INSTITUTO NACIONAL DE TECNICA AERONAUTICA

"ESTEBAN TERRADAS"

MADRID, SPAIN

# O P E N  F I R E S

# A N D

# T R A N S P O R T  O F  F I R E B R A N D S

Principal Investigator

C. Sánchez Tarifa

Colaborators:

P. Pérez del Notario

F. García Moreno

A. Liñán Martinez

A. Bollain Sánchez

MAY 31, 1962 - MAY 31, 1963

# OPEN FIRES AND TRANSPORT OF FIREBRANDS

- - - - -


## SUMMARY

### a) Open Fires

During the report period the research work on open fires has been directed, mainly, to the study of fire burning rates.

A theoretical model of the process of the combustion of a liquid fuel contained in a vessel has been developed. This model gives stationary as well as transient burning rates of the fuel and temperature distributions within the vessel as a function of the amount of heat received through the fuel surface.

Dimensionless results are shown as well as several numerical applications for n-heptane, iso-octane, benzene, ethyl-alcohol and dioxane.

An extense research program is being carried out, in order to verify the theoretical conclusions and in order to obtain basic information on the combustion process.

The research facilities are, essentially, the same ones described in First Annual Report, although they have been improved and several radiometers have been installed.

Several experimental results are shown as well as a comparison between theoretical and experimental results.

Some interesting conclusions are obtained on the Open Fires program which are included at the end of the Report.

### b) Transport of Firebrands

Theoretical and experimental studies on the problem of transport of firebrands have shown that an excellent approximation of the process is obtained by assuming that the firebrands fly at their terminal or final velocity of fall.

By means of numerical integrations of the differential equations of the process and by means of analytical calculations it is shown that in a matter of seconds the firebrands reach values of their velocities very close to the terminal velocity of fall.

Therefore, flight paths are calculated under such assumption and the experimental tests in the wind tunnel are carried out at wind speeds equal to the firebrand terminal velocity of fall.

This is achieved by reducing continuously the wind speed in the tunnel during the test, in order to keep equal the values of the aerodynamic drag and the weight of the particle. This is controlled by the position of the wire holding the firebrand or else by the recorded curves of such weight and drag.

An extense research program is also being carried out, with firebrands of several kind of woods (pinus pinaster, picea excelsa, quercus sessiliflora, populus tremuloides and ochroma lagopus) with spherical and cylindrical shapes and for different moisture contents.

The small wind tunnel described in First Annual Report is being used. A large wind tunnel has been designed and constructed and it will be soon utilized.

Several results are shown and discussed, including flight paths of the firebrands for several wind conditions.

Some important conclusions are obtained on the Transport of Firebrands program which are included at the end of the Report.

= = = = = = = = =

# I - OPEN FIRES

## 1-1 Introduction

The research work on Open Fires has been especially dedicated to the theoretical and experimental studies on burning rates.

A theoretical model of the process of the combustion of a liquid fuel contained in a cylindrical vessel has been developed, which gives the burning rates and temperature profiles within the fuel as functions of the amount of heat received by the fuel from the flame. Transient conditions have also been considered in order to evaluate the time needed to attain quasi-estationary combustion conditions, which in certain cases may be extremely long.

The research facilities utilized have been, basically, the same ones described in the First Annual Report. An improved system for measuring the fuel flow has been placed. A ring with four radiometers has been fitted around and over the fire, as well as a moving system of probes for measuring flames temperatures and convection speeds. Recording thermocouples have also been installed.

An experimental research program is being conducted using several types of fuels in order to verify the theoretical results and in order to obtain more information on the combustion process.

# BURNING RATES.

## THEORETICAL STUDIES

### I-2 Combustion Process in a Vessel

The combustion process of a fuel in a constant-level vessel can be divided into the following periods:

a) Heating and ignition

The fuel is heated from an external source (a flame) until its surface reaches the flash point temperature, and then, combustion begins.

b) Combustion and surface heating

When combustion starts the fuel surface temperature increases very rapidly until it reaches the boiling temperature.

c) Transient combustion at constant fuel surface temperature.

Combustion proceeds at constant fuel surface temperature. Temperature within the fuel increases and the burning rate also increases both tending towards stationary values.

The time required for periods a) and b) is very short as compared with the time of period c). However, these periods cannot be disregarded because they fix the initial temperature conditions for the transient combustion. For simplicity, periods a) and b) will be joined in only one period, which will be called heating and ignition, in which the fuel is heated until its surface reaches the boiling temperature. Burning rate (fuel consumption) will be disregarded throughout this process.

d) Stationary combustion

After a certain time combustion reaches, practically, stationary conditions, which can be directly calculated.

## I-3 General assumptions

The physical model of the transient or stationary combustion process will be based upon the following assumptions:

a) The fuel enters the vessel through its bottom at ambient temperature $T_o$. This temperature is kept uniform and constant throughout the bottom by means of water cooling at $T_o$. The fuel moves upwards till it reaches the surface where it is evaporated and burned. This fuel surface is kept at a constant level (fig.1).

In other models it will be assumed that part of the fuel is removed from the fuel surface without burning by means of overflow tubes.

b) One-dimensional conditions within the vessel will be considered by assuming that vessel diameter is large as compared to vessel depth and by assuming that conditions at the fuel surface are uniform.

c) Viscosity and gravitational forces are not considered. Density, thermal conductivity and specific heat of the fuel are taken as constant regardless of fuel temperature.

d) It will be assumed that a certain amount of heat $Q_s$ per unit surface and per unit time is transferred from the flame to the fuel through either conduction, radiation or convection. It will be assumed that $Q_s$ is absorbed at the fuel surface, disregarding the depth of the fuel required to absorb the heat transferred through

radiation. The values of $Q_s$ will be experimentally obtained.

e) Temperature at the fuel surface will be taken equal to the boiling temperature at ambient pressure.

f) For the case of the ignition period the general assumptions will be the same, except that combustion will be substituted by a heating process in which the fuel will be at rest.

## I-4 General Equations

Under the aforementioned assumptions the equations of conservation of mass and energy within the fuel are as follows:(*)

a) Continuity:

$$\rho V = \dot{m}_s = \text{constant} \qquad (1)$$

in which $\rho$ is the fuel density, $V$ the upwards velocity of the fuel and $\dot{m}_s$ is the burning rate or mass of fuel burnt per unit time and per unit area.

b) Energy:

Neglecting the kinetic energy of the fuel, the equation of energy expresses the transport balance of heat and internal energy.

$$\frac{\partial}{\partial X}\left(\lambda \frac{\partial T}{\partial X}\right) - \rho V \frac{\partial (cT)}{\partial X} = \rho \frac{\partial (cT)}{\partial t} \qquad (2)$$

or else:

$$V \frac{\partial T}{\partial X} + \frac{\partial T}{\partial t} = \frac{\lambda}{\rho c} \frac{\partial^2 T}{\partial X^2} \qquad (3)$$

c) Motion:

Neglecting the transfer of momentum within the fluid, the

(*) See Appendix for Notation.

equation of motion vanishes, reducing to:

$$P = \text{constant} \qquad (4)$$

throughout the fluid.

I-5 Boundary Conditions

a) Combustion

At the fuel surface we have the following boundary conditions:

$$X = X_s \quad ; \quad T = T_s \qquad (5)$$

$$Q_s = \dot{m}_s \, q_l + \lambda \left( \frac{\partial T}{\partial X} \right)_s \qquad (6)$$

in which $q_l$ is the latent heat of evaporation. This equation expresses the heat balance at the fuel surface.

At the fuel bottom, we have:

$$X = 0 \quad ; \quad T = T_o \qquad (7)$$

b) Ignition

During ignition, condition (5) does not exist and equation (6) is:

$$Q_s = \lambda \left( \frac{\partial T}{\partial X} \right)_s \qquad (8)$$

At the initial time $(t = o)$, we also have:

$$t = o \quad T(X) = T_o = \text{constant} \qquad (9)$$

For $T = T_s$, the resulting temperature distribution $T(X)$ will be the initial condition for studying transient combustion.

## I-6 Solution of the Equations

Introducing the dimensionless variables and parameters:

$$\theta = \frac{T}{T_s} \tag{10}$$

$$\delta = \frac{X}{X_s} \tag{11}$$

$$\tau = \frac{t}{X_s^2 a^2} \tag{12}$$

$$a^2 = \frac{\rho c}{\lambda} \tag{13}$$

$$\chi_s = \frac{Q_s X_s}{\lambda T_s} \tag{14}$$

$$\chi_1 = \frac{q_1}{T_s c} \tag{15}$$

$$\nu = a^2 X_s V \tag{16}$$

$$\theta_o = \frac{T_o}{T_s} \tag{17}$$

$$\theta_s = \frac{T_s}{T_s} = 1 \tag{18}$$

equation (3) and boundary conditions (7), (5), (9), (6) and (8) are expressed, respectively, as follows:

$$\nu \frac{\partial \theta}{\partial \delta} + \frac{\partial \theta}{\partial \tau} = \frac{\partial^2 \theta}{\partial \delta^2} \tag{19}$$

$$\theta_{\delta=0} = \theta_0 \; ; \text{ or : } \theta(0,\tau) = \theta_0 \tag{20}$$

$$\theta_{\delta=1} = \theta_s = 1 \; ; \text{ or : } \theta(1,\tau) = 1 \tag{21}$$

$$\theta_{\tau=0} = \theta_0 \; ; \text{ or : } \theta(\delta, 0) = \theta_0 \tag{22}$$

$$\chi_s = \chi_1 \nu + \left(\frac{\partial \theta}{\partial \delta}\right)_{\delta=1} \tag{23}$$

$$(\chi_s)_{\nu=0} = \left(\frac{\partial \theta}{\partial \delta}\right)_{\delta=1} \tag{24}$$

In the first place, the fundamental process of stationary combustion will be studied, and then, the transient processes of ignition and combustion will be considered.

## STATIONARY PROCESSES.

### I-7 Stationary Combustion

The equation governing the process is the ordinary differential equation:

$$\nu \frac{d\theta}{d\delta} = \frac{d^2\theta}{d\delta^2} \tag{25}$$

because the only variable is the dimensionless coordinate $\delta$.

Boundary conditions are as follows:

$$\theta(0) = \theta_0 \tag{26}$$

$$\theta(1) = 1 \tag{27}$$

$$\chi_s = \chi_1 \nu + \left(\frac{\partial \theta}{\partial \delta}\right)_{\delta=1} \qquad (28)$$

in which $\theta_o$ , $\chi_s$ and $\chi_l$ are constant and their values are given. Parameter $\nu$ , which gives the fuel velocity V and burning rate $\dot{m}_s = \rho V$ , is constant, but its value has to be determined.

Equation (25) is inmediately integrated, resulting:

$$\theta = \frac{1}{\nu}\left\{C_1 + \exp\left[\nu(\delta - C_2)\right]\right\} \qquad (29)$$

Boundary conditions (26) and (27), give:

$$C_1 = \frac{\nu(1 - \theta_o e^{\nu})}{1 - e^{\nu}} \qquad (30)$$

$$C_2 = 1 - \frac{1}{\nu} \log \nu \left(1 - \frac{1 - \theta_o e^{\nu}}{1 - e^{\nu}}\right) \qquad (31)$$

Resulting:

$$\theta = 1 - (1 - \theta_o) \frac{e^{\nu} - e^{\nu\delta}}{e^{\nu} - 1} \qquad (32)$$

The value of fundamental parameter $\nu$ is obtained from boundary condition (28) and from:

$$\left(\frac{\partial \theta}{\partial \delta}\right)_{\delta=1} = \nu e^{\nu} \frac{1 - \theta_o}{e^{\nu} - 1} \qquad (33)$$

Substituting this value into (28), it results:

$$\nu = \frac{1}{\chi_l}\left(\chi_s - \nu e^{\nu} \frac{1 - \theta_o}{e^{\nu} - 1}\right) \qquad (34)$$

from which the value of $\nu$ can be obtained.

When $\nu << 1$ , its value is approximately given by the expression:

$$\nu \approx \frac{\chi_s - (1 - \theta_o)}{\chi_l + (1 - \theta_o)} \tag{35}$$

or else:

$$\rho V = \dot{m}_s = \frac{Q_s - \frac{\lambda}{\chi_s}(T_s - T_o)}{q_l + c\,(T_s - T_o)} \tag{36}$$

Although the fuel velocity V is small, the motion of the fluid cannot be disregarded. For $V = o$ , we have:

$$\theta = \theta_o + (1 - \theta_o)\,\delta \tag{37}$$

and:

$$\nu = \frac{\chi_s - (1 - \theta_o)}{\chi_l} \tag{38}$$

or:

$$\dot{m}_s = \frac{Q_s - \frac{\lambda}{\chi_s}(T_s - T_o)}{q_l} \tag{39}$$

Temperature profile given by (32) may differ considerably from the straight line given by (37), and the values of the burning rates given by (36) or (39) may be quite different.

In figs. 2 through 7 temperature profiles $\theta = f(\delta)$ are shown for different values of parameters $\chi_s$ , $\chi_l$ , and $\theta_o$ , and in figs. 8, 9 and 10 dimensionless burning rates $\nu$ are plotted as functions of the same parameters.

It may be seen that for certain conditions, especially when the heat transfer parameter $\chi_s$ is large, the temperature profiles

re very sharp in the vicinity of the fuel surface. This is still etter shown in the figures with numerical values $\tau_1$, $\tau_2$ and $\tau_3$. herefore, a thermocouple placed at the fuel surface would measure n average value of the temperature. This might explain why the easured values of the temperature at the fuel surface are usually maller than the boiling temperature, which is the value predicted y theory.

It may be also seen that small values of $\chi_1$ increase the urning rates and that, on the contrary, large values of $\theta_o$ ncrease the burning rates for equal values of $\chi_s$ and $\chi_1$. Both esults are inmediately explained from physical considerations.

A numerical application for normal heptane has been carried ut. Figs. $\tau_1$, $\tau_2$, $\tau_3$ and $\tau_4$ show temperature profiles and burning ates for several values of the heat transferred to the fuel surface $Q_s$, temperature at the bottom of the vessel or temperature of the incoming fuel $T_o$, and vessel depth $X_s$.

The heat transferred from the flame to the fuel $Q_s$ is an experimental datum, which depends on the type of fuel and on the size of the vessel. Therefore, the values of the burning rates would only coincide with the experimental results for the correct value of $Q_s$, which will be experimentally determined.

The vessel depth (total fuel depth) $X_s$ does not influence the values of the burning rates above a certain value. But for small values of such parameter the burning rate depends considerably on it, decreasing as $X_s$ decreases until it reaches a minimum value under which combustion is not possible. Therefore, when

using vessels for studying open liquid fires, depths larger than those minimum values should be used.

In figs. 15 through 18 similar results are shown for benzene, from which the same conclusions could be derived.

Finally, figs. 19 and 20 show comparative results of temperature profiles and burning rates for normal-heptane, benzene, iso-octane and ethyl-alcohol.

## I-8 Stationary Combustion with Overflow

When using constant level cylindrical vessels for studying open fires, in order to keep the fuel at a constant level one or several overflow tubes are used. The overflow tubes can be placed outside the vessel, as shown in fig.4 of First Annual Report, but quite often, the overflow tubes are placed within the vessel. In this case it is necessary to introduce some modifications into the general equations of the process, since not all fuel which is heated up to the boiling temperature is evaporated and burned, but a certain percentage of it is returned down through the overflow tube. We will see that this return flow influences considerably the values of the burning rates.

The equation of energy:

$$\rho V \frac{dT}{dX} \equiv \dot{m}_s \frac{dT}{dX} = \lambda \frac{d^2T}{dX^2} \qquad (40)$$

is the same (25) than in the previous case. But in this case $\dot{m}_s = \rho V$ is the flow of fuel introduced into the vessel but it is not the amount of fuel which is evaporated and burned.

Boundary conditions (20), (21) and (22) do not change, but boundary condition (23) is now:

$$Q_s = \xi \dot{m}_s q_1 + \lambda \left( -\frac{dT}{dX} \right)_s \qquad (41)$$

or:

$$\chi_s = \chi_1 \xi \nu + \left( \frac{\partial \theta}{\partial \delta} \right)_{\delta=1} \qquad (42)$$

In these formulae $\xi \dot{m}_s$ is the fuel flow evaporated and burned, which is smaller than $\dot{m}_s$. The difference:

$$\dot{m}_r = \dot{m}_s (1 - \xi) \qquad (43)$$

is the return or overflow fuel. The experimenter can fix arbitrarily either $\dot{m}_s$ or $\dot{m}_r$.

The problem is solved in a similar way. Temperature distribution is given by (32), but the value of $\nu$ is now given by:

$$\xi \nu = \frac{1}{\chi_1} \left( \chi_s - \nu e^{\nu} \frac{1 - \theta_o}{e^{\nu} - 1} \right) \qquad (44)$$

in which the value of $\xi$ should be given. In fig. 21 the influence of $\xi$ on the burning rate is shown, and it can be seen that it can be very important. Therefore, when using the overflow system with tubes placed within the vessel, the influence of the overflow fuel must be taken into account, and it also gives an easy mean of changing burning rates and flames properties by varying the overflow rates.

When $\nu \gg 1$ its value is approximately given by the expres-

sion

$$\nu = \frac{\chi_s}{\xi \chi_l + 1 - \theta_o} \tag{45}$$

or else:

$$\rho V = \dot{m}_s = \frac{Q_s}{\xi q_1 + c (T_s - T_o)} \tag{46}$$

## BURNING RATES

## TRANSIENT PROCESSES

### I-9 Heating and Ignition

During the heating and ignition process it will be assumed that the amount of heat $Q_s$ transferred to the fuel is constant. As it was mentioned in paragraph I-2, the fuel surface temperature increases from its initial value up to the boiling temperature, and the burning rate $\dot{m}_s$ will be taken equal to zero throughout the process.

The partial differential equation of the process is:

$$\frac{\partial \theta}{\partial \tau} = \frac{\partial^2 \theta}{\partial \delta^2} \tag{47}$$

and boundary conditions are:

$$\theta (\delta, 0) = \theta_o \tag{48}$$

$$\theta (0, \tau) = \theta_o \tag{49}$$

$$\left(\frac{\partial \theta}{\partial \delta}\right)_{\delta=1} = \chi_s \tag{50}$$

The general solution of the parabolic partial differential equation (47) is:

$$\theta = C_1 + C_2 \delta + \sum_1^{\infty} A_n e^{-\omega_n^2 \tau} \sin(\omega_n \delta + \varphi_n) \qquad (51)$$

Condition (50) gives:

$$\omega_n + \varphi_n = \frac{2n-1}{2}\pi \qquad (52)$$

or:

$$C_2 = \chi_s \qquad (53)$$

Condition (49) gives:

$$\varphi_n = 0 \qquad (54)$$

or

$$C_1 = \theta_o \qquad (55)$$

From (54) and (52):

$$\omega_n = \frac{(2n-1)\pi}{2} \qquad (56)$$

resulting:

$$\theta = \theta_o + \chi_s \delta + \sum_1^{\infty} A_n \exp\left[-(2n-1)^2 \pi^2 \tau/4\right] \sin \frac{(2n-1)\pi\delta}{2} \qquad (57)$$

Finally, condition (48) gives:

$$\sum_1^{\infty} A_n \sin(2n-1)\frac{\pi}{2}\delta = -\chi_s \delta \qquad (58)$$

From which, by multiplying by $\sin\left[(2m-1)\pi\delta/2\right] d\delta$ and integrating from $\delta = 0$ up to $\delta = 1$, it is obtained:

$$A_n = \frac{8\chi_s}{\pi^2 (2n-1)^2}(-1)^n \qquad (59)$$

Resulting, finally, for the dimensionless temperature:

$$\theta = \theta_0 + \chi_s \delta + \frac{8\,\chi_s}{\pi^2} \sum_1^{\infty} \frac{(-1)^n}{(2n-1)^2} \exp\left[-\frac{(2n-1)^2 \pi^2 \tau}{4}\right] \sin\frac{(2n-1)\pi\delta}{2} \qquad (60)$$

The ignition period ends when $\theta = \theta_s$. The corresponding time $\tau_s$ is given by the expression:

$$\sum_1^{\infty} \frac{1}{(2n-1)^2} \exp\left[-\frac{(2n-1)^2 \pi^2}{4}\tau_s\right] = -\frac{\pi^2}{8\,\chi_s}(1 - \theta_0 - \chi_s) \qquad (61)$$

For this value of $\tau_s$ the distribution of temperatures is given by (60) for $\tau = \tau_s$.

In fig.22 the dimensionless time $\tau_s$ required to reach the boiling temperature is represented as a function of heat parameter $\chi_s$ for several values of $\theta_0$, and in fig. 23 a numerical application for normal-heptane is included.

In all practical cases, the actual time $t_s$ is very small, but if $Q_s$ is small, especially for large values of the vessel depth, such time may be very long and it could not even be possible to reach the boiling temperature, for very small values of the heat transferred $Q_s$.

## I-10 Transient Combustion

In order to study the transient combustion process the complete equation (3) should be used. However, the analytical integration of this complete equation does not appear as feasi-

ble(*)

The problem can be solved by means of numerical integration of the equation. However, an approximated analytical solution can be obtained by disregarding the influence of term $V\partial T/\partial X$ on the differential equation (3), and obtaining the value of velocity $V$ or burning rate $\dot{m}_s$ through boundary condition (6).

Term $V\partial T/\partial X$ is usually small as compared with terms $\partial T/\partial t$ and $\lambda/\rho c\ \partial^2 T/\partial X^2$, because the flow velocity $V$ is very small. By comparing terms $V\partial T/\partial X$ and $\lambda/\rho c\ \partial^2 T/\partial X^2$ for the stationary case and from results obtained through numerical integration of the complete equation in a representative case, it has been estimated that the error introduced in the value of the burning rate by disregarding such term is, usually, of the order of 20-40%, although in certain cases it may be larger. However, this approximation presents the inconvenience that it does not fulfill boundary conditions for $t = \infty$, for which the solution of the problem should tend towards the stationary solution of equation (3).

---

(*) Through the change of variable:

$$\frac{\partial \Psi}{\partial X} = \rho \quad ; \quad \frac{\partial \Psi}{\partial t} = -\rho V = -\dot{m}_s$$

equation (3) is transformed into the equation:

$$\frac{\partial T}{\partial t} = \frac{\rho \lambda}{c} \frac{\partial^2 T}{\partial \Psi^2} \ .$$

which could be integrated, but boundary conditions (5) and (7) cannot be introduced into the general solution of this equation.

A better approximation of the problem is obtained by means of a solution of the form:

$$T = T_e (X) + T_t (X , t) \tag{62}$$

or

$$\theta = \theta_e (\delta) + \theta_t (\delta , \tau) \tag{63}$$

in which $T_e (X)$ is the stationary solution of (3) and $T_t (X , t)$ is the transient term obtained by integrating such equation (3) for $V \partial T / \partial X = 0$ (*).

Boundary conditions are as follows:

$$\theta (0 , \tau) = \theta_o \tag{64}$$

$$\theta (1 , \tau) = 1 \tag{65}$$

$$\chi_s (\tau) = \chi_1 \nu + \left( \frac{\partial \theta}{\partial \delta} \right)_{\delta = 1} \quad (**) \tag{66}$$

This last boundary condition gives the dimensionless burning rate $\nu$. Furthermore: for $\tau = 0$, temperature distribution $\theta (\delta)$ should be the one given by (60) for $\tau = \tau_s$.

---

(*) This solution (62) fulfills all boundary conditions but it does not fulfill the complete equation (3). Solution (62) implies that terms:

$$(V_e - V) \frac{\partial T_e}{\partial X} - V \frac{\partial T_t}{\partial t} \simeq 0$$

have been taken equal to zero. It may be shown that this is a better approximation that the one obtained by simply taking $V \dfrac{\partial T}{\partial X} = 0$.

(**) A value $\xi = 1$ has been considered.

The stationary term $\theta_e(\delta)$ is given by (32). Therefore, the problem consists in the attainment of transient term $\theta_t(\delta,\tau)$.

This term is given by the transient term of the solution of equation:

$$\frac{\partial\theta}{\partial\tau} = \frac{\partial^2\theta}{\partial\delta^2} \tag{67}$$

with boundary conditions (64) and (65). This term is:

$$\theta_t(\delta,\tau) = \sum_1^\infty A_n\, e^{-n^2\pi^2\tau} \sin n\pi\delta \tag{68}$$

Therefore, solution (63) is:

$$\theta = 1 - (1-\theta_o)\frac{e^\nu - e^{\nu\delta}}{e^\nu - 1} + \sum_1^\infty A_n\, e^{-n^2\pi^2\tau} \sin n\pi\delta \tag{69}$$

Coefficients $A_n$ are determined by equalizing the expressions of $\theta$ given by (60) and (69) for $\tau = \tau_s$ and $\tau = 0$, and then, by multiplying by $\sin m\pi\delta$ and by integrating from $\delta = 0$ to $\delta = 1$. It results:

$$A_n = -\frac{2}{\pi}(1-\theta_o)\left(\frac{e^\nu}{e^\nu-1} - 1\right)\frac{(-1)^n - 1}{n} + \frac{2}{\pi}\frac{1-\theta_o}{e^\nu - 1}\frac{n}{\frac{\nu^2}{\pi^2}+n^2}\left[e^\nu\,(-1)^n - 1\right] -$$

$$-\frac{64}{\pi^3}\chi_s(-1)^n n \sum_{m=1}^\infty \exp\left[-\frac{(2m-1)^2\pi^2}{4}\tau_s\right]\left\{(2m-1)^2\left[(2m-1)^2 - 4\pi^2\right]\right\}^{-1} \tag{70}$$

Dimensionless burning rate is obtained from boundary condition (66) and from the value of $(\partial\theta/\partial\delta)_{\delta=1}$ obtained from

(69). It results:

$$\nu = \frac{\chi_s - \sum_1^{\infty} A_n \, n\pi(-1)^n \, e^{-n^2\pi^2\tau}}{\chi_1 + (1 - \theta_o)\,\frac{e^{\nu}}{e^{\nu} - 1}} \qquad (71)$$

in which $A_n$ is given by (70).

In figure 24 dimensionless temperature profiles $\theta = f(\delta)$ are shown as a function of dimensionless time $\tau$. The initial heating and ignition period, from $\tau = 0$ to $\tau = \tau_s$ is also included. It may be seen that such time $\tau_s$ is very small. It is also interesting to point out that temperature profiles are especially sharp during transient conditions.

Fig.25 shows dimensionless burning rates $\nu$ as a function of time. In this case the starting of combustion ($\nu = 0$) has been taken as the initial time ($\tau = 0$).

Figs. 26 and 27 show similar results of normal-heptane, for an assumed value of $Q_s$ equal to 0.1 cal/cm$^2$. For this value of $Q_s$ the time required to reach conditions close to the asymptotic stationary values is of the order of 30 minutes.

Results obtained by disregarding the motion of the fluid $\left(V \frac{\partial T}{\partial X} = 0\right)$ have been also included, showing that the approximation utilized is considerably better.

Finally, figs. 28 and 29 show the overhelmingly importance of vessel (fuel) depth $X_s$ on the time needed to reach conditions close to the stationary asymptotic values. In fig. 28 curves

$\dot{m}_s = f(t)$ are shown for several values of $X_s$. It may be seen that the stationary value of the burning rate depend little on $X_s$ above $X_s = 5$ cm, and the time needed to reach a value of $\dot{m}_s$ equal to 95% of the stationary value changes from 40 minutes to 120.

This might explain why some experimenters could not reach stationary conditions when studying liquid fires using deep vessels(*), and it also shows that vessel depth has to be selected carefully according to its size and to the type of fuel which is going to be studied.

## BURNING RATES

## EXPERIMENTAL STUDIES

### I-11 Research Facilities

The research facilities which are being used to study open liquid fires are, basically, the same ones as describedin First Annual Report, although they have been considerably improved. A general sketch of them is shown in fig. 30.

A new constant-pressure volumetric system for measuring the fuel consumption has been constructed. It gives more accurate readings and more flexibility for measuring large or small fuel consumptions.

The overflow tube has been placed in the center of the

---

(*) Ref. 7 of First Annual Report.

vessel. We have seen that the overflow rate influences considerably the process. By setting different overflow rates, the burning rate, the heat emitted by radiation and several other variables can be continuously modified, which may give very important informations on several aspects of the problem.

A grid with different sized holes has been placed at the bottom of the vessel, in order to have a more uniform distribution of the incoming fuel.

A ring with four Kipp and Zonen Radiometers has been placed over the fire, and their signals are registered in a recording Hartman and Braun instrument.

A moving system of probes has been placed. Several pressure and temperature probes have been attached to a moving carriage, which can be displaced by remote control along horizontal and vertical axis. This system permits measurements of flame temperatures and velocities at continuously variable location during the experiments.

Finally, an optical pyrometer has been acquired and the reflectivity of an aluminum mirror in the wavelength region of the red light has been measured at the Optical laboratory of the INTA, in order to measure flames temperatures by optical means.

I-12 Research Program

An extense experimental program is presently being conducted, compri$sing the following measurements:

1º) Burning rates and temperature profiles within the fuel.

2º) Radiant heat emitted by the flame

3º) Flame size and flame lateral surface (from movie pictures)

4º) Flame temperatures at several locations.

From these measurements information is being obtained on the following subjects:

a) Values of the heat transferred from the flame to the fuel as well as its laws of variation with several parameters, such as fuel properties, vessel size, flame temperature, etc. (This heat transferred will also be directly measured by placing a small radiometer at the end of a tube inserted in the vessel.)

b) With the values of the heat transferred to the fuel, burning rates and temperature profiles will be calculated following the theoretical model already described. These results will be compared with those directly measured.

c) Scaling laws. The influence of vessel size, vessel depth and flame size on the problem will be studied. For a given vessel and for the same fuel, flame size can be varied considerably by changing the overflow rate.

Pure chemical species are mainly being used as fuels, especially normal-heptane, benzene, octane and ethyl-alcohol. Ethylene-dioxide (dioxane) is also being used, mixed with water in several proportions.

Information on several problems of liquid fuel-fire is being studied, especially in connection with radiation properties and

heat balances of flames.

This experimental program and the comparison of theoretical and experimental results is in full progression now, and it will constitute one of the main subjects on open fires for the next annual period. Some preliminary results will be given in the present Report.

Figs. 31, 32 and 33 show three examples of the type of measurements which are being carried out.

Figs. 34 and 35 show the values of $Q_R$ , $Q_R/A_f$ and $Q_R/\xi \dot{m}_s q_r A_v$ as function of time. $Q_R$ is the total heat emitted by radiation, through the upper hemisphere calculated from data of figs.31 and 32. $Q_R/A_f$ is the average value of the radiant heat emitted per unit area of the flame, and $Q_R/\xi \dot{m}_s q_r A_v$ is the ratio of such radiant heat to the heat released by combustion, ($q_r$ = heat of reaction).

Finally, assuming that all heat received by the fuel is transferred through radiation, and taking as the value of such radiant heat the average value of $Q_R/A_f$, the value of $Q_s$ may be estimated. From the value of $Q_s$, and with the values of the overflow coefficient $\xi$ of figures 31 and 32, the values of the burning rates for n-heptane may be calculated by applying the theoretical model already described. In this way, curves of fig. 36 have been calculated and the calculated values of $\xi \dot{m}_s$ are compared with the values directly measured with the volumetric motor.

There is a fair agreement between the calculated and

the measured values, although, as it could be expected, the calculated values are somewhat smaller. Vessel diameter is 25 cm, and for this size some appreciable amount of heat should be transferred through conduction. Therefore, the estimated value of $Q_s$ is probably smaller than its actual value, which might explain the slight discrepancy between calculated and measured values of the burning rates.

## II. TRANSPORT OF FIREBRANDS

### II-1 INTRODUCTION

During the report period the following work has been performed on the firebrand program:

a) Continuation of the theoretical work on flight paths.

b) Modifications of the research facilities and constructions of new ones.

c) Continuation of the experimental work on lifetimes, weight and aerodynamic drag histories and flight paths of burning particles of wood.

The theoretical research has been applied to the study of actual flight paths, by means of numerical integration of the differential equations of the process. From these studies a simplified model of flight paths has been derived, which gives an excellent approximation of the process. This model assumes that the firebrand always flies at its terminal velocity of fall.

The experimental results mentioned in paragraph c) were at first determined by burning wood particles in a small wind tunnel at constant wind speeds.

According to the aforementioned conclusion that the firebrandsfly at their terminal velocity of fall, the experimental work is presently being carried out at variable wind speed. By changing progressively the throttling of the tunnel the wind speed is kept continuously equal to the terminal velocity of fall of the burning particle, which decreases throughout the combustion process tending towards zero.

A remote control of the wind speed of the tunnel has been fitted, and a larger wind tunnel has been designed and constructed, which will be soon utilized.

## THEORETICAL STUDIES

### II-2 Flight Paths

The two-dimensional equations which control the motion of a burning particle under stationary wind conditions are as follows:

$$\frac{d\,w_x}{dt} + \frac{\rho\, C_D\, A}{2\,m}\, w\, w_x = 0 \qquad (72)$$

$$\frac{dw_y}{dt} + \frac{\rho\, C_D\, A}{2m}\, w\, w_y - g = 0 \qquad (73)$$

These equations were derived in First Annual Report.(*)

(*) See Notation in Appendix

Parameter:

$$\alpha = \frac{\rho C_D A}{2 m} \tag{74}$$

is a function of time as well as of the relative wind velocity $w$.

The experimental part of the research program consists in the determination of function $\alpha = f(w, t)$ for several initial sizes and shapes of the firebrand, kind of woods and moisture contents. At the same time lifetimes or burn-out time of the firebrands $t_b = f(w, t)$ are determined.

From the experimental values of $\alpha$, and under given wind conditions $u(x, y)$, from equations (72) and (73) the flight paths are determined:

$$X = \int_o^{t_b} (u_x - w_x)\, dt \tag{75}$$

$$Y = \int_o^{t_b} (u_y - w_y)\, dt \tag{76}$$

The burn-out time $t_b$ can be longer or shorter that the time required for a firebrand to reach the ground ($t_{y=o}$). In the first case the firebrand reaches the ground still burning and in the second case the firebrand burns out in the air. When $t_b = t_{y=o}$ a maximum horizontal range is reached.

## II-3 Terminal Velocity of Fall (Final Velocity)

In First Annual Report flight paths were obtained by taking an average value of parameter $\alpha$. For $\alpha$ constant an analytical

solution of system (72), (73) was obtained and one of the principal conclusions was that the burning particles reach very rapidly their final velocity or terminal velocity of fall, characterized by conditions:

$$w_x = 0 \tag{77}$$

$$w_y = w_f = \sqrt{\frac{g}{\alpha}} \tag{78}$$

Several numerical integrations of system (72) (73) have been performed for different representative cases, by taking the experimental values of parameter $\alpha$ (w, t). Adam's method has been utilized, by using expression:

$$w_{x,n+1} = w_{x,n} + \frac{1}{2}\left[\left(\frac{dw_x}{dt}\right)_n - \left(\frac{dw_x}{dt}\right)_{n-1}\right]\Delta t \tag{79}$$

and a similar expression for $w_y$.

In figs. 37 and 38 two representative cases are shown for "pinus pinaster" spheres with initial diameters of 17 mm and 25 mm. An initial value of $w_{x,o} = 20$ m/sec has been taken and for the vertical component two cases have been considered: $w_{y,o} = 20$ m/sec and $w_{y,o} = 0$. The first would correspond to the initial flight of a firebrand taken upwards by the convection column produced by the fire. The second case would correspond to a firebrand leaving the convection column at a certain height being thrown into a horizontal wind at a zero vertical component of its velocity.

The experimental values of the terminal velocities of fall are also shown in the figures. It may be seen that in all cases

in a matter of seconds both components of the velocity $w_x$ and $w_y$ tend very rapidly towards zero and towards $w_f$ respectively.

In fig.39 the time needed for the particles to reach a value very close to its asymptotic value ($w_x = o$ $w_y = w_f$) is compared with the burn-out time, and it may be seen that it is extremely small. Therefore, it is justified to assume that the firebrand is always flying at its terminal velocity of fall for the calculation of flight paths. However, since some cases may exist for which such approximation could not be admissible; in the following paragraphs two expressions are derived which give a maximum value of the error introduced by the aforementioned assumption.

## II-4 Maximum Errors in the Flight Paths

The errors introduced into the horizontal and vertical distances reached by a firebrand owing to the introduction of the assumption that the firebrands always fly at $w_x = o$ and $w_y = w_f$, may be expressed by the expressions:

$$\varepsilon_x = \frac{\int_o^{t_f} w_x \, dt}{u_x t_f - \int_o^{t_f} w_x \, dt} \approx \frac{\int_o^{t_f} w_x \, dt}{u_x \, t_f} \qquad (80)$$

$$\varepsilon_y = \frac{\left| \int_{t_1}^{t_2} (w_f - w_y) \, dt \right|}{u_y (t_2 - t_1) - \int_{t_1}^{t_2} w_y \, dt} \approx \frac{\left| \int_{t_1}^{t_2} (w_f - w_y) \, dt \right|}{u_y \, (t_2 - t_1)} \qquad (81)$$

In these expressions $t_f$ is the final time, equal to $t_{y=o}$ or to $t_b$ (to the one which is the longest) and $t_2 - t_1$ is the time during which the firebrand is climbing ($t_1 = 0$ , $w_{y,o} = u_y$ , $w_y > w_f$) or falling ($t_2 = t_f$ , $w_{y,o} = 0$ , $w_f > w_y$).

Expressions will be derived giving the maximum or limiting values for $\xi_x$ and $\xi_y$ .

According to equation (72), the derivative $dw_x/dt$ and the relative velocity $w_x$ are always of opposite sign. Considering that parameter $\alpha$ increases as time progresses and that in the normal case the initial relative velocity $w_{x,o}$ is positive(*) , we have

$$\left| \frac{dw_x}{dt} \right| \geqslant \alpha_o \, w \, w_x \geqslant \alpha_o \, w_x^2 \qquad (82)$$

in which $\alpha_o$ is the initial value of parameter $\alpha$ . Integrating, it results:

$$w_x \leqslant \frac{w_{x,o}}{1 + \alpha_o \, w_{x,o} \, t} \qquad (w_{x,o} > 0) \qquad (83)$$

which is introduced into (80), gives:

$$\xi_x \leqslant \frac{\log (1 + \alpha_o \, w_{x,o} \, t_f)}{\alpha_o \, u_x \, t_f} = \frac{\log (1 + \alpha_o \, u_x \, t_f)}{\alpha_o \, u_x \, t_f} \qquad (84)$$

because normally $w_{x,o} = u_x$ .

It may be easily verified that in all cases of practical

---

(*) In First Annual Report velocities $w_x$ and $w_y$ were defined "as relative velocities of the wind with respect to the firebrand". This definition was adopted in order to have positive numerical values of such velocities.

interest is $\alpha_o u_x t_f \gg 0$ and, therefore, $\xi_x$ is very small. For the cases of figs. 37 and 38 $\alpha_o u_x t_f$ is larger than 125 and $\xi_x$ is small than a 4%.

For very small values of $t_f$ or for a very low velocity of the wind $\xi_x$ may have large values, but both cases are of no practical interest because the distances reached by the firebrands would be very small.

Parameter $\alpha$ is inversely proportional to a linear dimension of the burning particle, and the final time, taking equal to the burnt-out time (for maximum fire range), is roughly proportional to a linear dimension of the particle. Therefore, the maximum error given by (84) does not depend on the size of the particle.

Similarly, for the vertical component $w_y$ and considering the case of a free fall ($t_1 = t_o$ , $t_2 = t_f$ , $w_{y,o} = 0$ , $w_f > w_y$) , we have:

$$\frac{dw_y}{dt} = g - \sqrt{w_x^2 + w_y^2} \qquad w_y \leq g - \alpha_o w_y^2 \qquad (85)$$

from which it is obtained by integration:

$$w_y \leq \frac{\gamma}{\alpha_o} \frac{e^{2\gamma(t-t_o)} + 1}{e^{2\gamma(t-t_o)} - 1} = w_{f,o} \frac{e^{2\gamma(t-t_o)} - 1}{e^{2\gamma(t-t_o)} + 1} \qquad (86)$$

where:

$$\gamma = \sqrt{\alpha_o g} \qquad (87)$$

$$w_{f,o} = \sqrt{\frac{g}{\alpha_o}} = (w_f)_{t=t_o} \qquad (88)$$

$t_o$ is the time at which the particle starts falling, and $\alpha_o$ and $w_{f,o}$ are the corresponding values of coefficient $\alpha$ and terminal velocity $w_f$ .

In formula (86) it may be verified that in a few seconds $w_f$ changes from zero to a value very close to $w_{f,o}$ .

Since $w_f \gg w_y$ and $w_f \ll w_{f,o}$ , formula (81) gives:

$$\varepsilon_y \ll \frac{\int_{t_o}^{t_f} (w_{f,o} - w_y)\, dt}{u_y\,(t_f - t_o)} \qquad (89)$$

and taking (88) into (89), it results:

$$\varepsilon_y \ll \frac{1}{u_y\,(t_f - t_o)} \left\{ w_{f,o}\,(t_f - t_o) - w_{f,o} \left[ \frac{1}{\gamma} \log \frac{1 + e^{2\gamma(t_f - t_o)}}{2} - (t_f - t_o) \right] \right\} \qquad (90)$$

It may be easily verified that if $t_f - t_o$ or $u_y$ are not too small, $\varepsilon_y$ is very small and tends towards zero when $t_f - t_o$ tends towards infinity.

## EXPERIMENTAL RESULTS .

### II-5 Research Facilities

All experimental data have been obtained in the small wind tunnel described in First Annual Report. A remote control of the

throttle andaby-pass intake have been fitted in order to carry out the tests at variable wind speed.

Another wind tunnel has been designed and constructed, similar to the small wind tunnel, but considerably larger (fig. 40). This wind tunnel uses an axial 6 HP blower and a fixed exhaust and wind speed control system, but two calibrated intake nozzles can be adjusted, one of 52 cm in diameter and other of 32 cm.

Wind speeds up to 40 m/sec can be reached in the tunnel and pieces of wood up to 10 cm in length or diameter can be tested.

The nozzles are calibrated jet engines intakes. Wind velocity is determined by measuring the static pressure at four points located around the periphery of the test section, wind speed is controlled by means of a throttle andaby-pass intake.

The firebrand is supported by means of a thin steel wire. The weight and aerodynamic drag are measured by means of a two-components strain-gauges balance or else, the particle is allowed to hang freely from the wire, till it reaches a 45º angle from the vertical position, when the weight and the aerodynamic forces are in equilibrium.

A four channels recording equipment has been recently acquired, for registering the strain-gauges signals as well as the pressure signal from an electric micromanometer which will be acquired.

II-6 Research Program

The theoretical treatment of the problem of transport of firebrands is well established. Also, a quite satisfactory experimental technique has been determined and the research facilities are almost finished.

An extense experimental research program is now being carried out, and it will constitute the bulk of the work on the firebrand problem for the next reporting period.

The comparison, analysis and scaling laws of results will be made when all experimental data are available. Therefore in the present Report only some typical results will be advanced.

Transport of firebrands of pine wood ("pinus pinaster"), spruce ("picea excelsa"), poplar ("populus tremuloides"), oak ("quercus sessiliflora")(*) and balsa wood ("ochroma lagopus") are or will be studied with moisture contents of 2% and 25%.

At present definite geometrical initial shapes have been selected: spheres, cylinders and plates. Later on, natural shapes will also be studied.

Until now, most of the experimental work has been realized with shperical firebrands of pinus pinaster wood. Some results have also been obtained with spruce and poplar firebrands and some data with cylindrical initial shapes are also available.

All results have been obtained in the small wind tunnel.

---

(*) It has not been possible to obtain "querqus rubra" wood.

The experimental technique has been as follows:

The wood particles are suspended by a thin steel wire at the test section. The particle is ignited with the flame of a butane torch, keeping the flame on the particle during a time which is determined by the condition that the burn-out time of the firebrand has a maximum value compatible with complete combustion.

At first, some experiments were carried out by burning wood particles at constant wind speed. Afterwards, once it was established that the firebrands fly at their terminal velocity of fall along practically the whole flight paths, the experiments were made by varying the tunnel wind speed keeping its value equal throughout the test to the decreasing terminal velocity of fall of the burning particle. Until now, such condition has been controlled by the position of the wire, which is mantained at a 45º angle throughout the test.

In the large wind tunnel when using the Micrograph recorder, such condition of equal values of both velocities will be established by the recorded curves of weight and aerodynamic drag of the firebrand. Both values will be kept equal throughout the test by reducing continuously the tunnel wind speed.

At present, the wind velocity has to be read very frequently by an experimenter during the test. A direct reading non-recording micromanometer is being used. It is intended to use an electric micromanometer, and its signal will be recorded on the Micrograph.

Figs. 41 and 42 show typical results obtained with pinus spheres. Wood is not an homogenous substance, and when burning spheres of equal initial size a severe scattering of results is unavoidable. Therefore, average values for each initial diameter have to be taken as shown in such figures.

In Figs. 43, 44 and 45 average values of the terminal velocity of fall or final velocity $w_f$ as function of time are shown for different sized spheres of pine, spruce and poplar woods.

In the last part of the combustion process of the firebrand, the particle very frecuently breaks. Therefore, the last part of the curves is not well determined. However, this has little influence on the over-all combustion process.

Fig.46 shows similar results obtained with cylindrical firebrands. The cylinders are held in a transverse position regarding to the wind speed because in a free flight this position would be approximately taken by the firebrand(*).

From the results shown in figs. 41 through 46 the flight paths of the firebrands are calculated with formulae (75) and (76) once the wind conditions are established.

In Research Progress Report No. 3 some examples of flight paths were shown.

Figs. 47 and 48 show the flight paths for spherical and

---

(*) In a free fall a particle balances around the position of maximum stability, which is the position of maximum aerodynamic drag.

ylindrical firebrands under a wind model which assumes a vertical convection column and a horizontal wind.

The firebrands are assumed to be taken upwards by the convective wind and in some point of the convection column they are thrown away and picked up by the horizontal wind.

It may be seen that there exists a critical height $Y_m$ for which the firebrand reaches a maximum distance on the ground still burning. This maximum distance is the "maximum range $X_m$" of fire spread.

If the firebrands leave the convection column at heights lower than $Y_m$ they reach the ground still burning but at distances smaller than $X_m$. On the other hand, if the particles leave the convection column at heights higher than $Y_m$ they burn out in the air before reaching the ground.

Finally, figs. 49 and 50 show flight paths for spheres and cylinders for a wind model in which the convection column is assumed to be inclined and with a given width. Results are qualitatively similar to those already discussed.

A comparison and discussion of results for several shapes, types of wood, moisture contents, wind models, etc. will be left for the next Report, when all the experimental data already programmed will be available.

## PRINCIPAL CONCLUSIONS

The principal conclusions included in the present Report are as follows:

a) OPEN FIRES

1) Burning rates and temperature profiles are theoretically obtained as functions of the heat received by the fuel per unit time.

2) When it is assumed that such heat is transferred exclusively through radiation, a fair approximation of the process is obtained, for normal-heptane fuel and for vessels larger than 25 cm in diameter.

3) Vessel or total fuel depth influences considerably the process when it is smaller than a certain minimum value.

4) Liquid depth influences considerably the time required to achieve quasi-stationary conditions, and that time may be extremely long.

5) From 3 and 4 it follows that vessel depth has to be chosen between certain limits. These limits depend considerably on the heat $Q_s$ received by the fuel, that is to say, on the characteristics and size of the flame, and therefore, on the type of fuel.

6) Temperature profiles are very sharp in the vicinity of the fuel surface. Therefore, a thermocouple placed at the fuel surface would measure an average value of the temperature,

somewhat smaller than its superficial value, which should be very close to the boiling temperature at ambient pressure.

Temperature profiles are especially sharp for transient combustion.

The amount of overflow fuel taken from the vessel influences considerably the combustion process. The overflow rate may be used as an additional variable of the process. Large overflow rates reduce both the burning rate and the flame size, and conversily.

TRANSPORT OF FIREBRANDS

The firebrands reach in a few seconds velocities very close to their terminal velocity of fall characterized by conditions $w_x = 0$ and $w_y = w_f$ .

Only when the burn-out time $t_f$ is very small or the wind speed very low condition 1) might not hold, but these cases are of no practical interest.

There exists a critical height $Y_m$ at which if the firebrand leaves the convection column it reaches a maximum horizontal distance $X_m$ still burning.

$X_m$ is the maximum range from the flame front for which fire spread may be produced by firebrands of given initial size and for given wind conditions.

In the worst conditions $X_m$ may reach values of the order of several kilometers, even for small firebrands and for moderate wind conditions.

Madrid, june 1963

# A P P E N D I X

## NOTATION.

$a$ . . . Parameter defined by (13)

$A$ . . . Cross section area of a firebrand

$A_n$ . . . Coefficient

$A_f$ . . . Flame area

$A_v$ . . . Fuel surface area

$c$ . . . Specific heat of the fuel

$C_1$ . . . Constant

$C_2$ . . . Constant

$C_D$ . . . Drag coefficient

$D$ . . . Vessel diameter. Also, firebrand diameter

$g$ . . . Gravitational constant

$m$ . . . Mass of a firebrand (also a number)

$\dot{m}_r$ . . . Overflow or return flow of fuel

$\dot{m}_s$ . . . Fuel flow within the vessel

$n$ . . . Number

$P$ . . . Pressure

$Q_R$ . . . Radiant-heat emitted by the flame per unit time, through the upper hemisphere

$Q_g$ . . . Heat received by the fuel per unit area and per unit time

$q_l$ . . . Latent heat of evaporation

$q_r$ . . . Heat of the reaction of combustion

$t$ . . . Time

$t_b$ . . . Burn-out time

$t_{y=o}$ . . . Time at which a firebrand reaches the ground

$t_f$ . . . Final time, equal to $t_b$ or $t_{y=o}$

$u$ . . . Wind speed

$V$ . . . Velocity of the fuel or absolute velocity of a firebrand

$w$ . . . Relative velocity of the wind with respect to a firebrand

$w_f$ . . . Final or terminal velocity of fall

$X$ . . . Horizontal coordinate for firebrand motion. Also, coordinate for fuel motion within a vessel

$X_m$ . . . Maximum range reached by a firebrand

$X_s$ . . . Vessel (fuel) depth

$Y$ . . . Vertical coordinate for firebrand motion

$Y_m$ . . . Critical height reached by a firebrand for maximum range

$\alpha$ . . . Parameter defined by (74)

$\delta$ . . . Dimensionless coordinate defined by (11)

$\varepsilon$ . . . Error

$\theta$ . . . Dimensionless temperature defined by (10)

$\chi_s$ . . . Dimensionless heat transferred to the fuel surface defined by (14)

$\chi_l$ . . . Dimensionless heat of evaporation defined by (15)

$\lambda$ . . . Thermal conductivity of the fuel

$\nu$ . . . Dimensionless burning rate defined by (16)

$\rho$ . . . Fuel or air density

$\tau$ . . . Dimensionless time defined by (12)

$\omega_n$ . . . Coefficients

$\varphi_n$

$\psi$ . . . Function

Subscripts

o . . . . Indicates initial values

e . . . . Indicates stationary conditions

s . . . . Indicates at the fuel surface

t . . . . Indicates transient conditions

x,y . . . . Indicate X and Y axis directions.

FIG. 1

# SCHEMATIC MODEL FOR THE COMBUSTION OF THE FUEL WITHOUT OVERFLOW TUBES

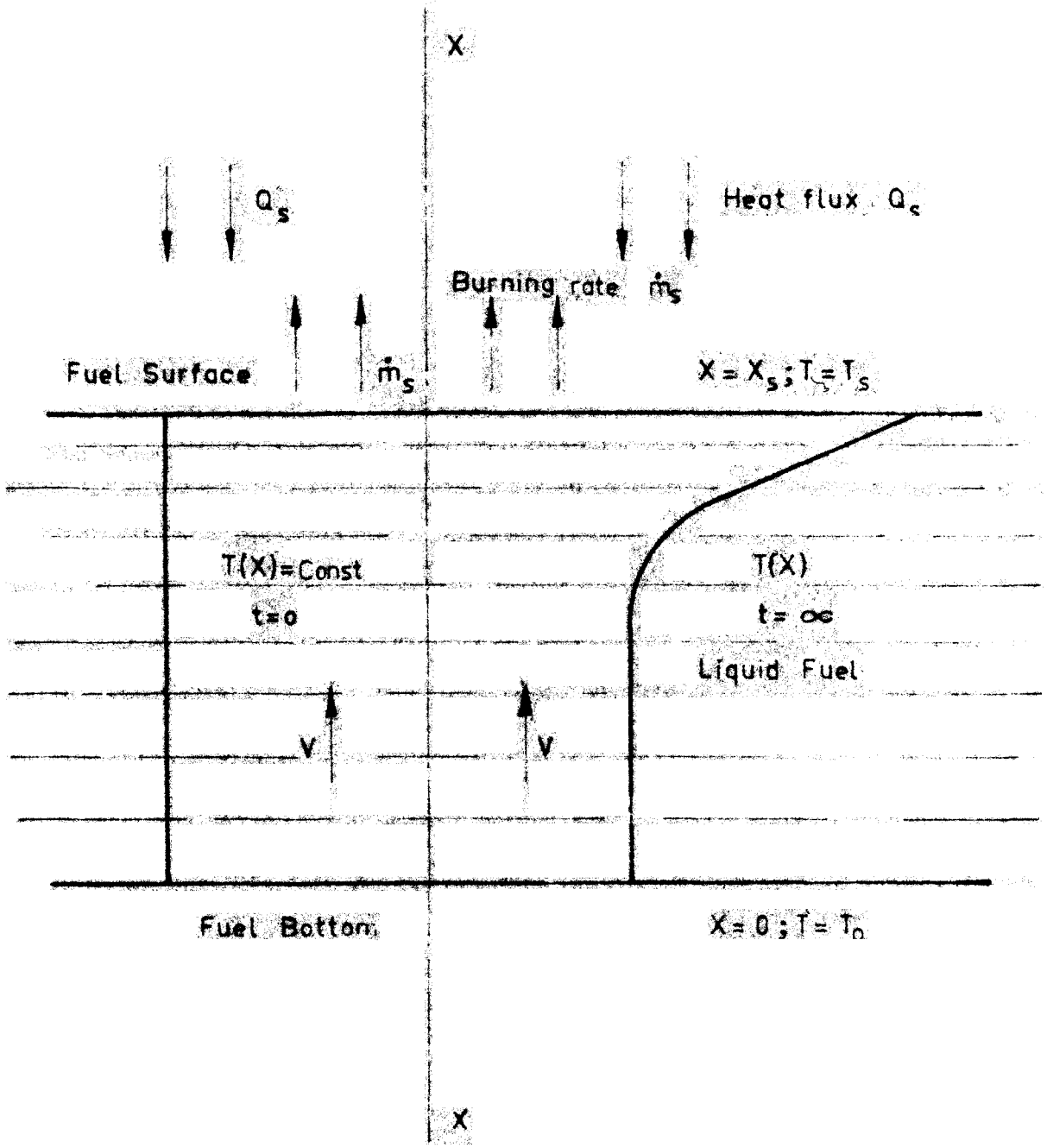

FIG. 2

$\chi_s = 5.0$

$\chi_l = 0.7$

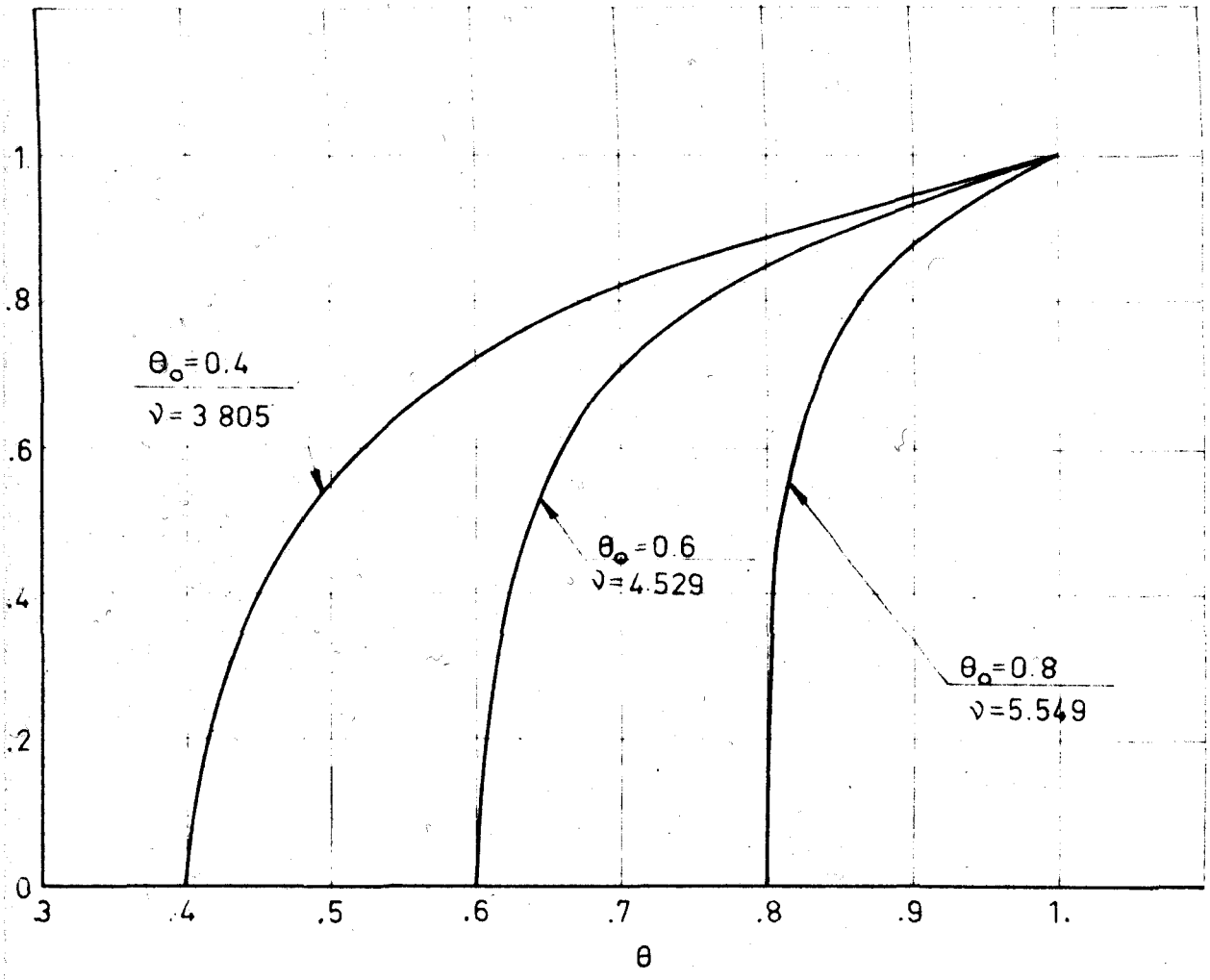


STATIONARY COMBUSTION

DIMENSIONLESS TEMPERATURE PROFILES

FIG. 3

$\chi_s = 1.5$

$\chi_l = 0.7$

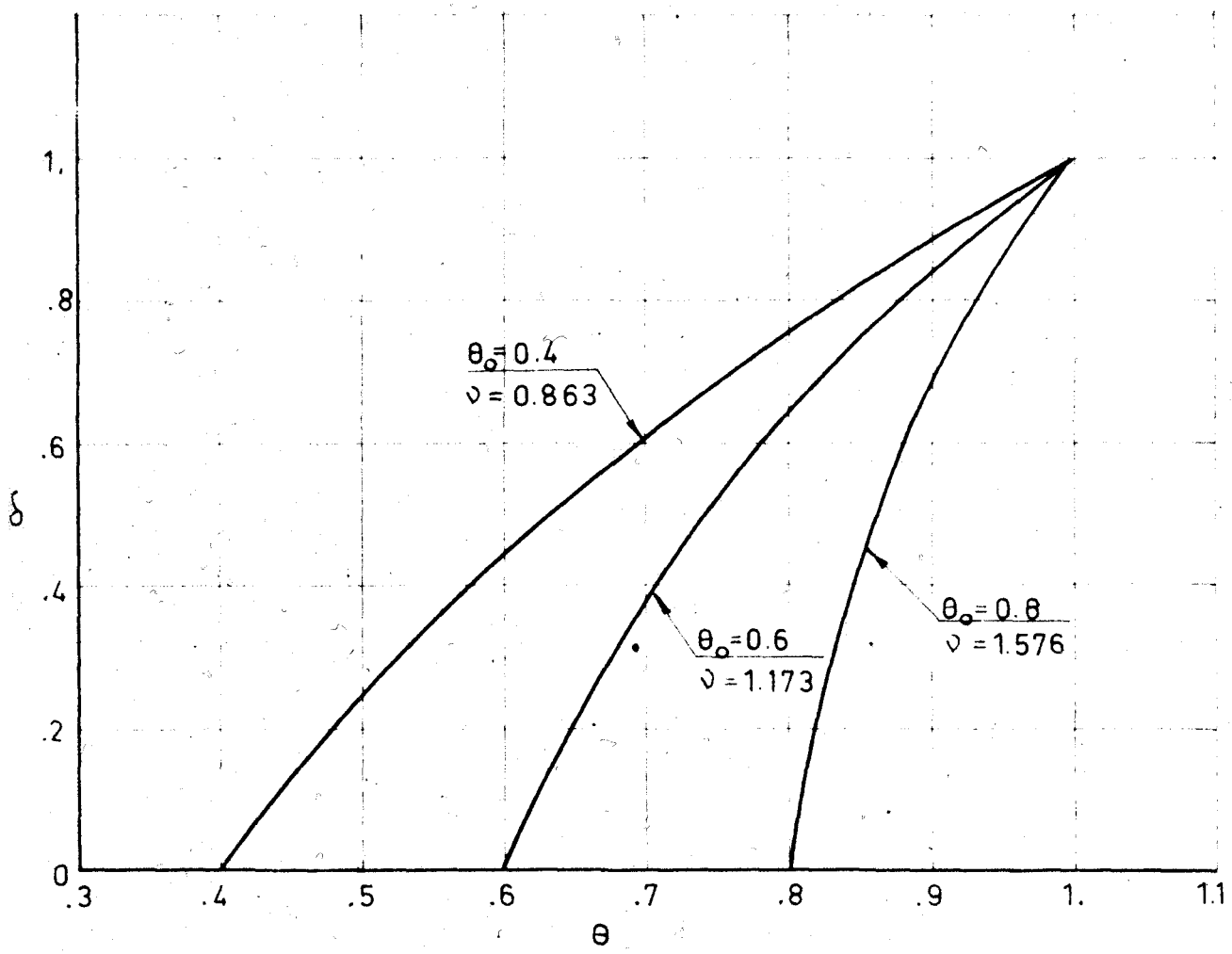


STATIONARY COMBUSTION

DIMENSIONLESS TEMPERATURE PROFILES

FIG 4

$\chi_s = 0.5$

$\chi_l = 0.7$

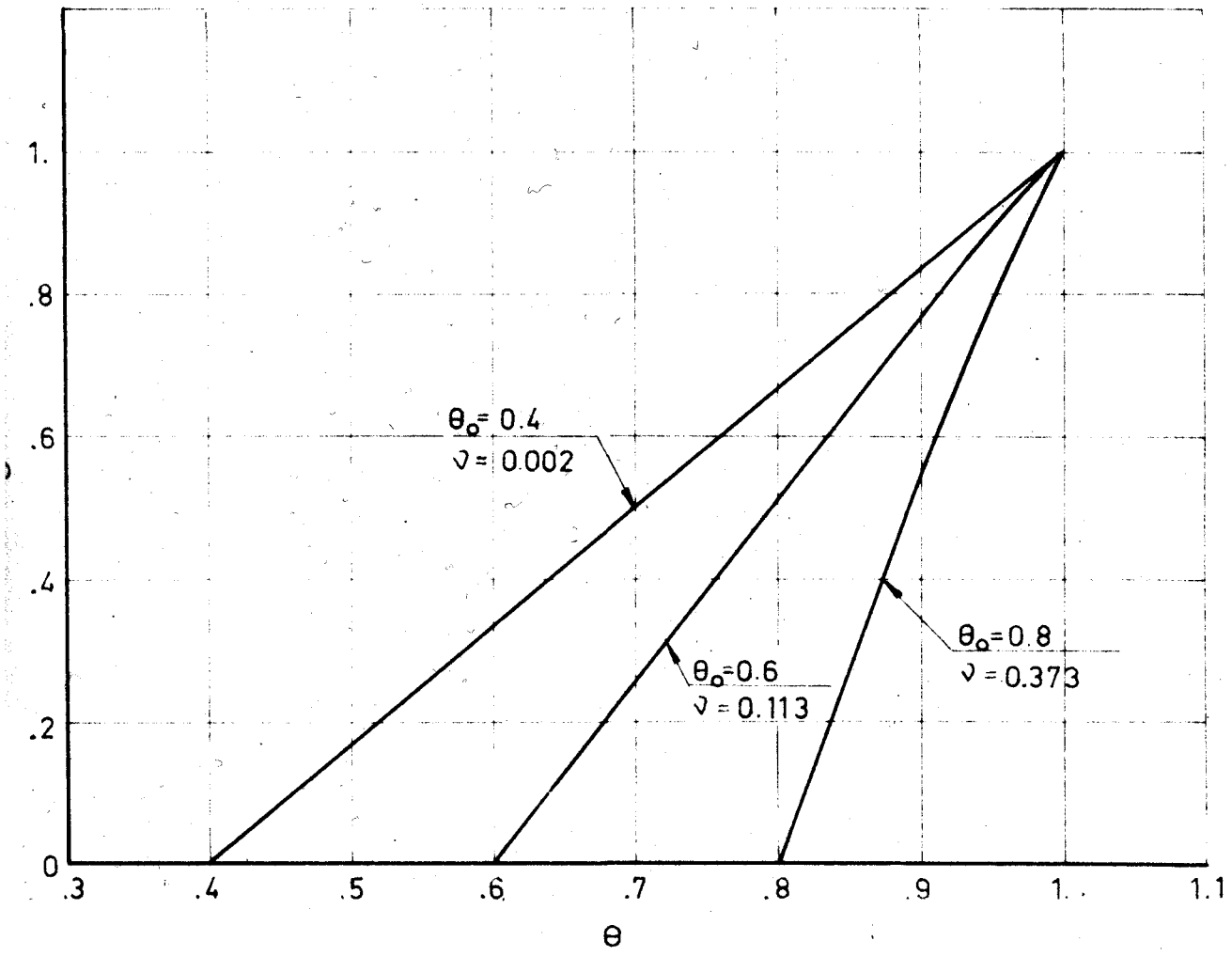


STATIONARY COMBUSTION

DIMENSIONLESS TEMPERATURE PROFILES

FIG. 5

$\chi_s = 5.0$

$\chi_l = 0.3$

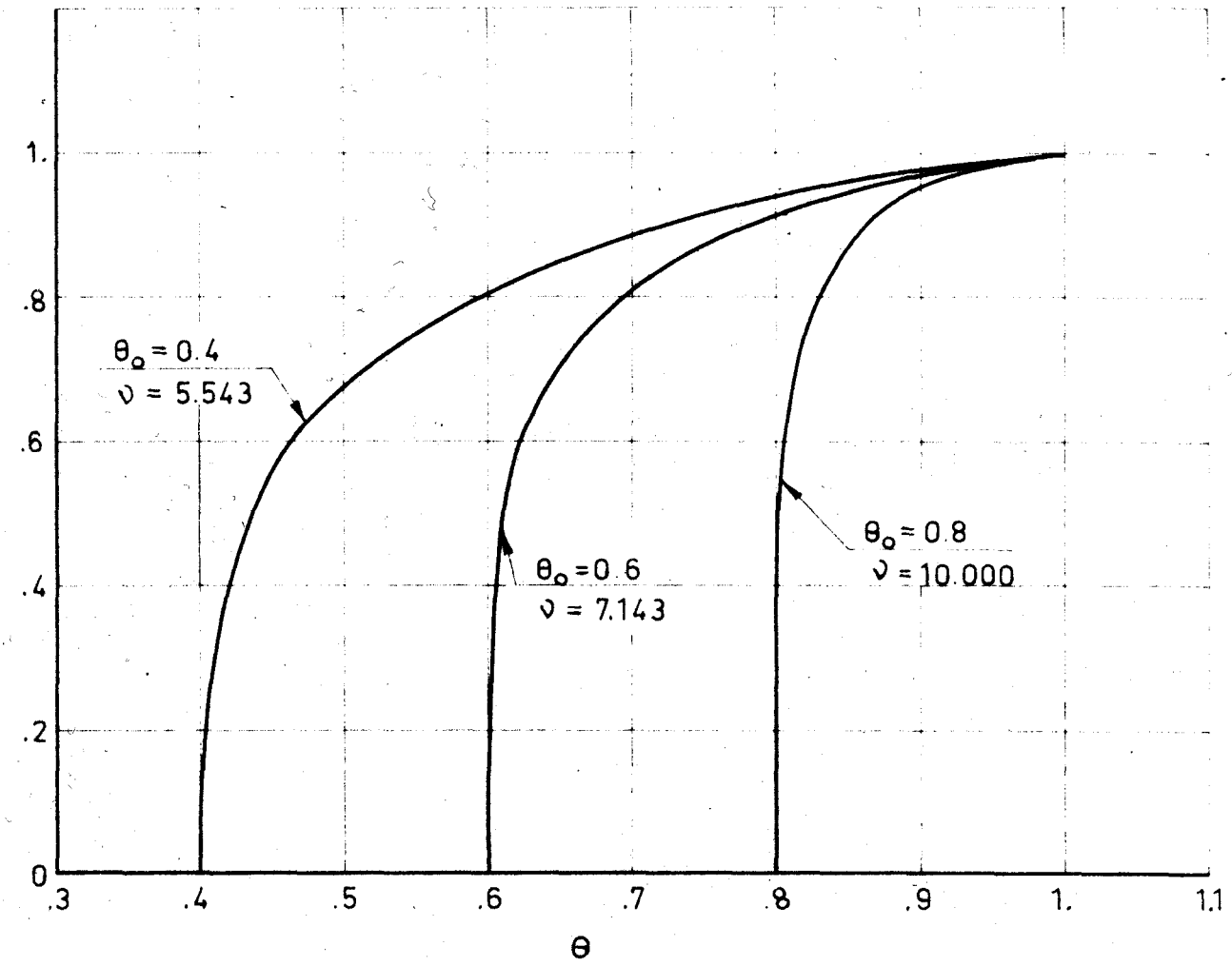


STATIONARY COMBUSTION

DIMENSIONLESS TEMPERATURE PROFILES

FIG. 6

$\chi_s = 1.5$

$\chi_l = 0.3$

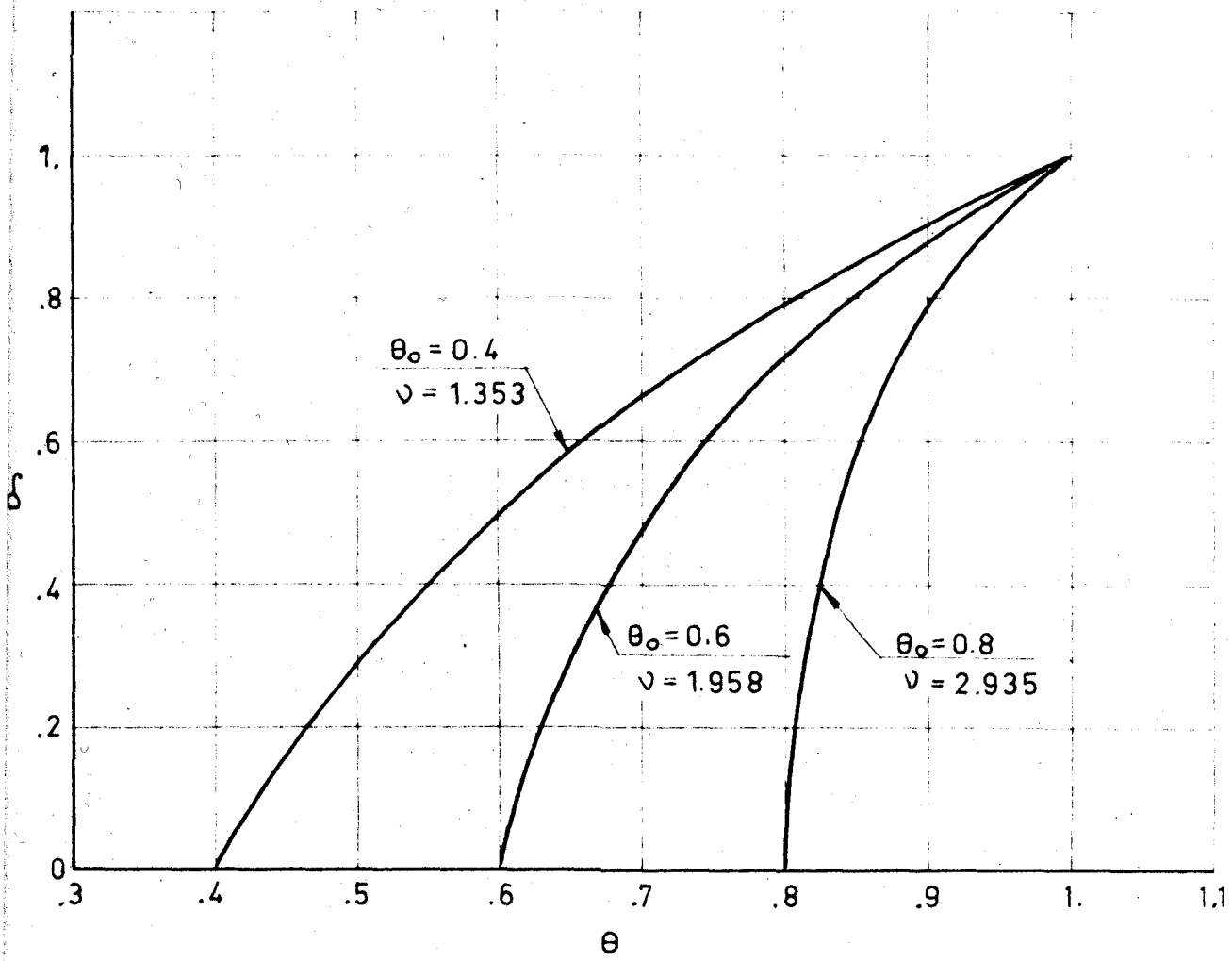


STATIONARY COMBUSTION

DIMENSIONLESS TEMPERATURE PROFILES

FIG. 7

$\chi_s = 0.5$

$\chi_l = 0.3$

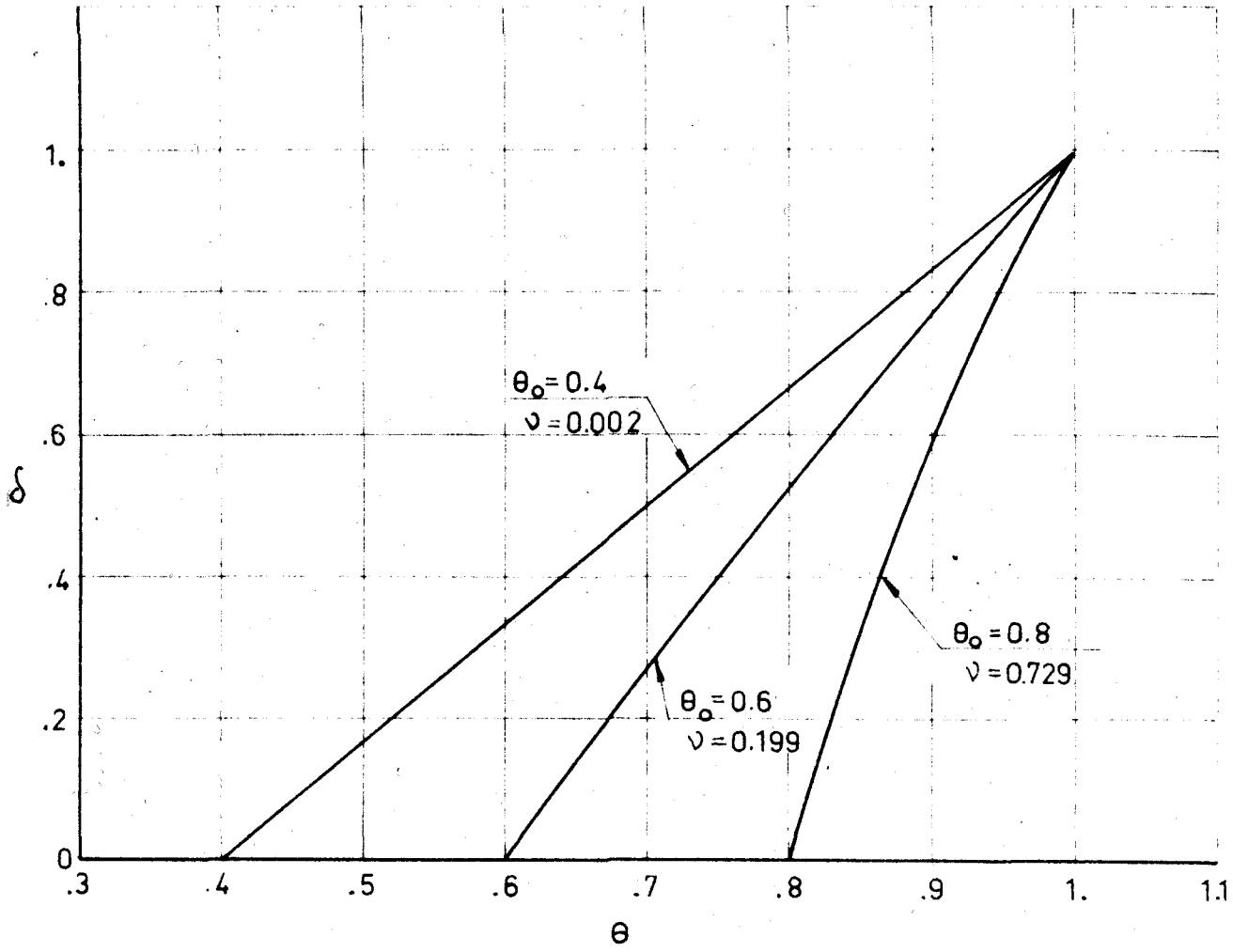


STATIONARY COMBUSTION

DIMENSIONLESS TEMPERATURE PROFILES

FIG. 8

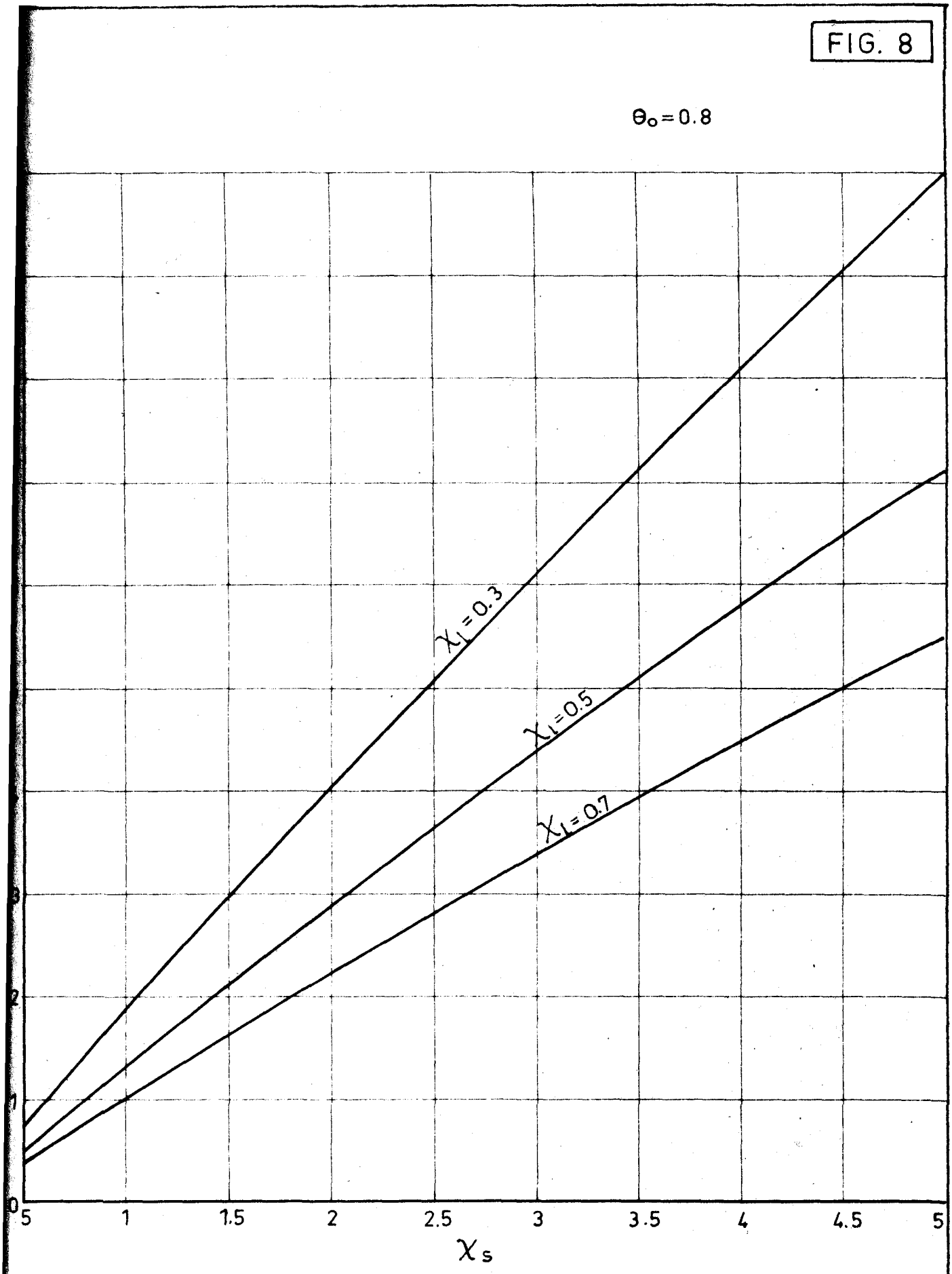


STATIONARY COMBUSTION

DIMENSIONLESS BURNING RATES

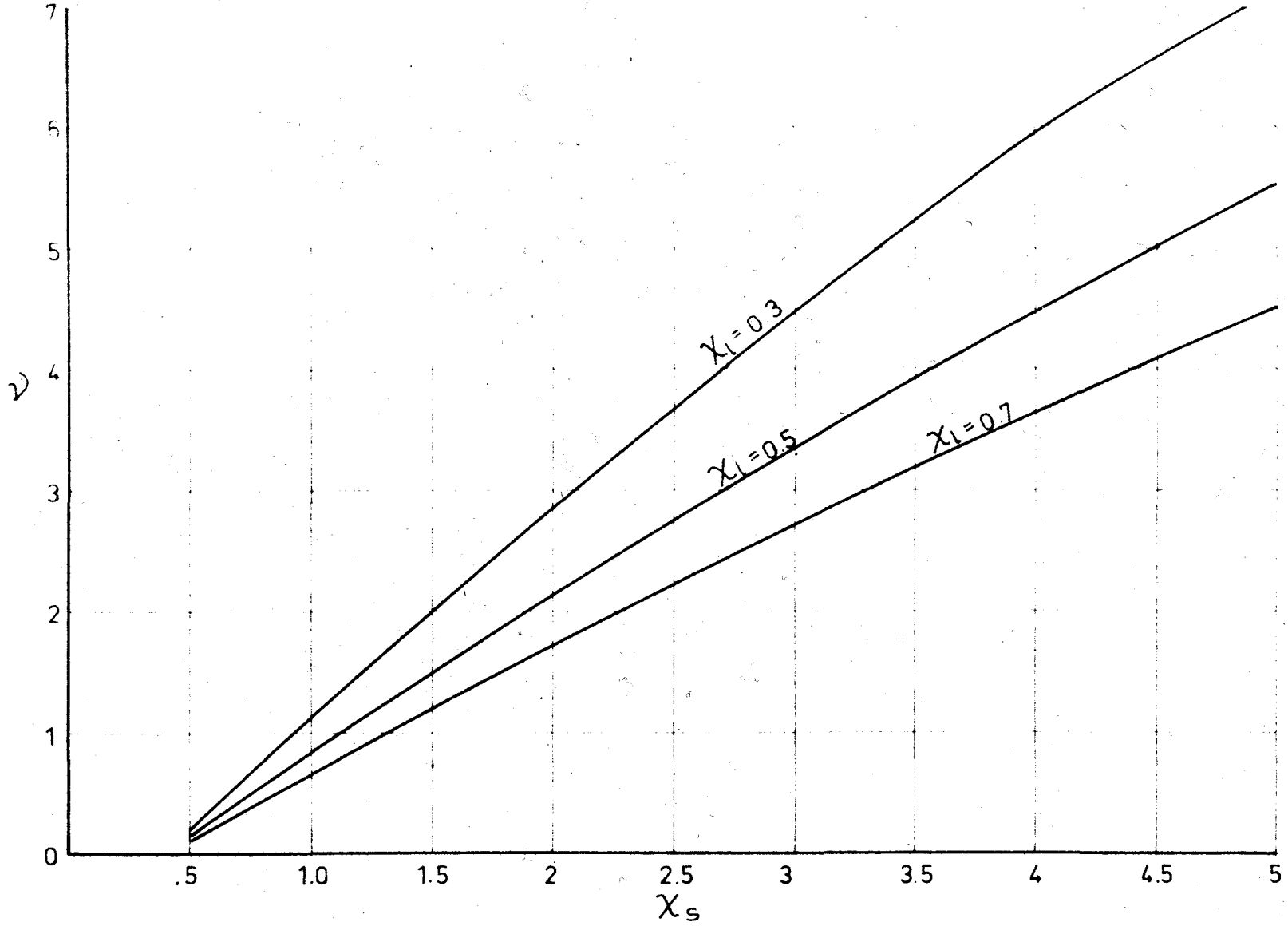


STATIONARY COMBUSTION

DIMENSIONLESS BURNING RATES

FIG. 6

$\theta_o = 0.4$

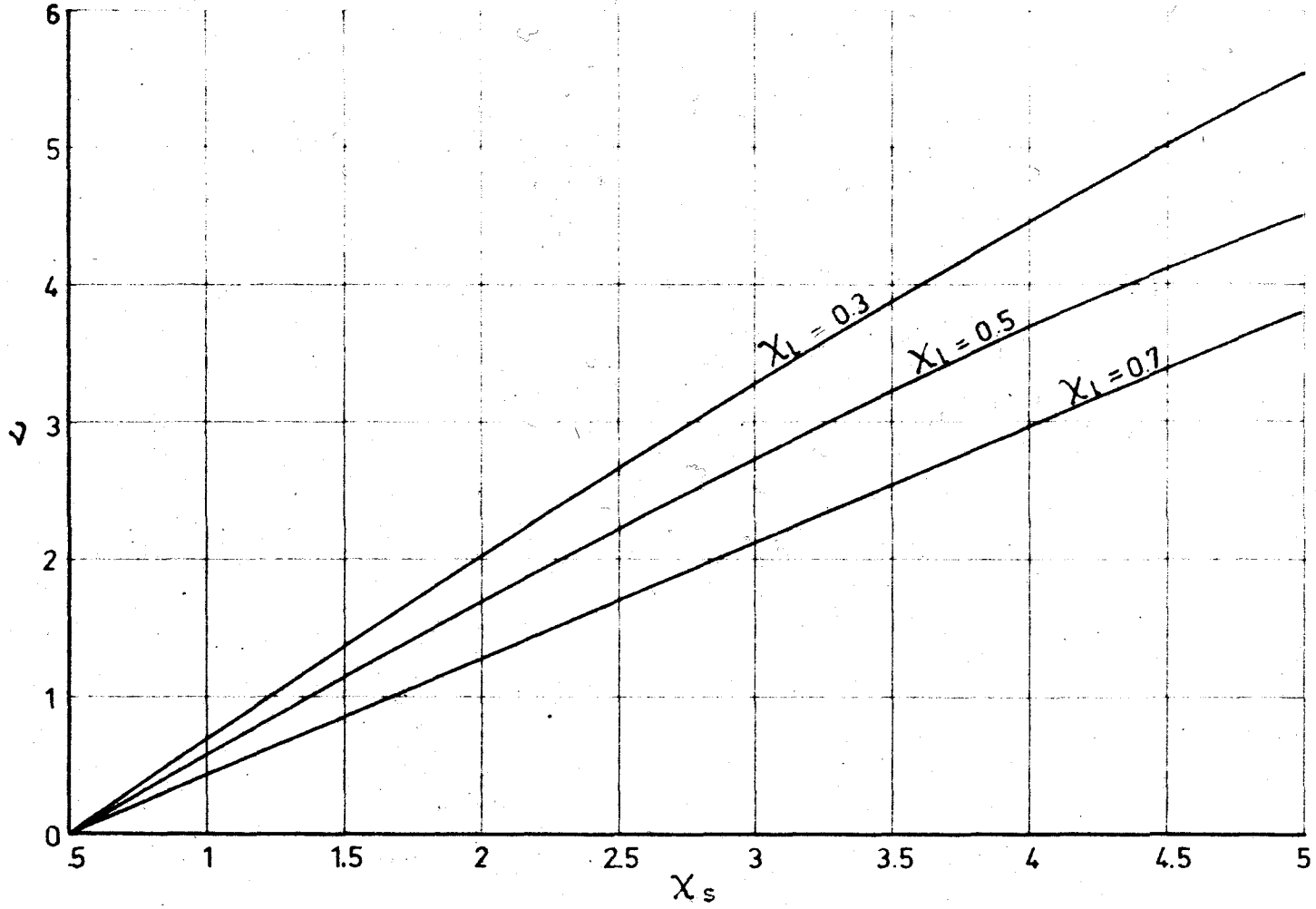


STATIONARY COMBUSTION

DIMENSIONLESS BURNING RATES

FIG. 10

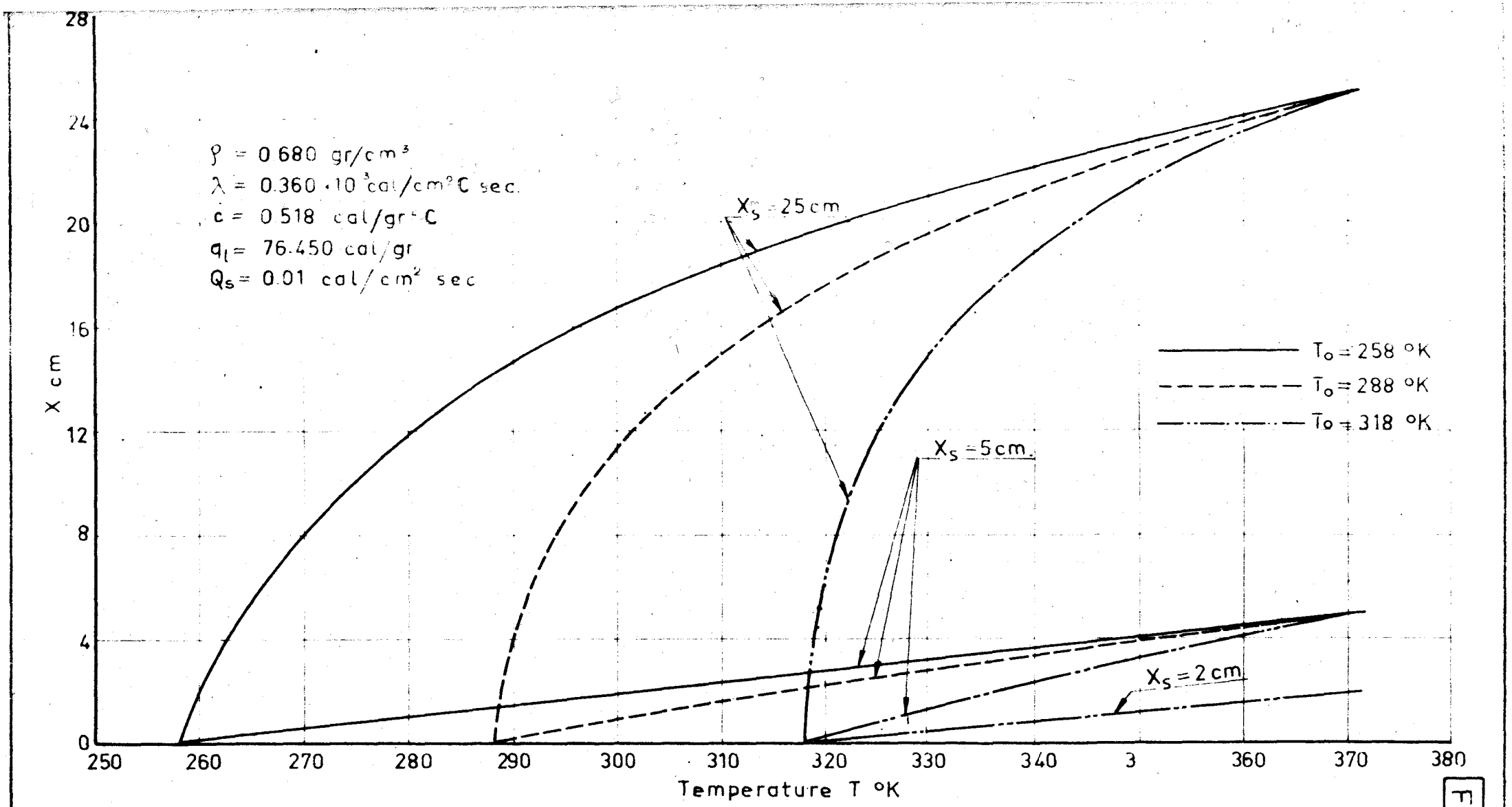


STATIONARY COMBUSTION

N-HEPTANE

TEMPERATURE PROFILES

FIG. 11

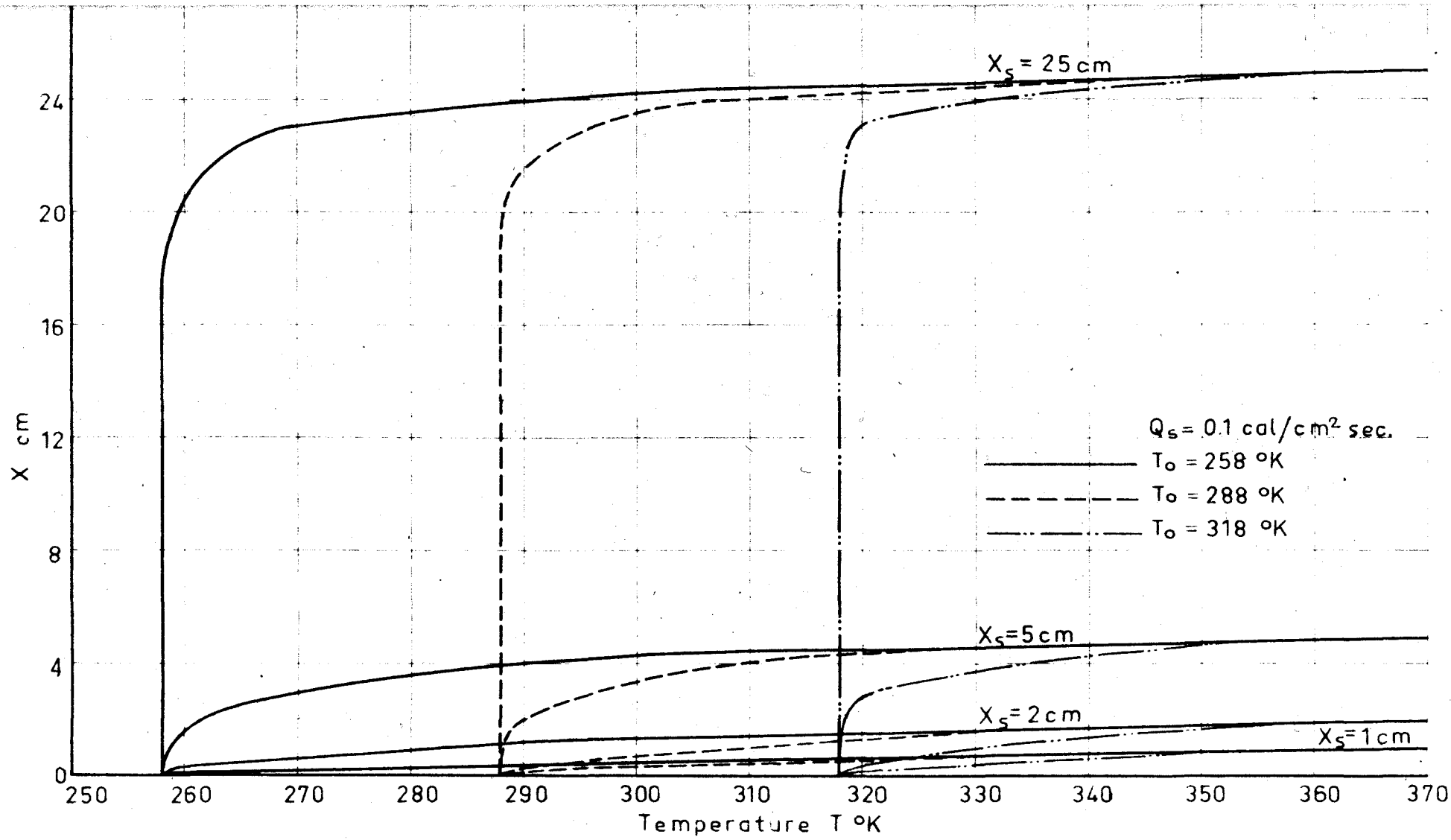


STATIONARY COMBUSTION

N-HEPTANE

TEMPERATURE PROFILES

FIG. 12

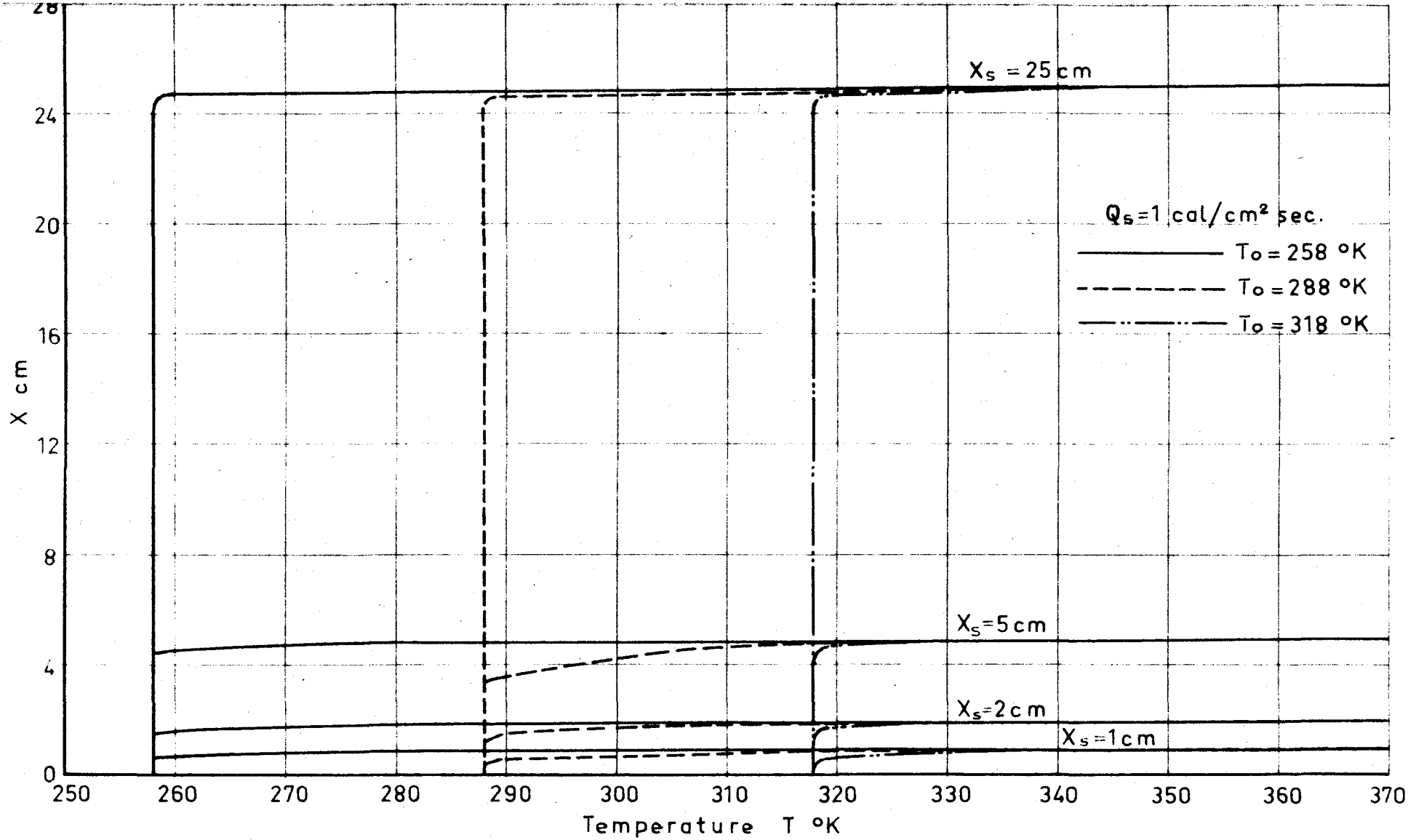


STATIONARY COMBUSTION

N-HEPTANE

TEMPERATURE PROFILES

FIG. 13

FIG. 14

$\rho = 0.680\ gr/cm^3$

$\lambda = 0.360 \times 10^{-3}\ cal/cm\,°C\ sec.$

$c = 0.518\ cal/gr\,°C$

$q_e = 76.450\ cal/gr$

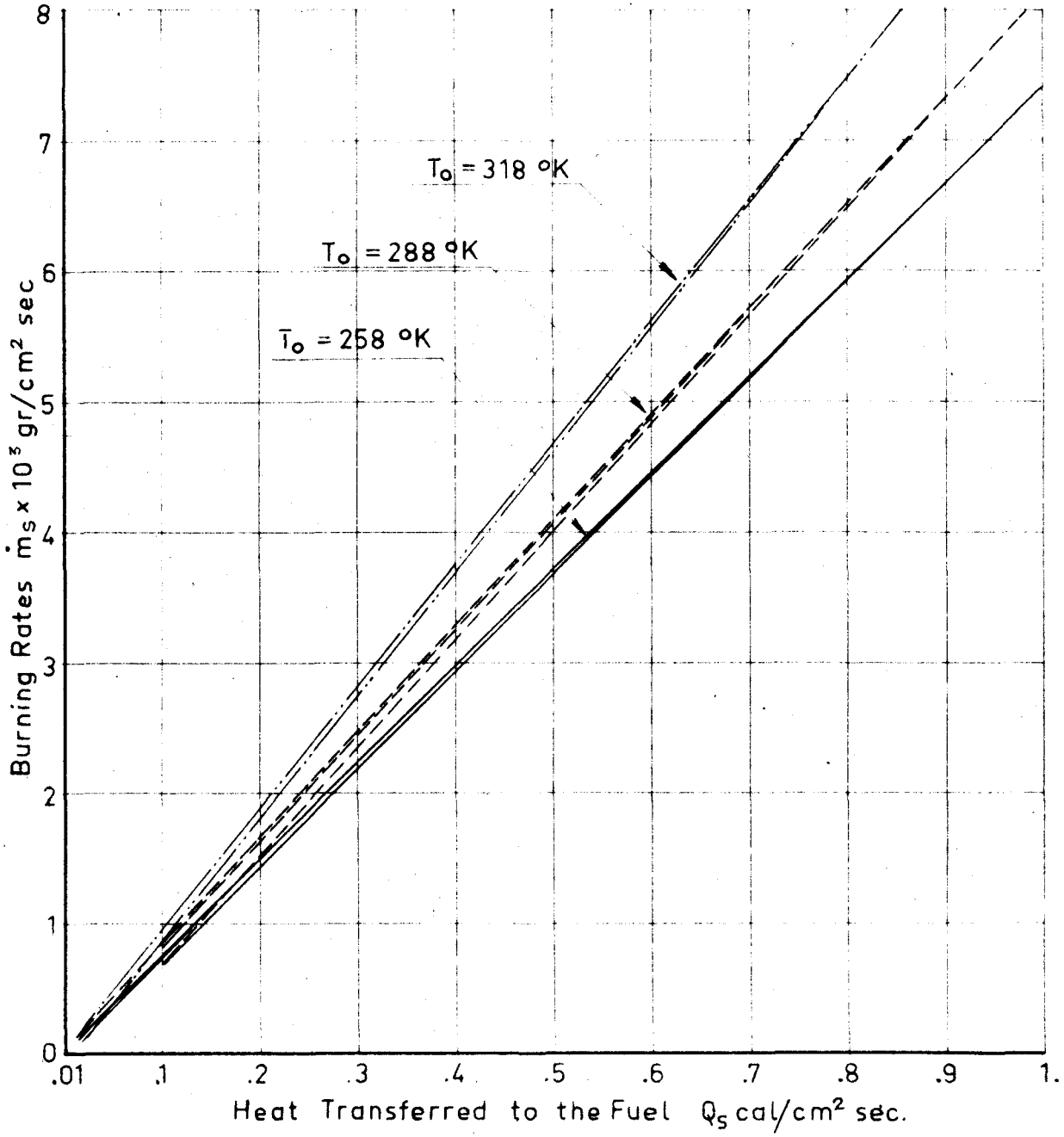


STATIONARY COMBUSTION

N-HEPTANE

BURNING RATES

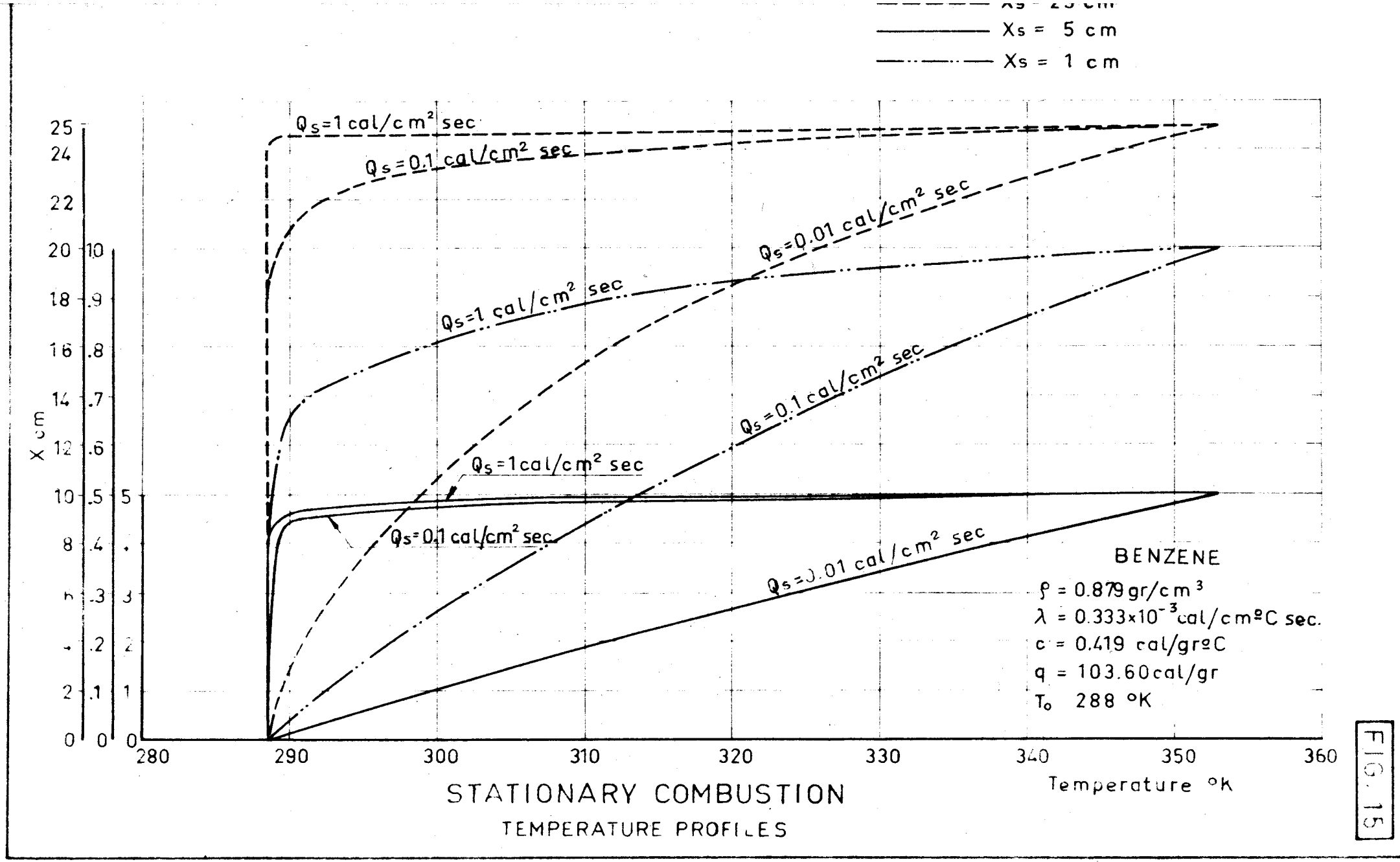


STATIONARY COMBUSTION

TEMPERATURE PROFILES

FIG. 15

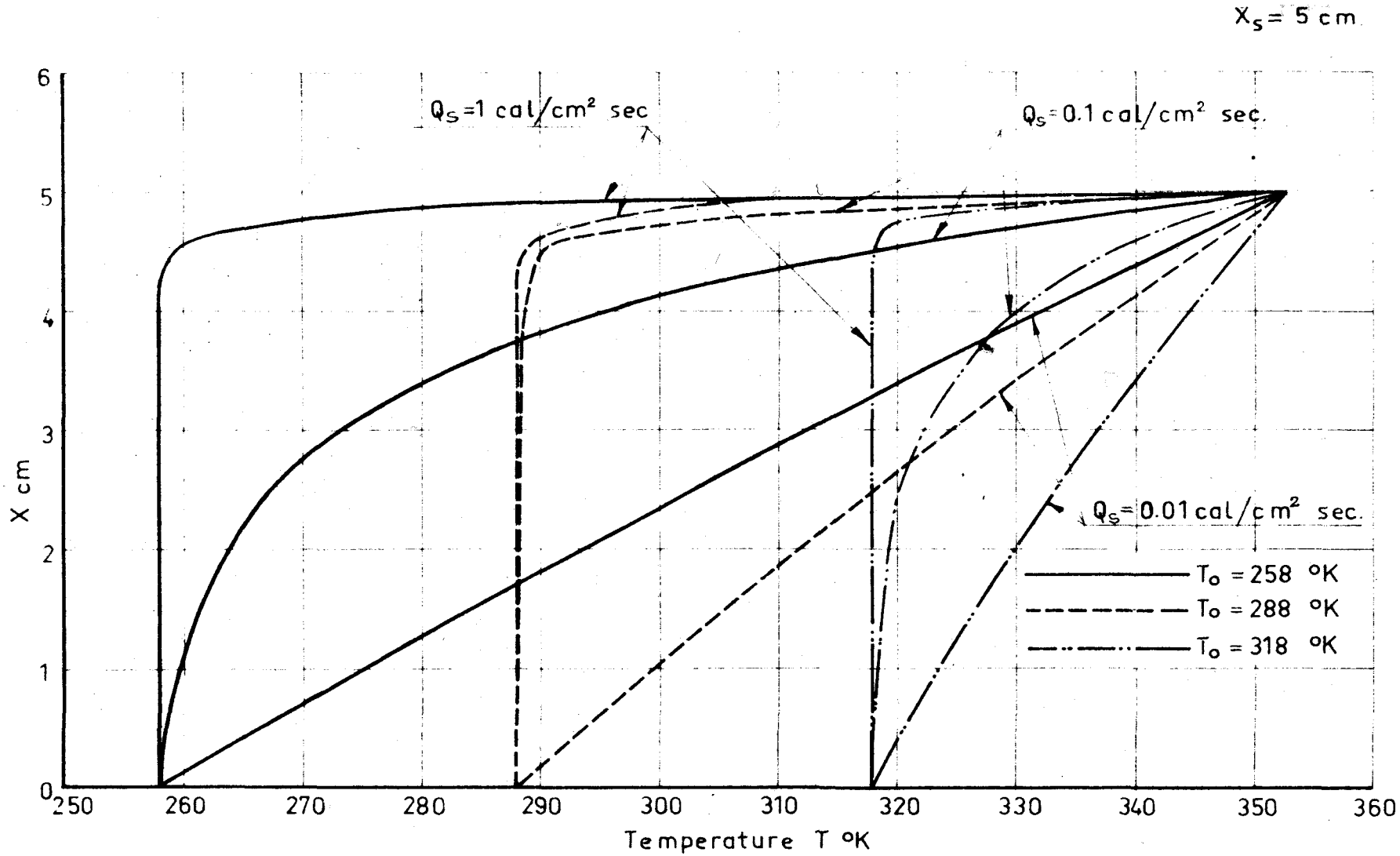


STATIONARY COMBUSTION

BENZENE

TEMPERATURE PROFILES

FIG. 16

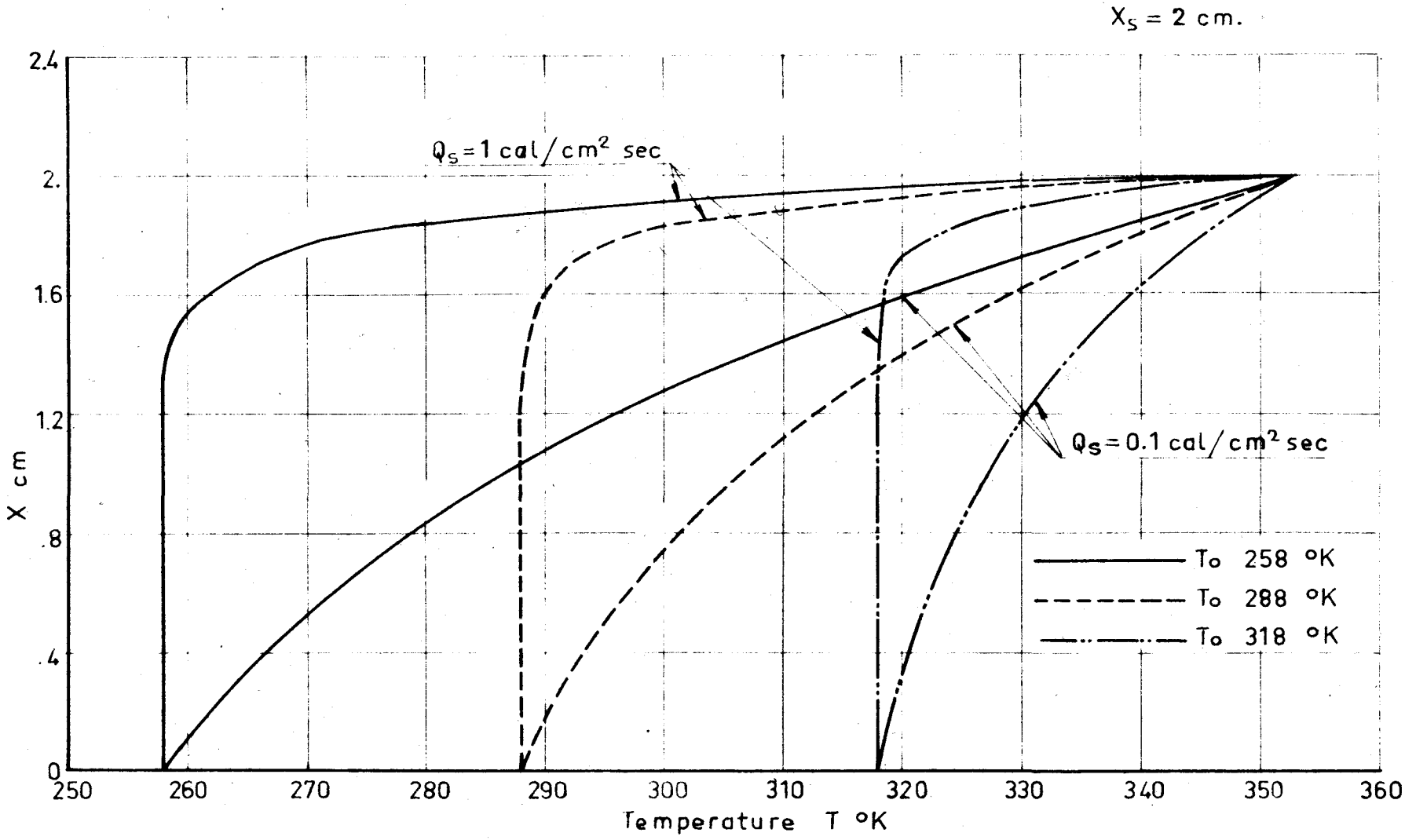


STATIONARY COMBUSTION

BENZENE

TEMPERATURE PROFILES

FIG. 17

FIG. 18

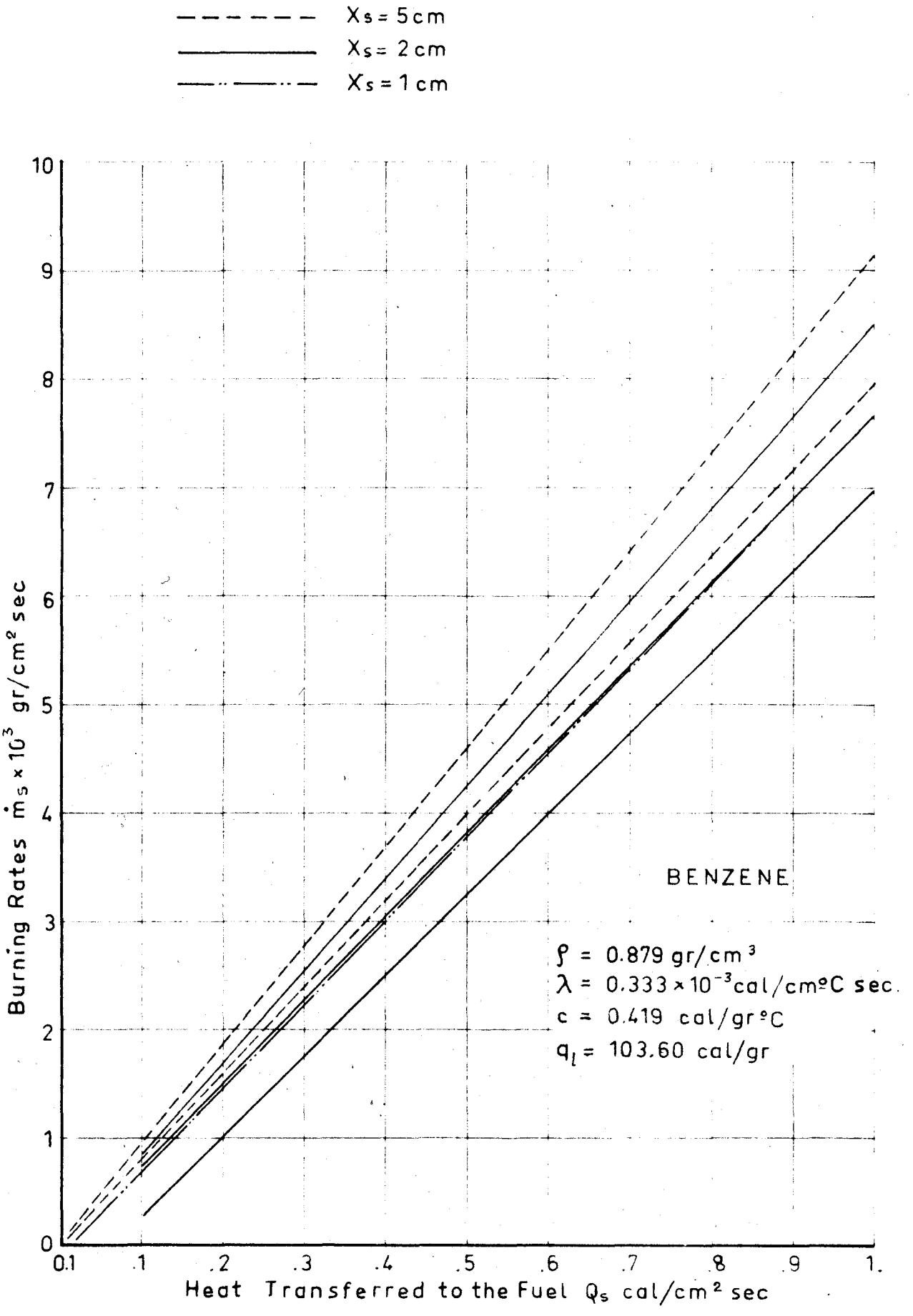


STATIONARY COMBUSTION

BURNING RATES

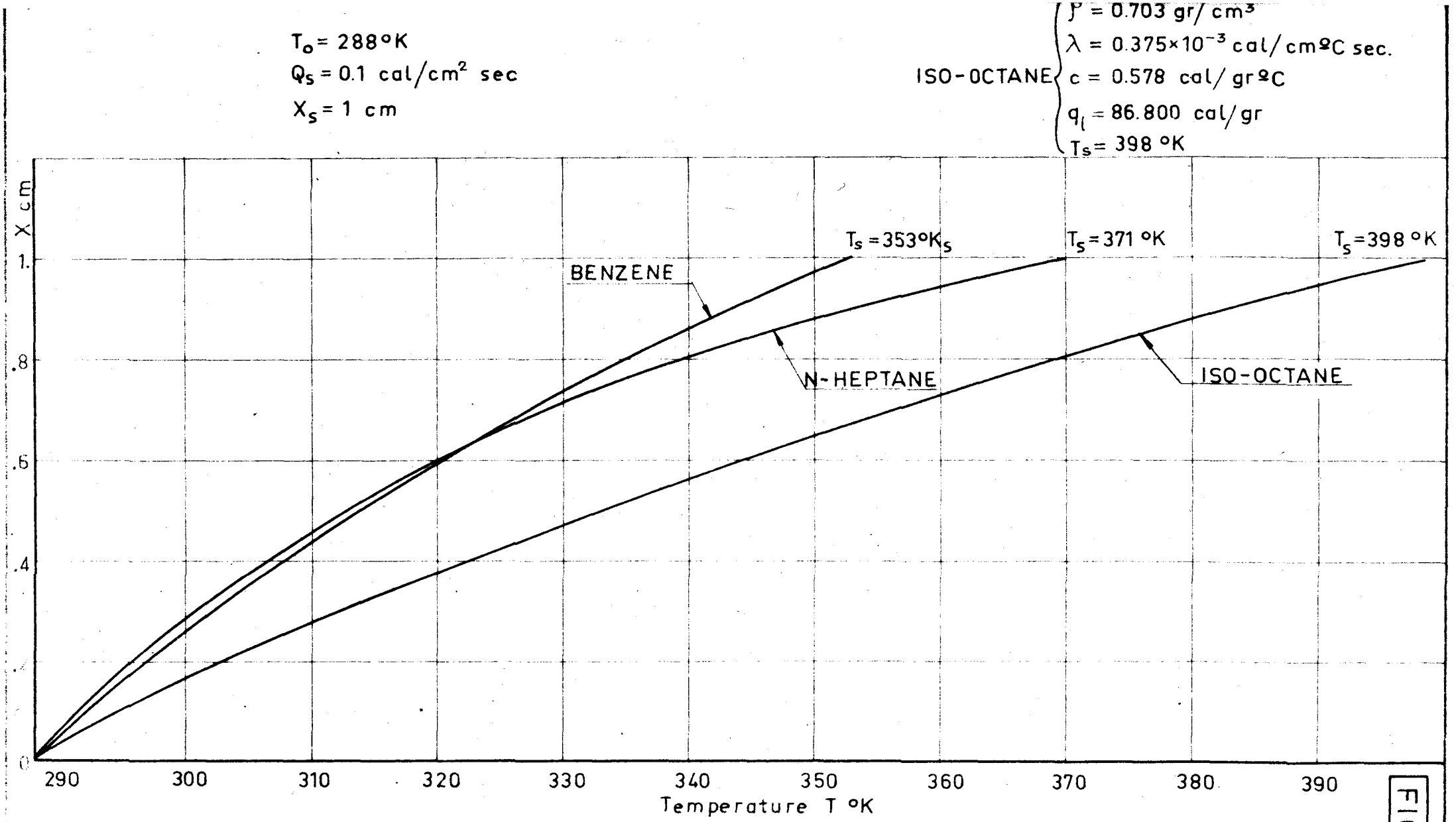


FIG. 19

STATIONARY COMBUSTION

TEMPERATURE PROFILES FOR SEVERAL FUELS

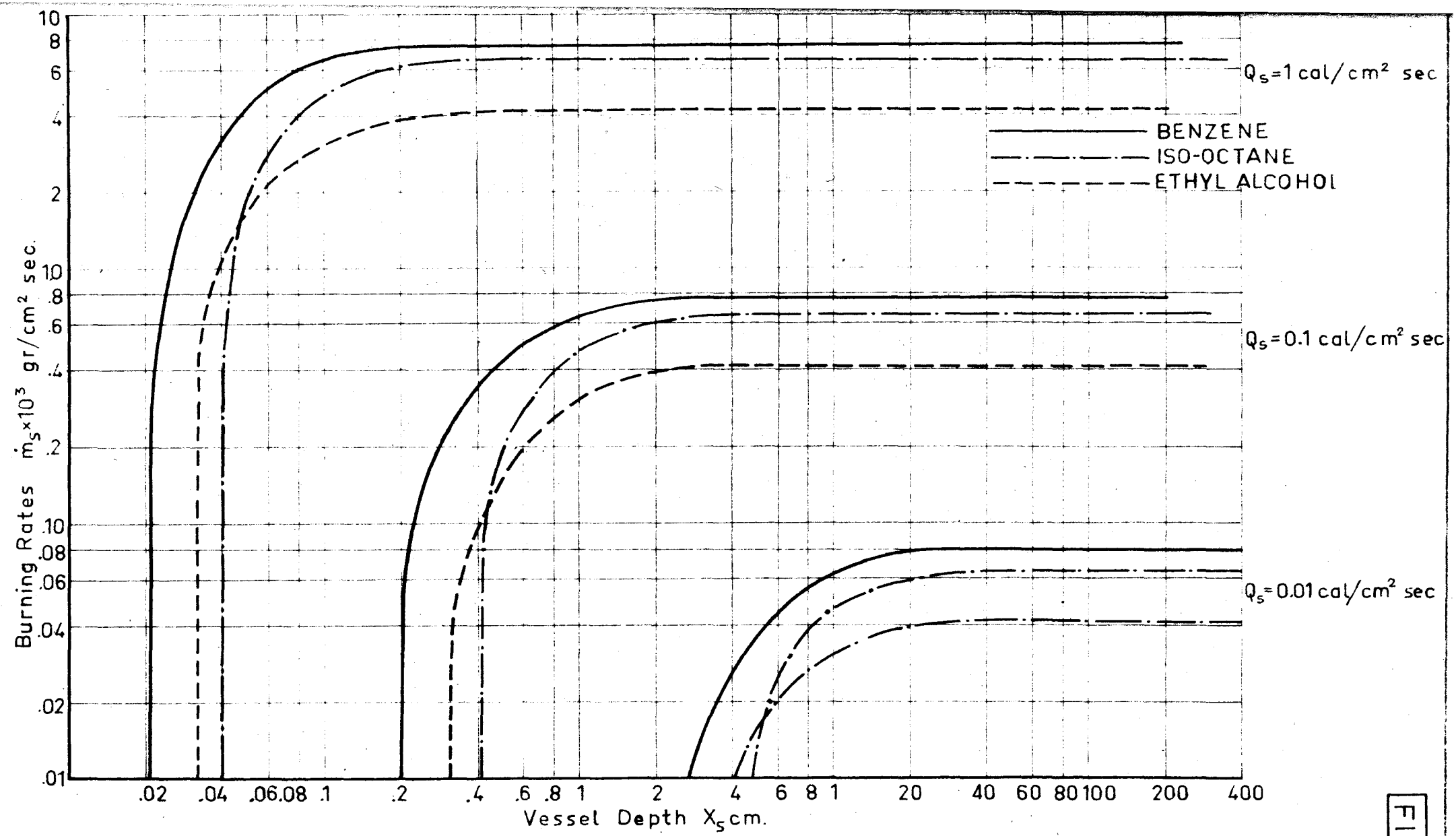


FIG. 20

# STATIONARY COMBUSTION

## BURNING RATES FOR SEVERAL FUELS

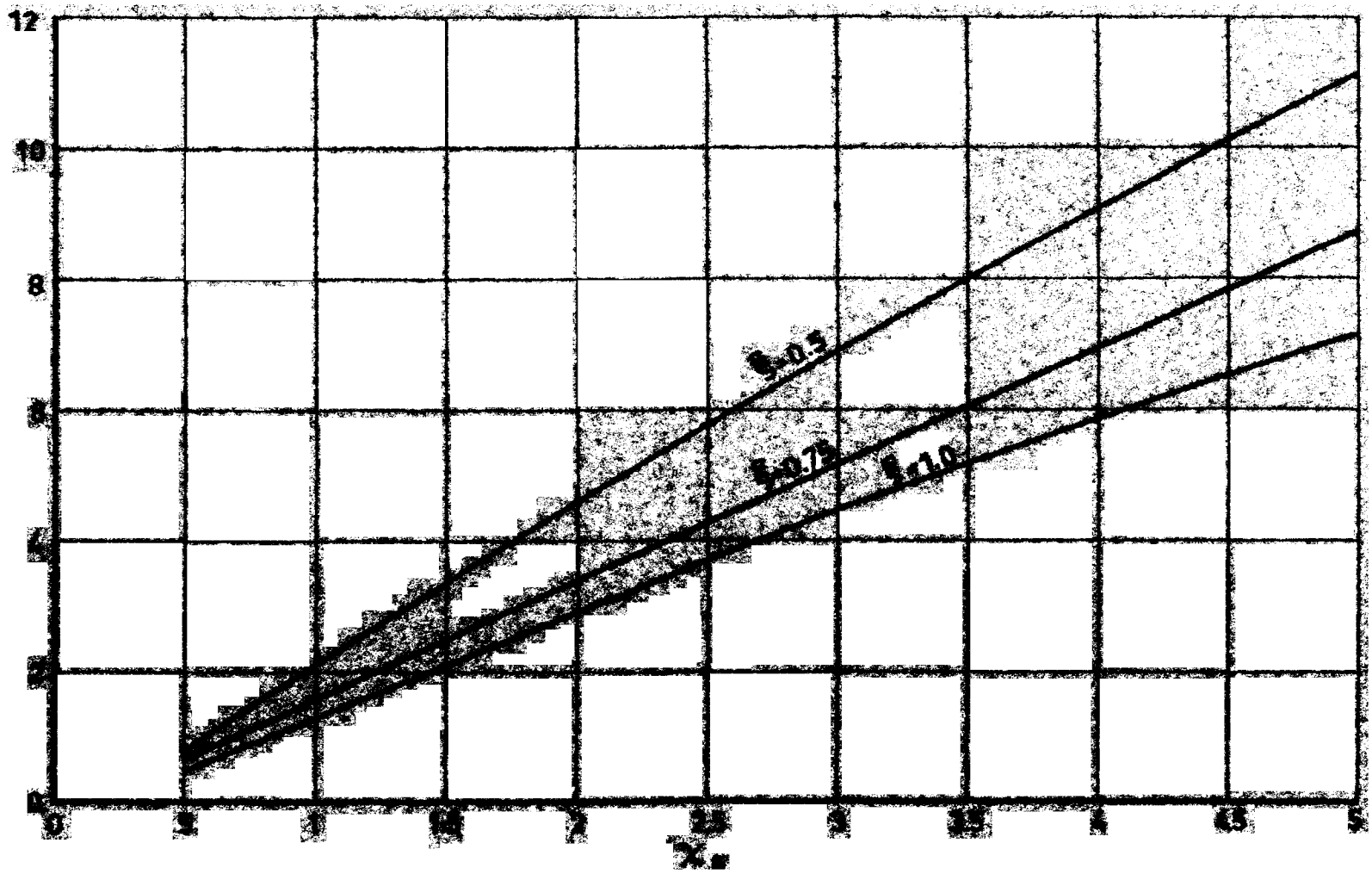


STATIONARY COMBUSTION

INFLUENCE OF THE OVERFLOW ON BURNING RATES

FIG. 21

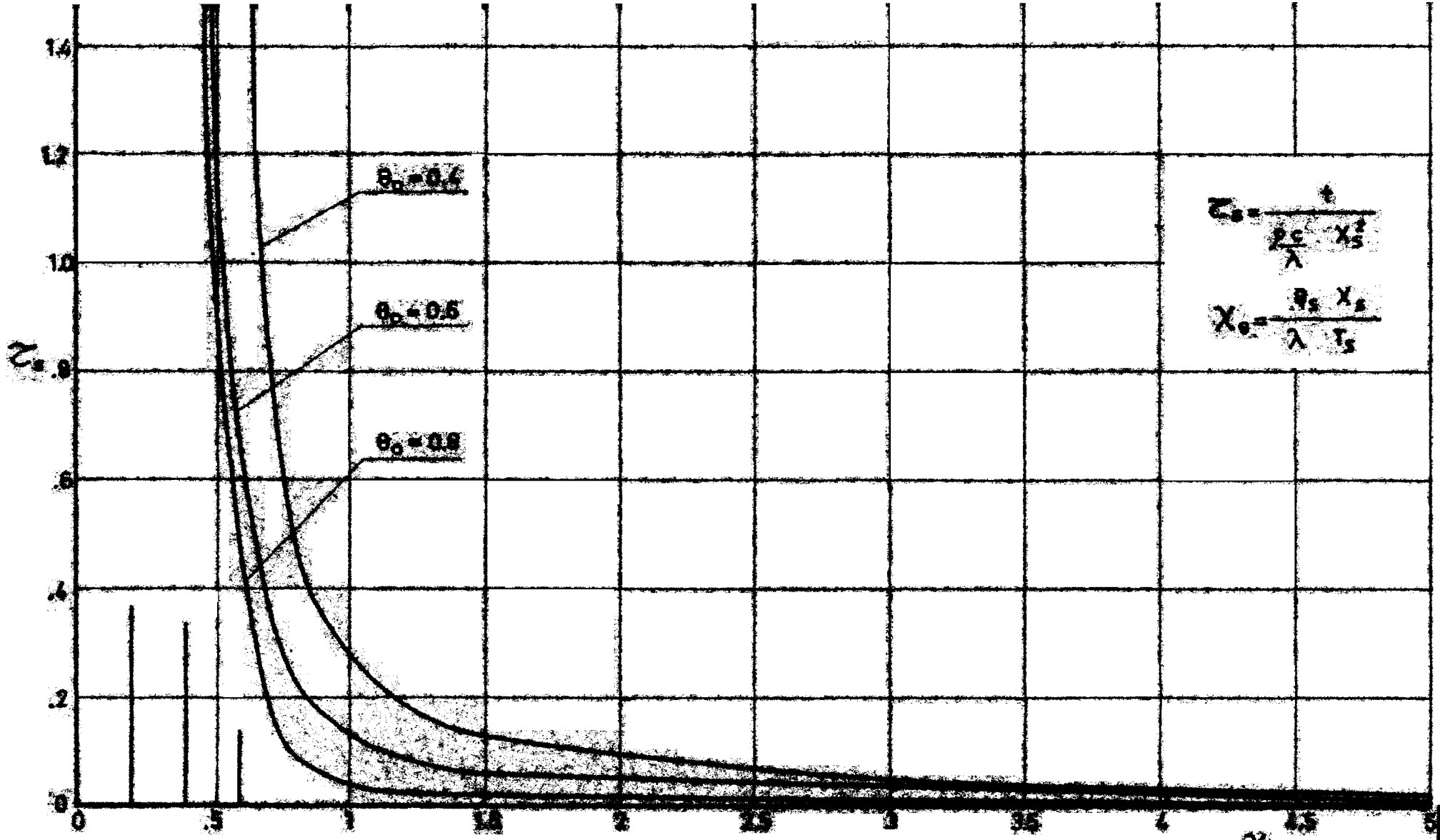


IGNITION AND HEATING

DIMENSIONLESS TIME REQUIRED TO REACH BOILING TEMPERATURE

FIG. 22

# IGNITION AND HEATING

FIG. 23

## TIME REQUIRED TO REACH BOILING TEMPERATURE

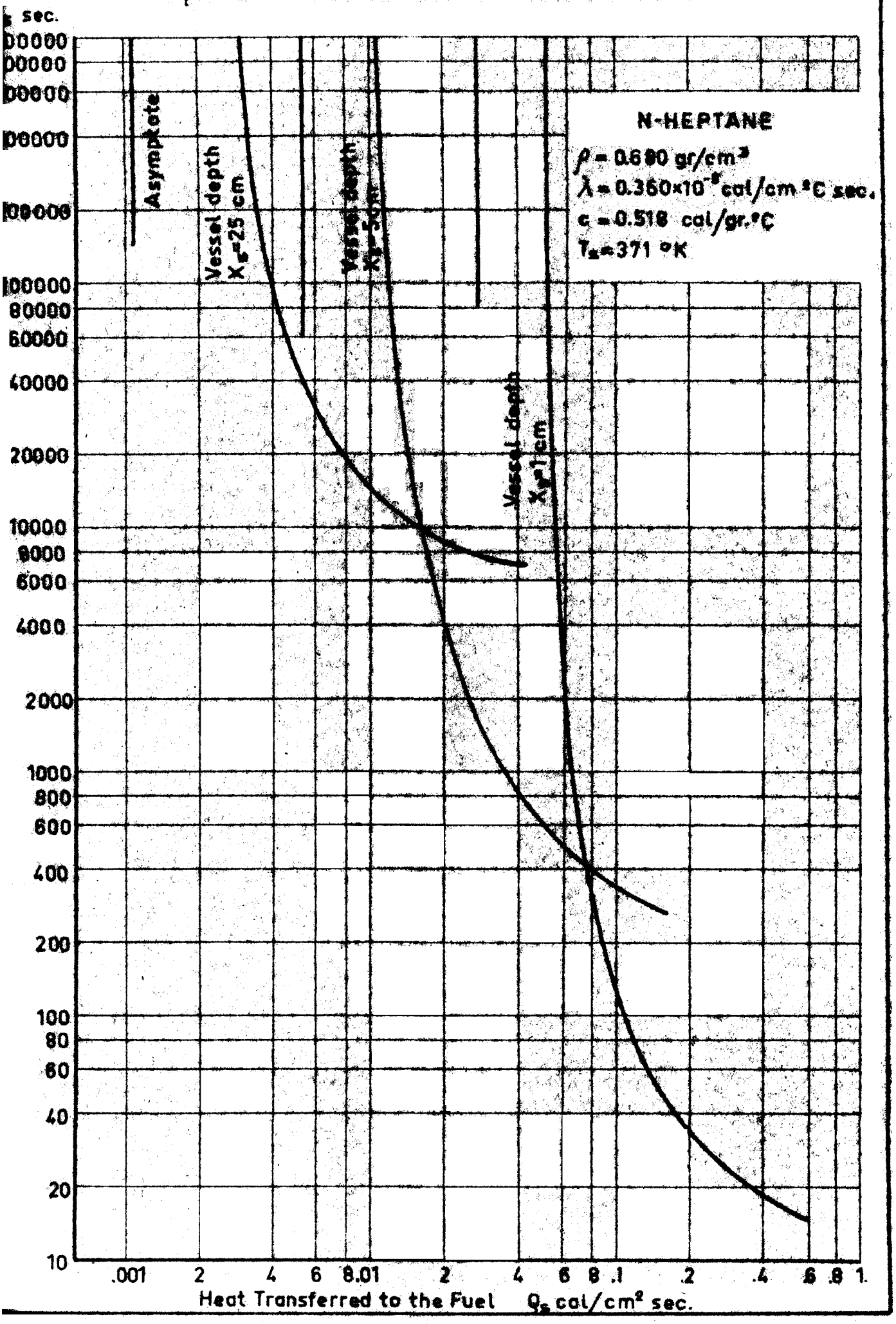

FIG. 24

$\theta_0 = 0.776$
$X_s = 3.739$
$X_l = 0.398$

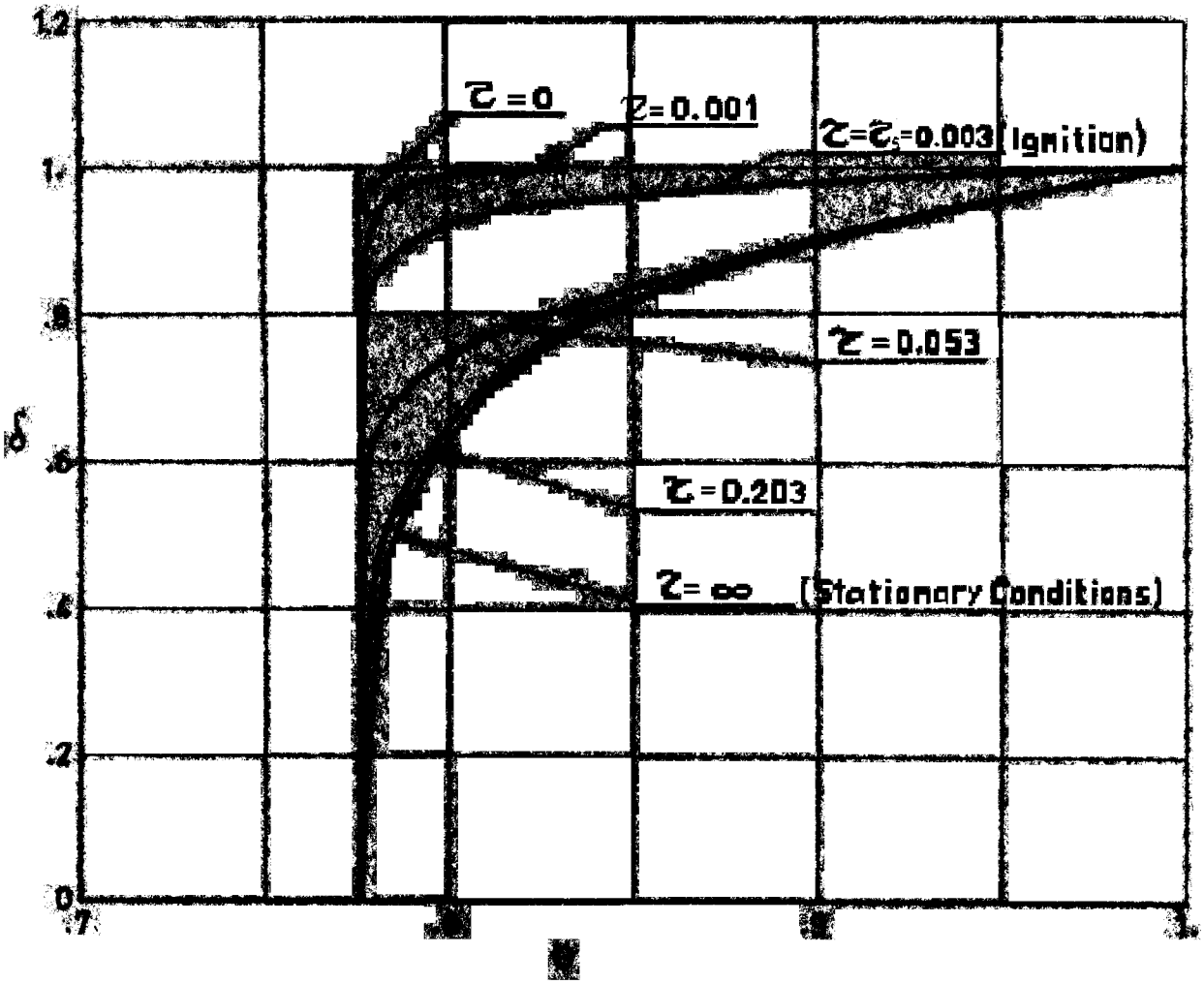


## TRANSIENT COMBUSTION

### DIMENSIONLESS TEMPERATURE PROFILES

FIG. 25

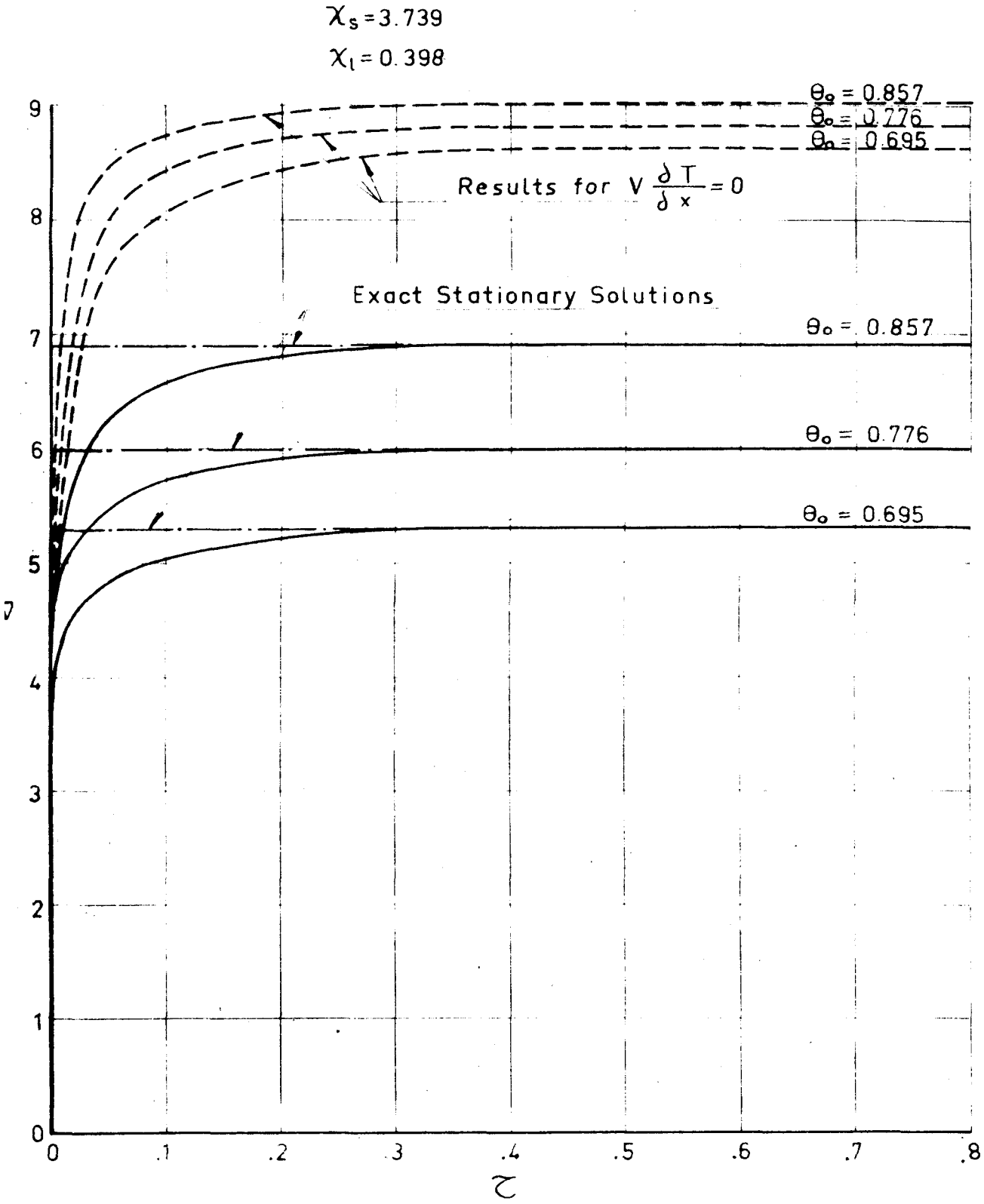


TRANSIENT COMBUSTION

DIMENSIONLESS BURNING RATES

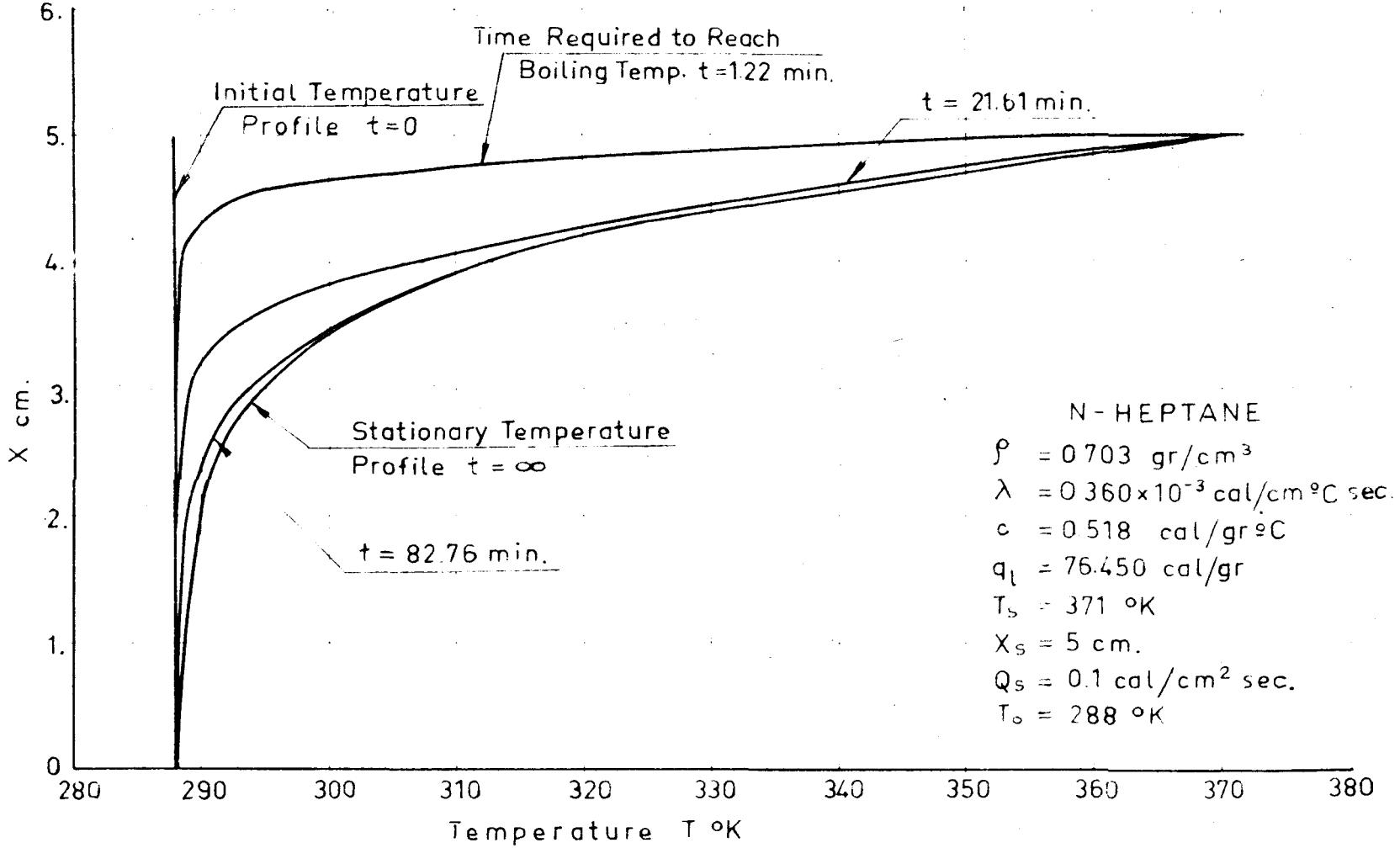


TRANSIENT COMBUSTION

TEMPERATURE PROFILES

FIG. 7

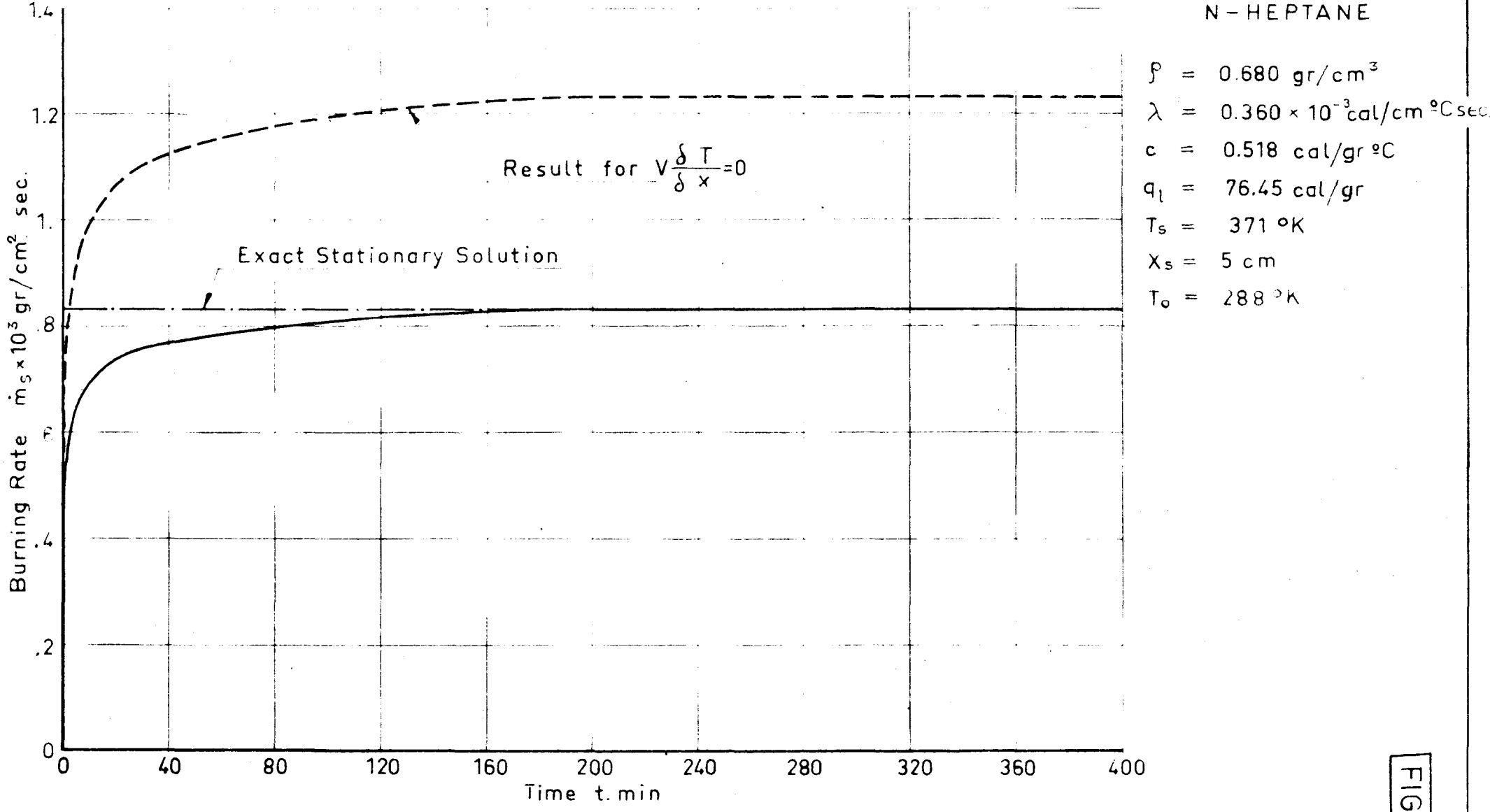


TRANSIENT COMBUSTION

BURNING RATES AS A FUNCTION OF TIME

FIG. 27

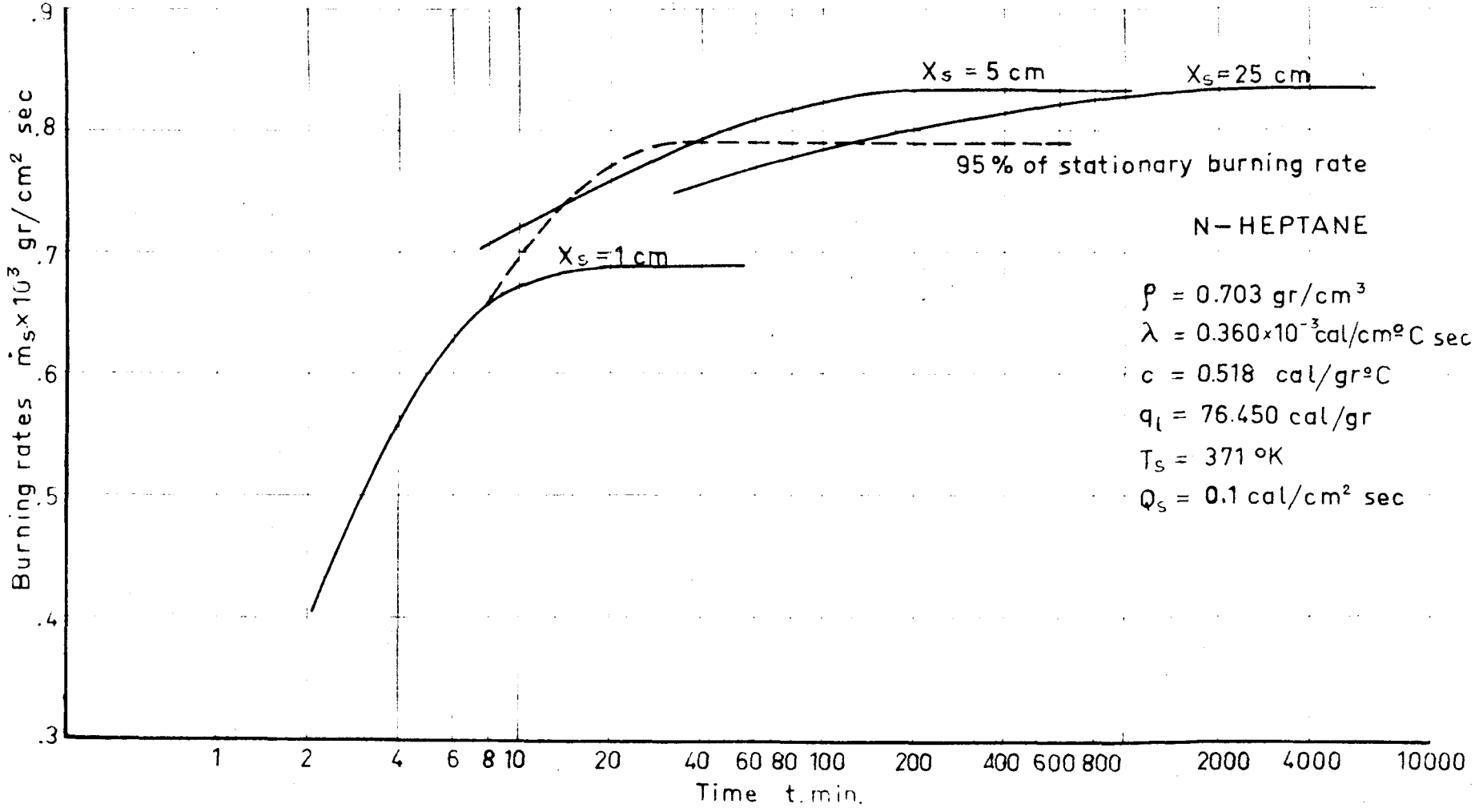


TRANSIENT COMBUSTION

BURNING RATES

FIG. 28

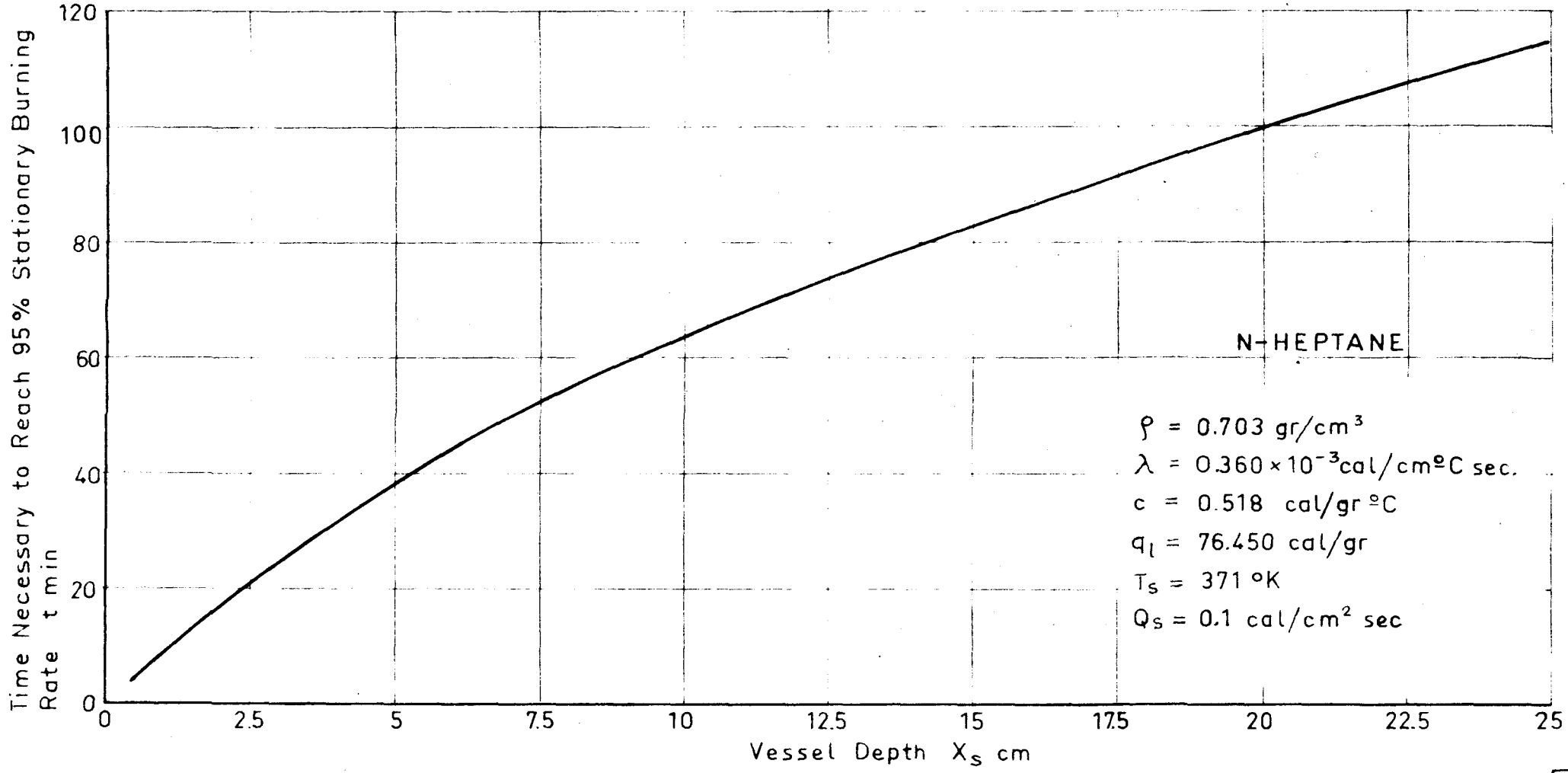


FIG. 29

TRANSIENT COMBUSTION

TIME NECESSARY TO REACH 95% STATIONARY BURNING RATE

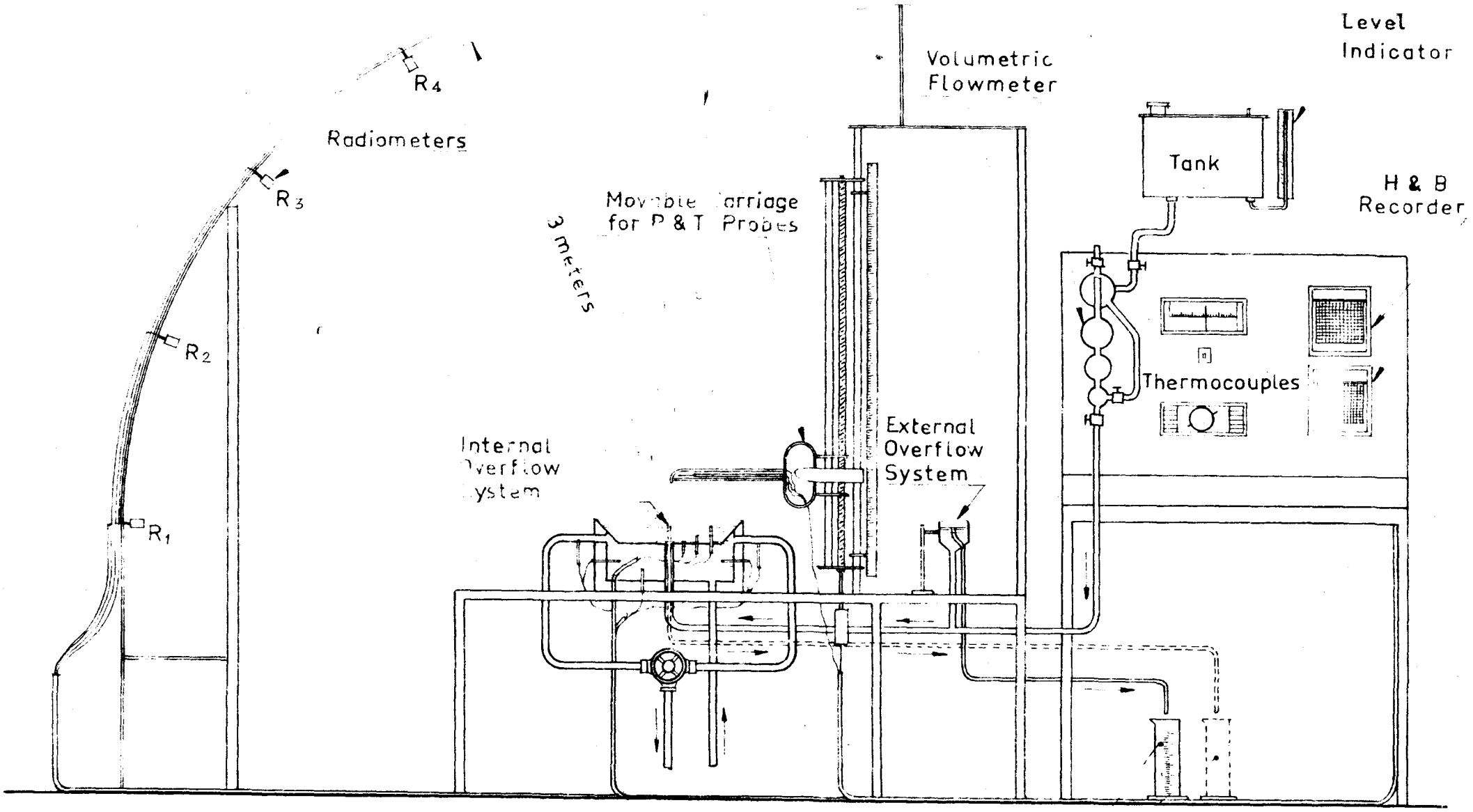


SCHEMATIC DIAGRAM OF RESEARCH FACILITIES FOR STUDYING OPEN FIRES.

Fig. 30

FIG. 31

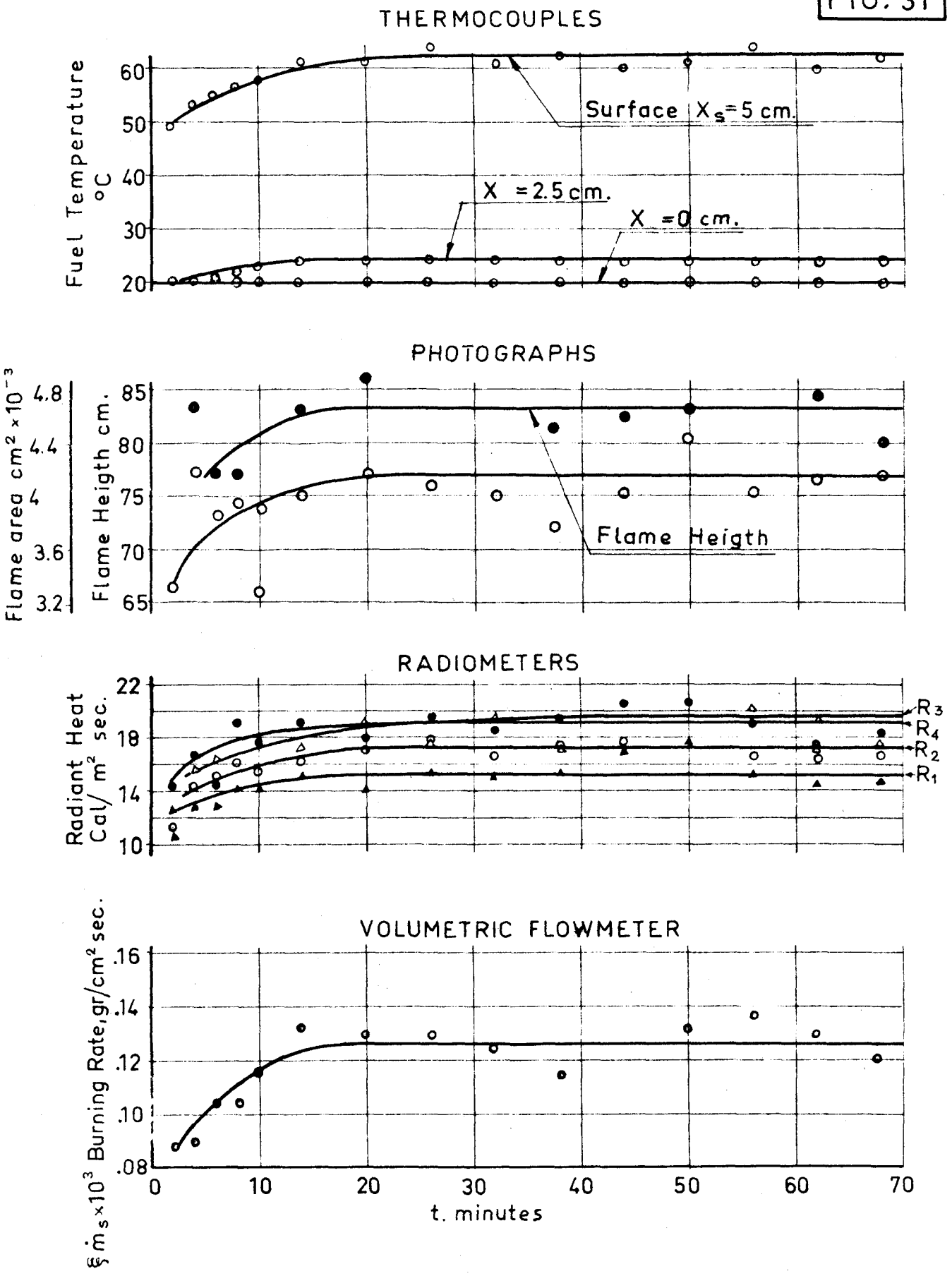


NORMAL HEPTANE
Test N.16

$T_o$=293°K
Vessel Diameter $D_V$=25 cm
Vessel Depth $X_S$ = 5 cm
$\dot{m}_S$= 0.00532

FIG. 32

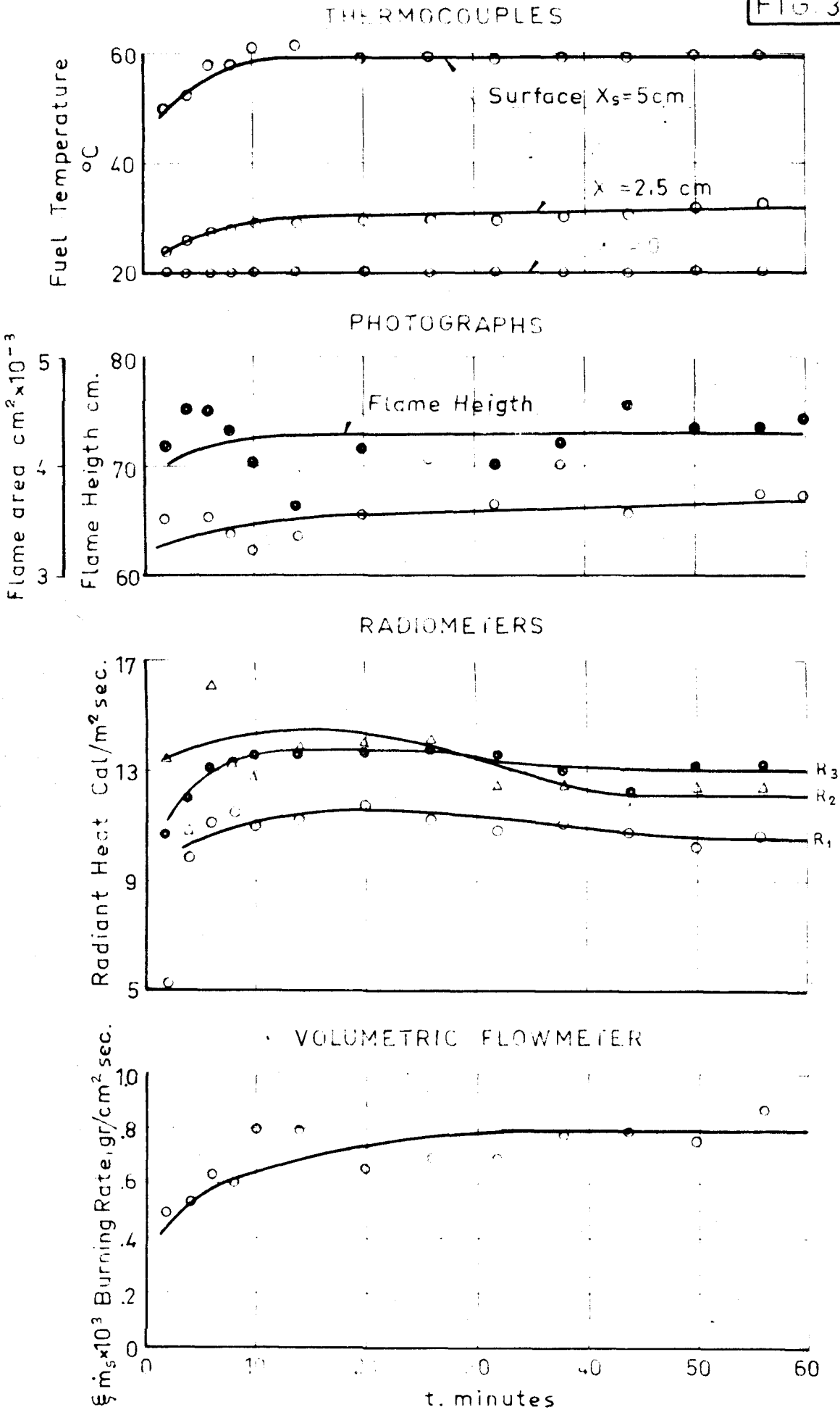


NORMAL-HEPTANE

Test N. 6

$T_o = 293\ ^oK$

Vessel Diameter $D_v = 25$ cm

Vessel Depth $X_s = 5$ cm

$\dot{m}_s = 0.00617$

FIG. 33

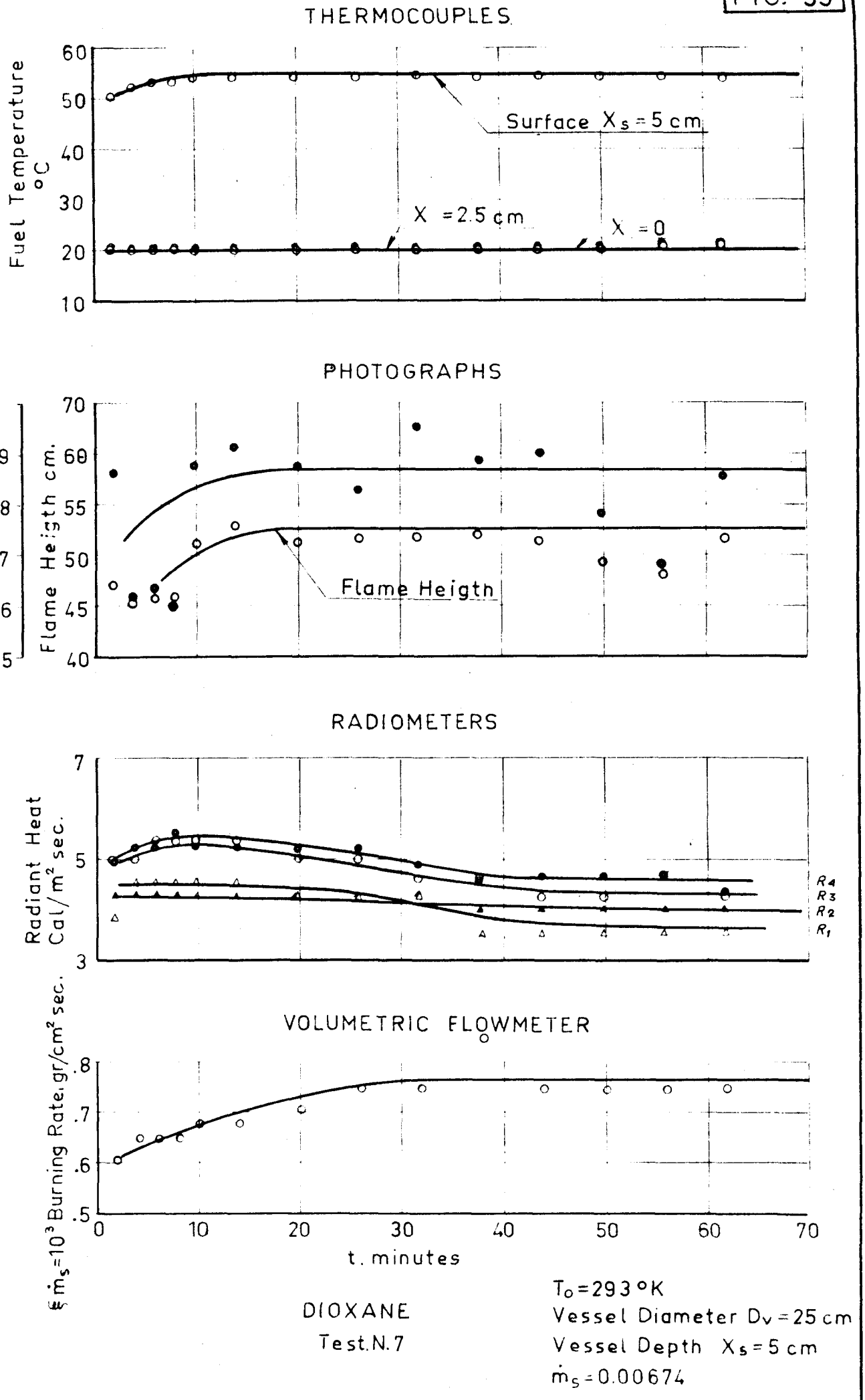


DIOXANE

Test.N.7

$T_o = 293$ °K

Vessel Diameter $D_v = 25$ cm

Vessel Depth $X_s = 5$ cm

$\dot{m}_s = 0.00674$

FIG. 34

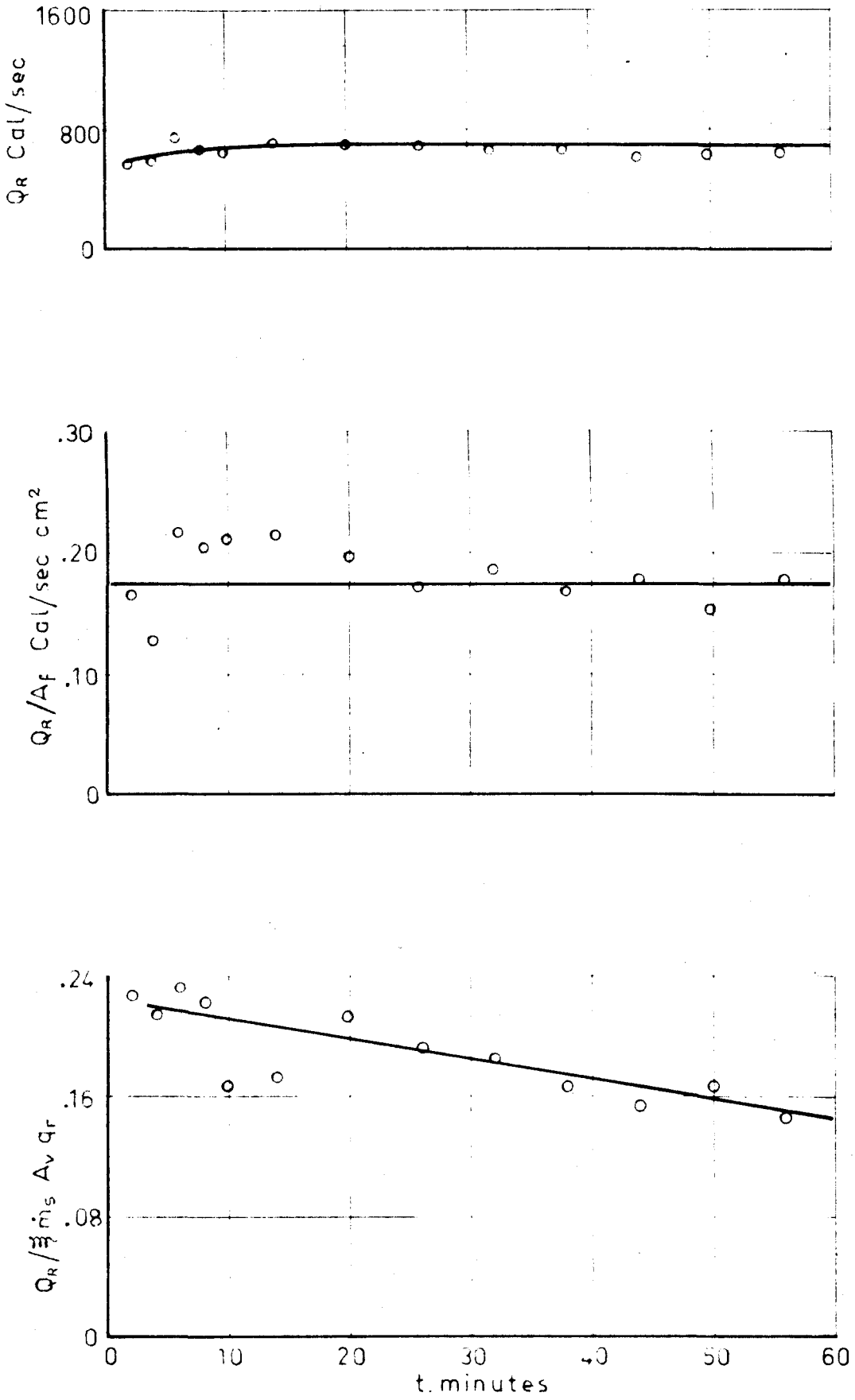


NORMAL-HEPTANE

Test N.6

FIG. 35

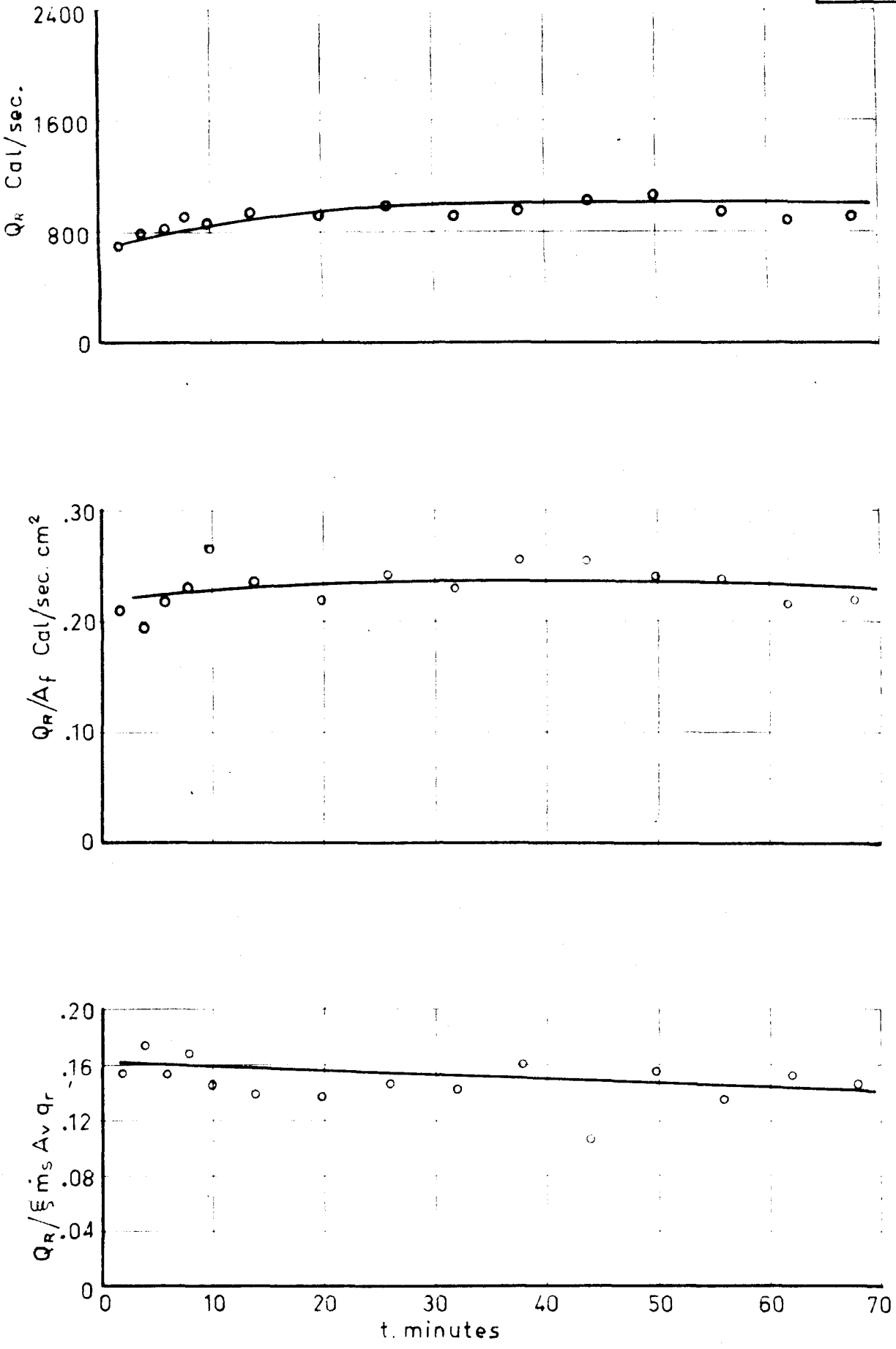


NORMAL-HEPTANE
Test N. 16

FIG. 36

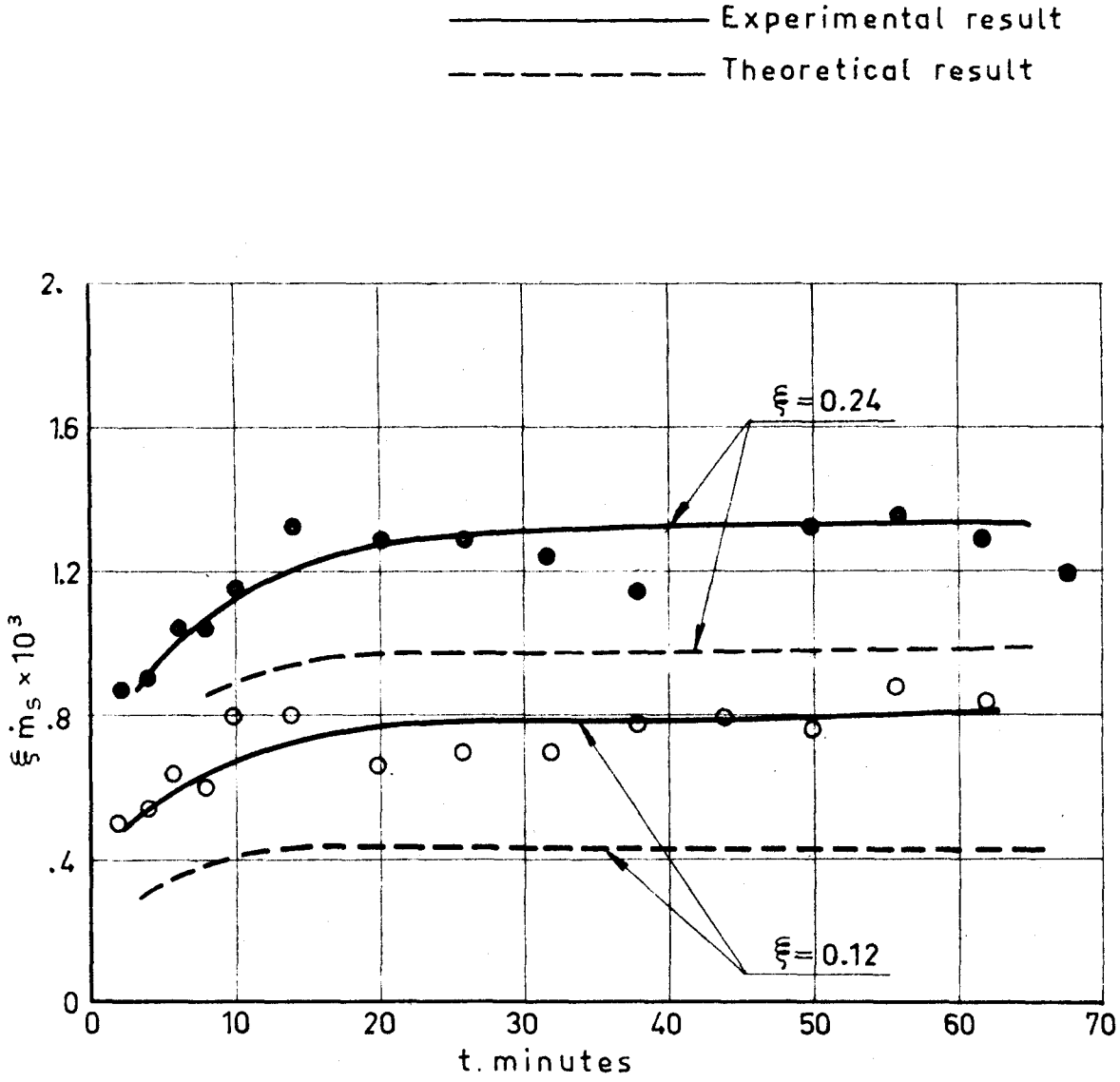


COMPARISON OF RESULTS

FIG. 37

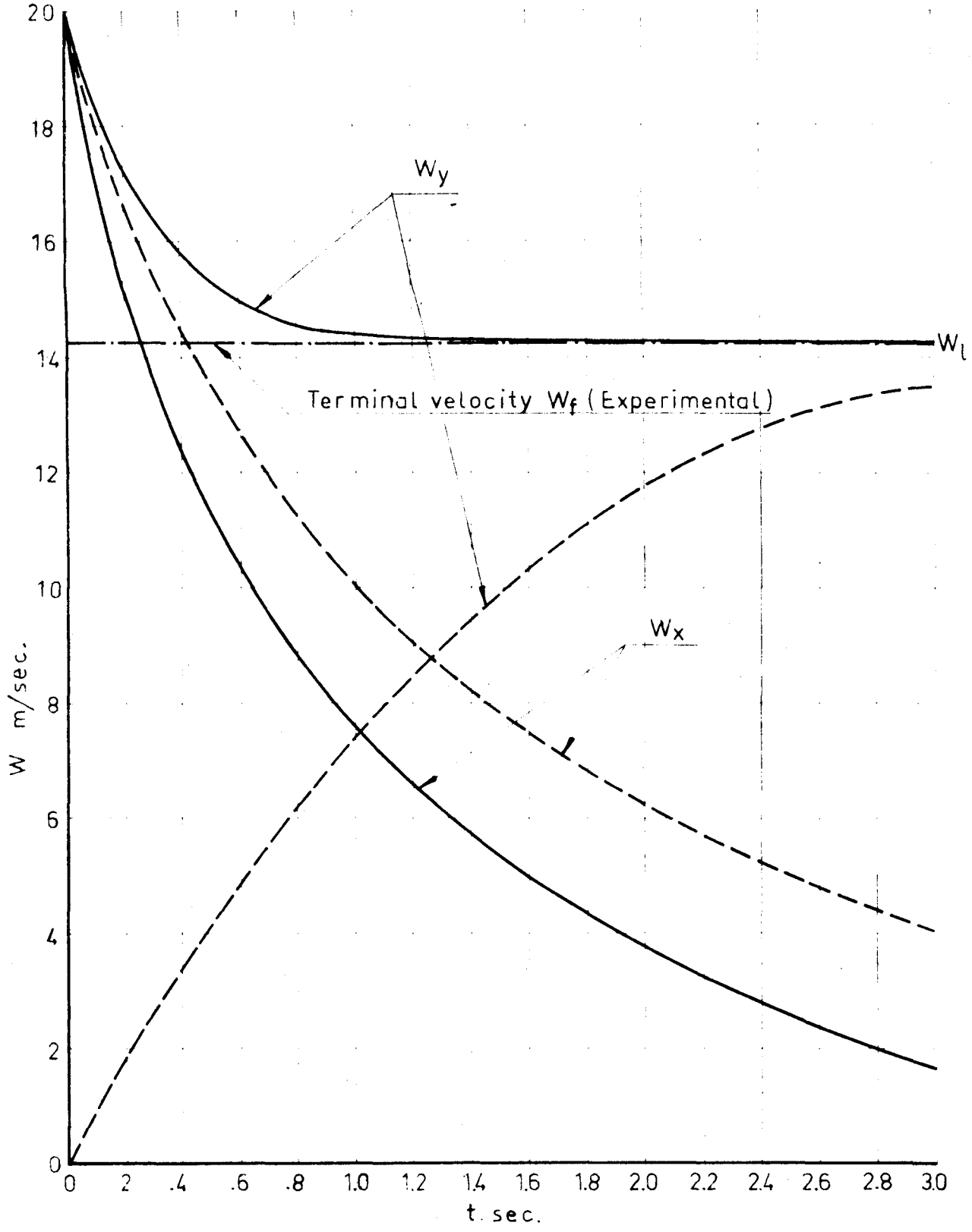


NUMERICAL INTEGRATION OF SYSTEM $\begin{cases} W'_x = -\alpha |W| W_x \\ W'_y = g - \alpha |W| W_y \end{cases}$

PINUS PINASTER SPHERE $D_o = 17$ mm

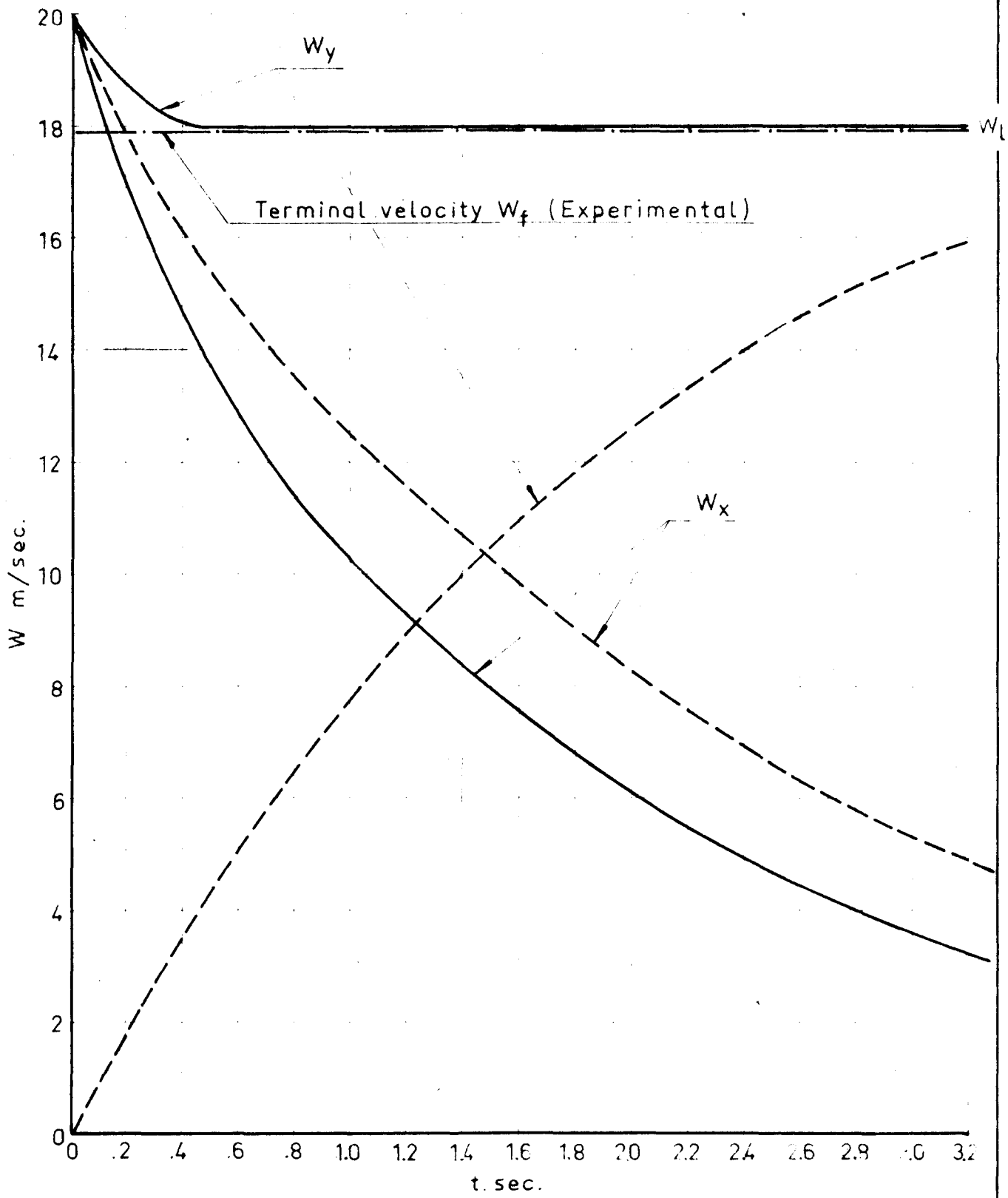


$W_{x_o}$ = 20 m/sec.
——— $W_{y_o}$ = 20 m/sec.
– – – – – – $W_{y_o}$ = 0

NUMERICAL INTEGRATION OF SYSTEM

$$W_x' = -\alpha |W| W_x$$
$$W_y' = g - \alpha |W| W_y$$

PINUS PINASTER SPHERE $D_o$ = 22 mm.

FIG. 39

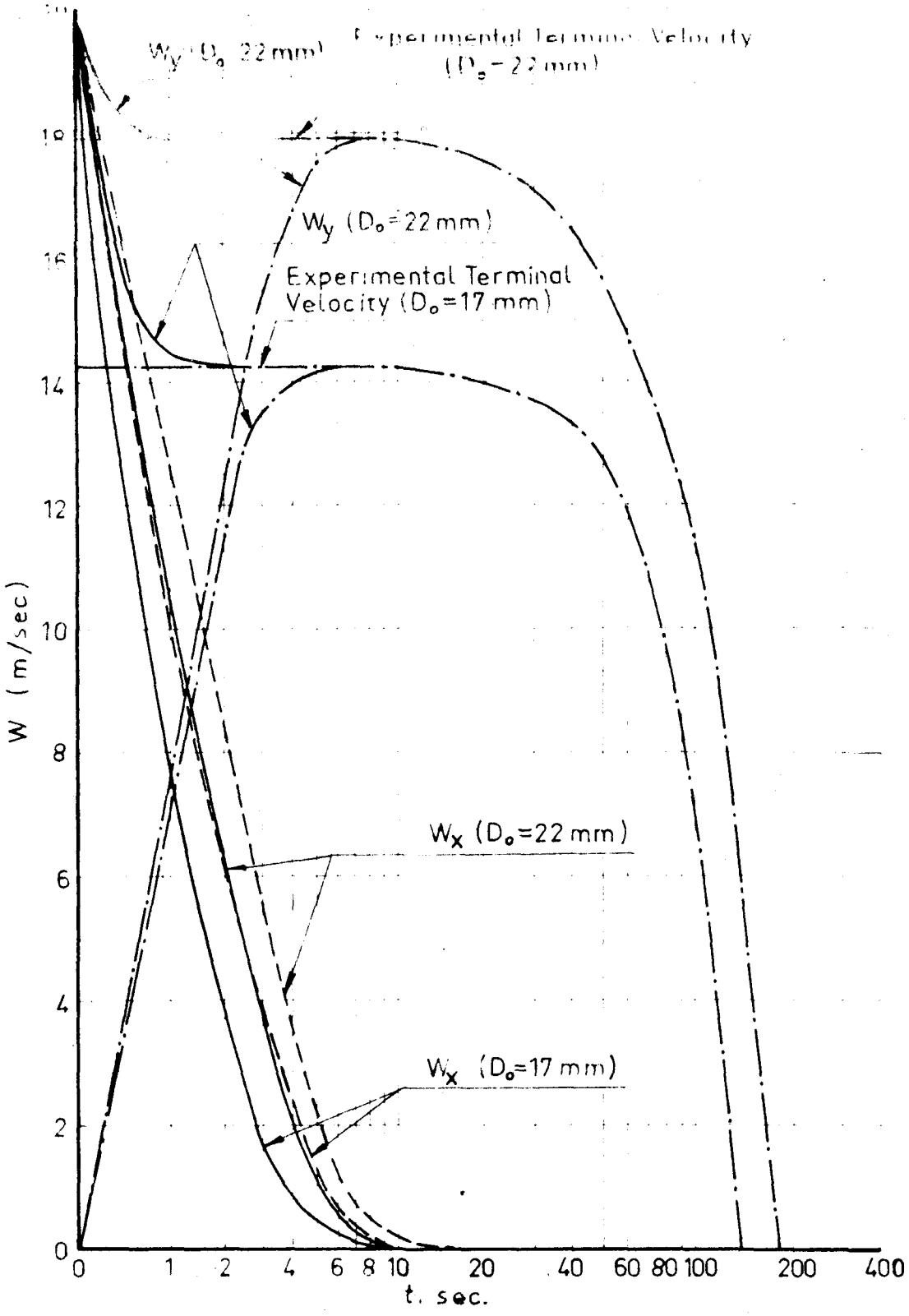


NUMERICAL INTEGRATION OF EQUATIONS
COMPARISON OF RESULTS.

# SUCTION WIND TUNNEL FOR TESTING LARGE FIREBRANDS

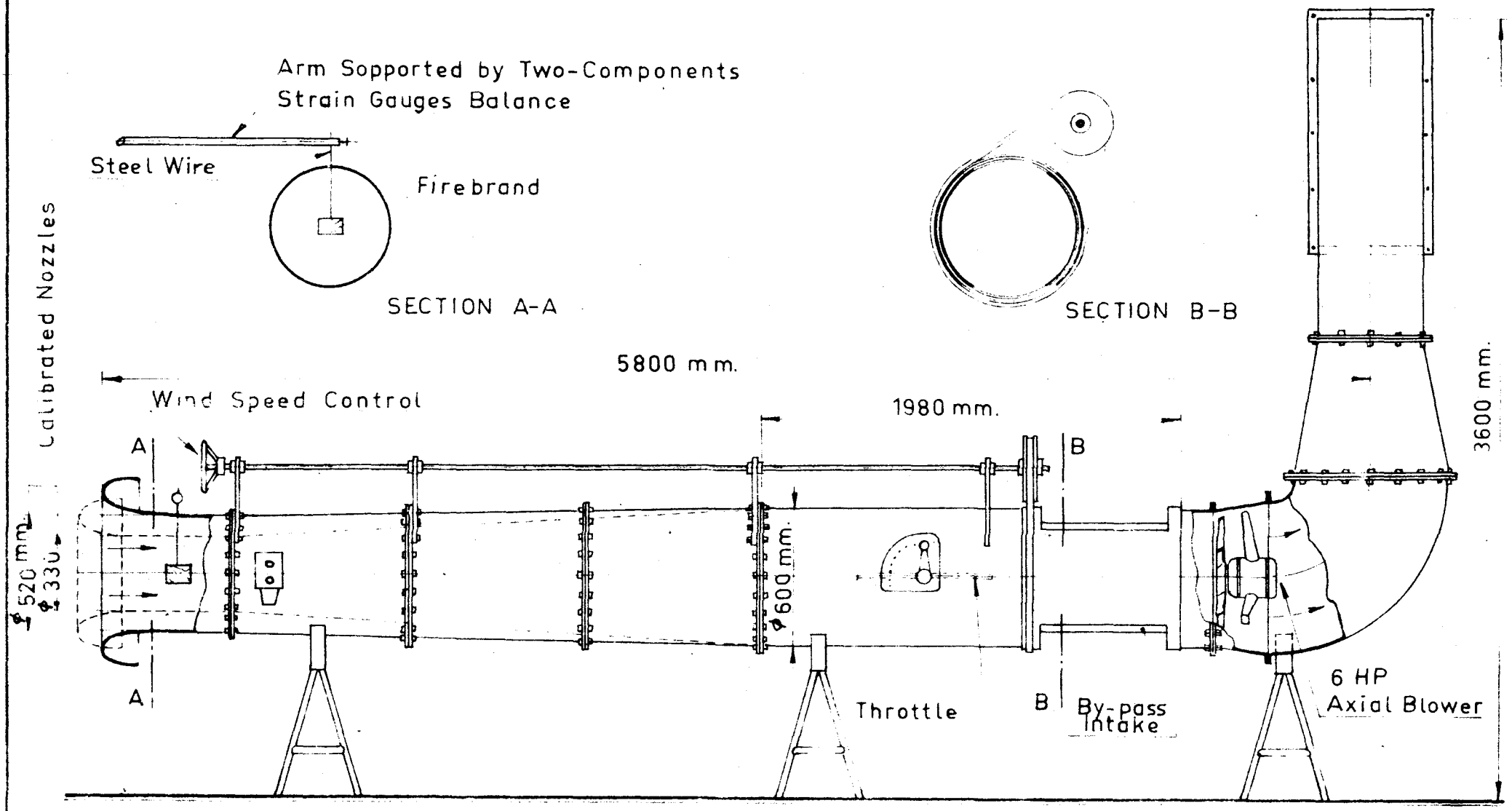


FIG 40

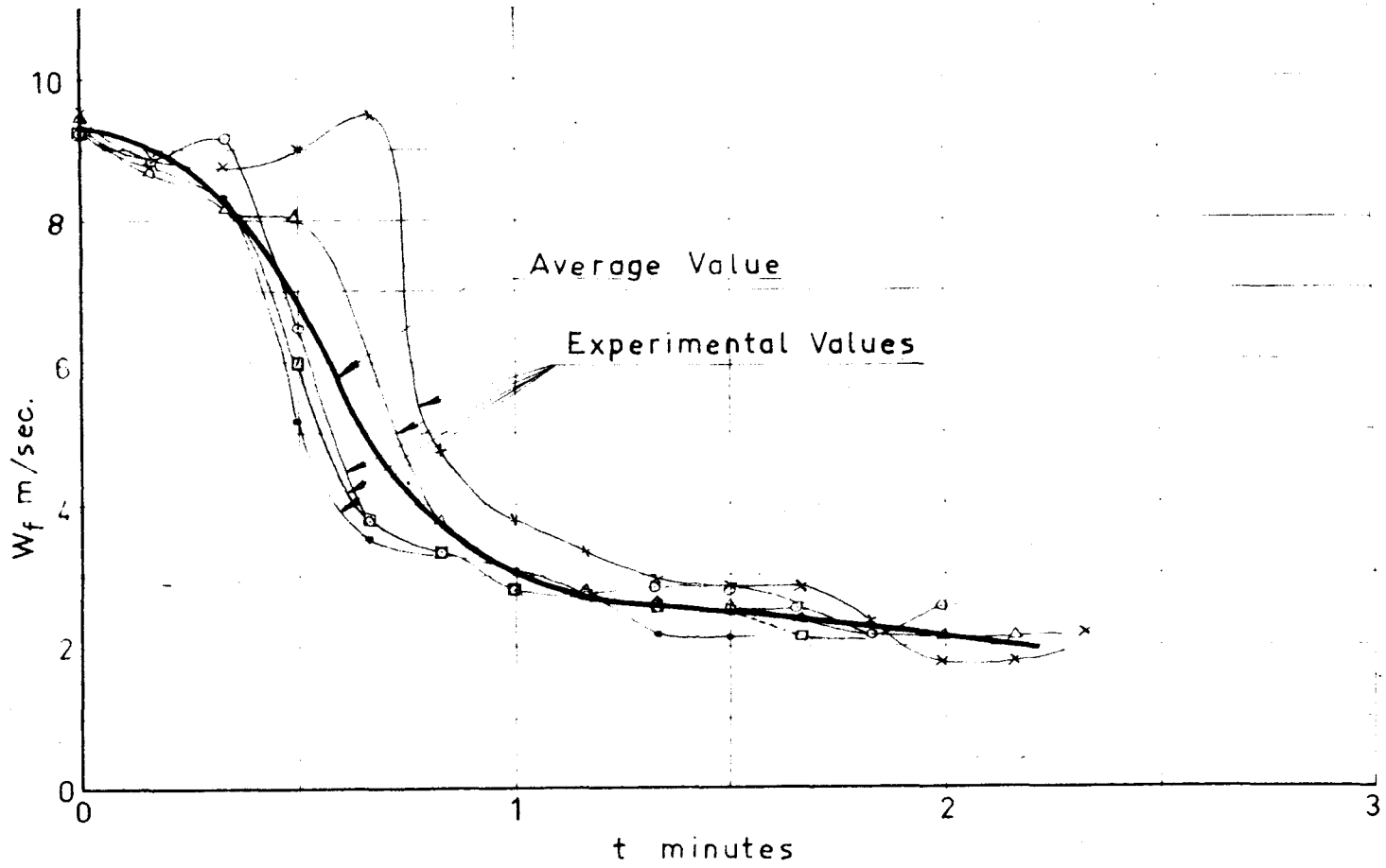


SPHERES. INITIAL DIAMETER $D_o$=10 mm

PINUS PINASTER WOOD

M.C.= 2 %

FIG. 41

FIG. 42

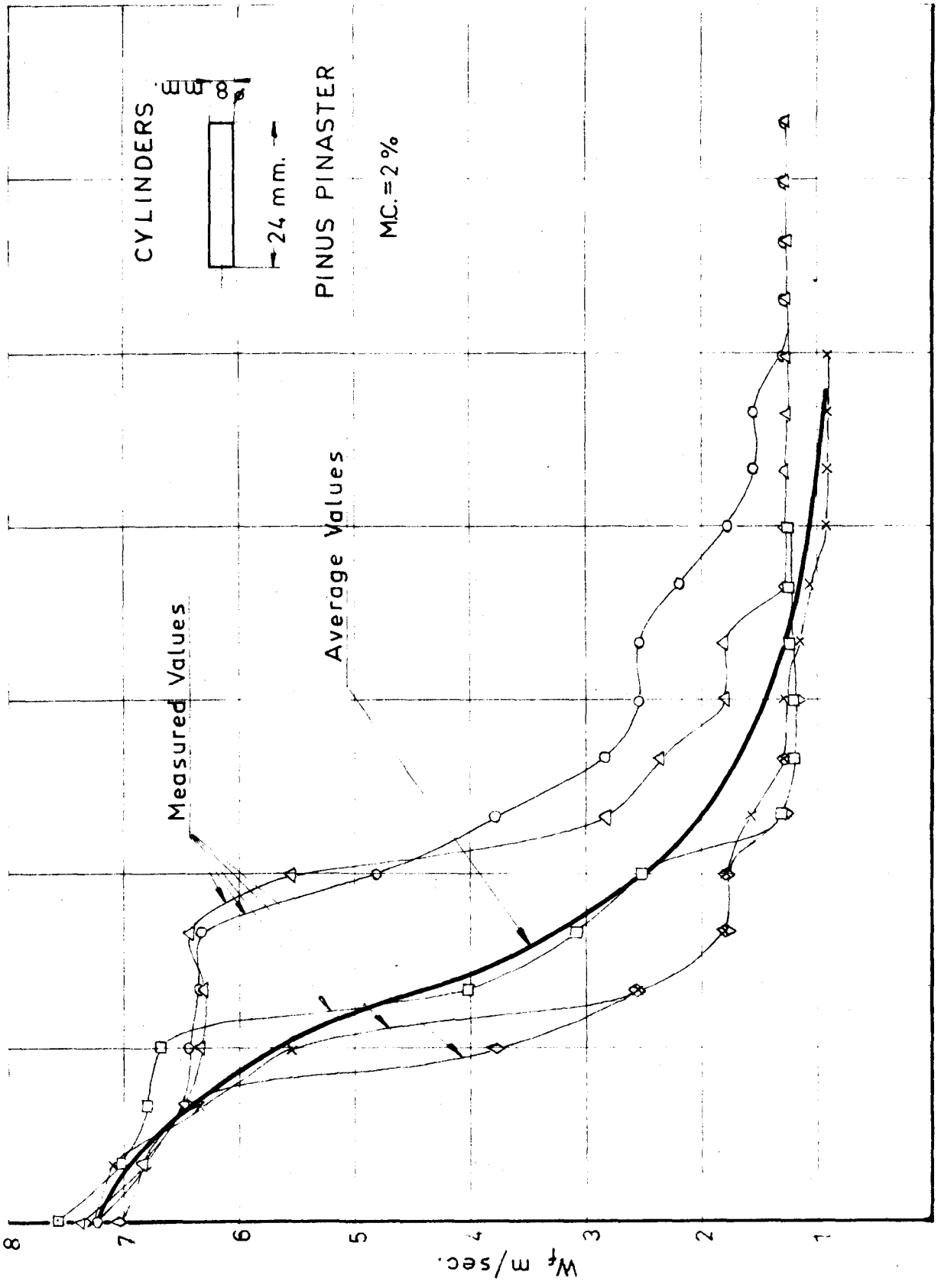


EXPERIMENTAL FINAL VELOCITIES

FIG. 43

SPHERES
PINUS PINASTER
M.C.= 2 %

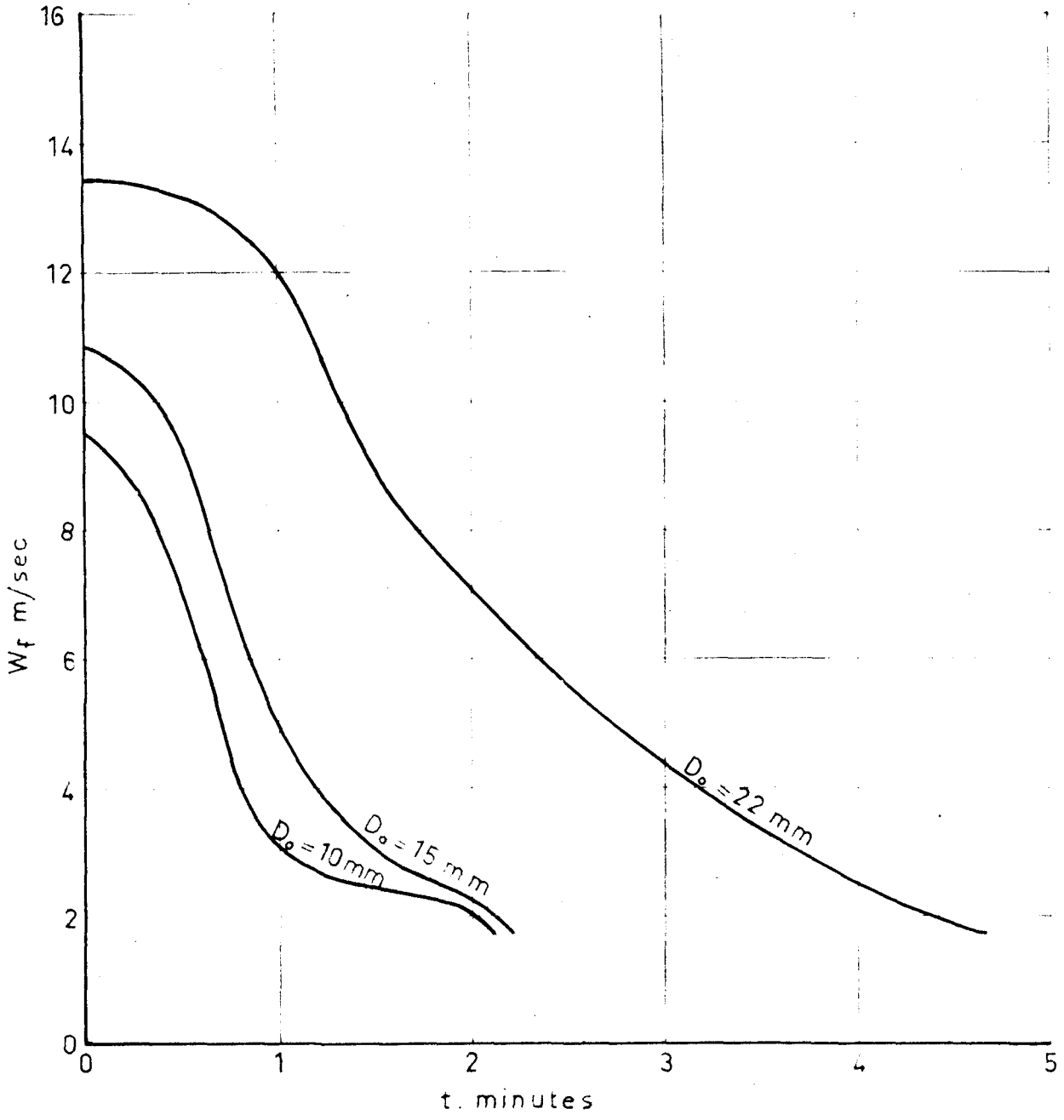


EXPERIMENTAL FINAL VELOCITIES

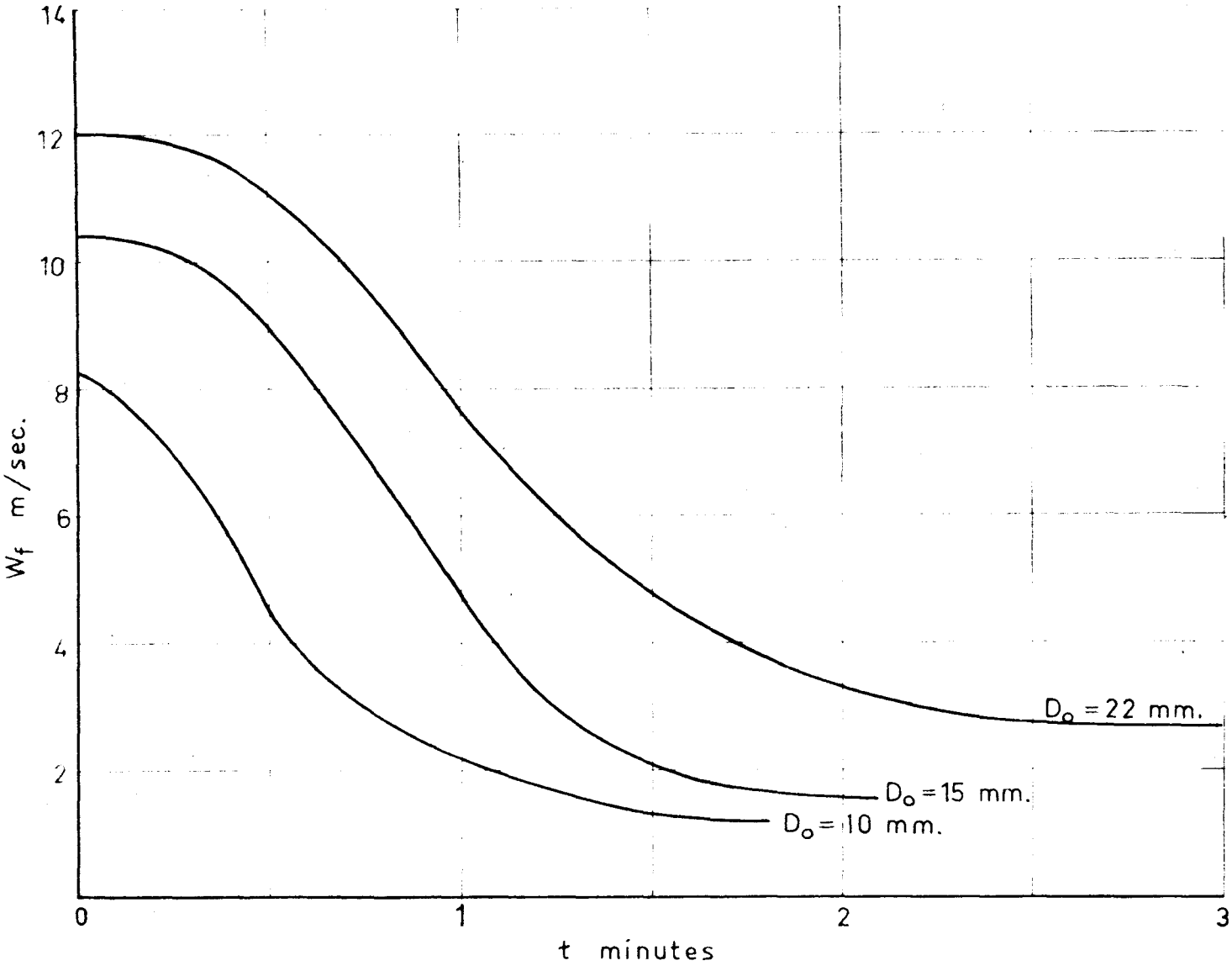


SPHERES
"PICEA EXCELSA"

M.C. = 2%

EXPERIMENTAL FINAL VELOCITIES $W_f$

FIG 44

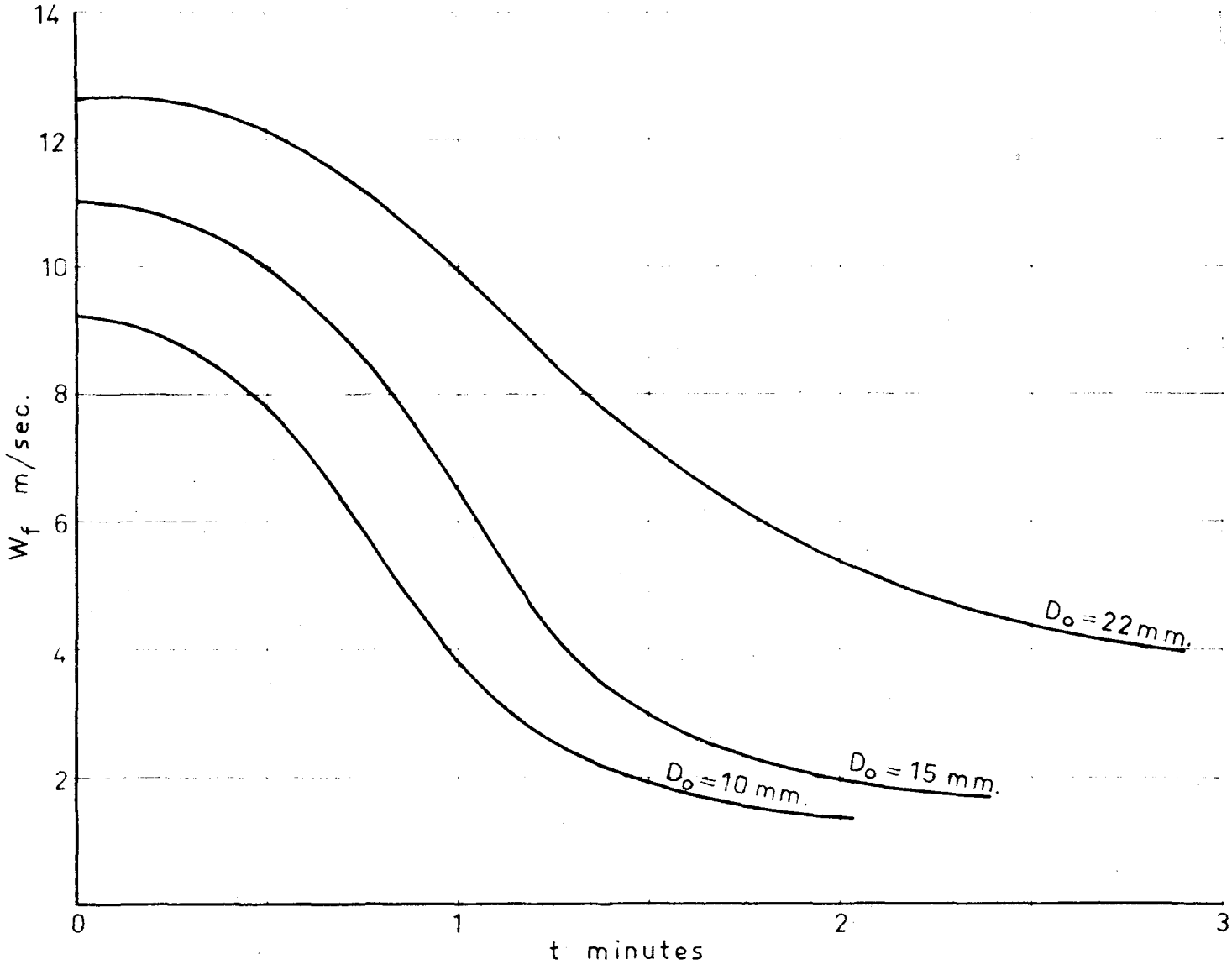


SPHERES
"POPULUS TREMULOIDES"
M.C.= 2 %

EXPERIMENTAL FINAL VELOCITIES

FIG. 45

FIG. 46

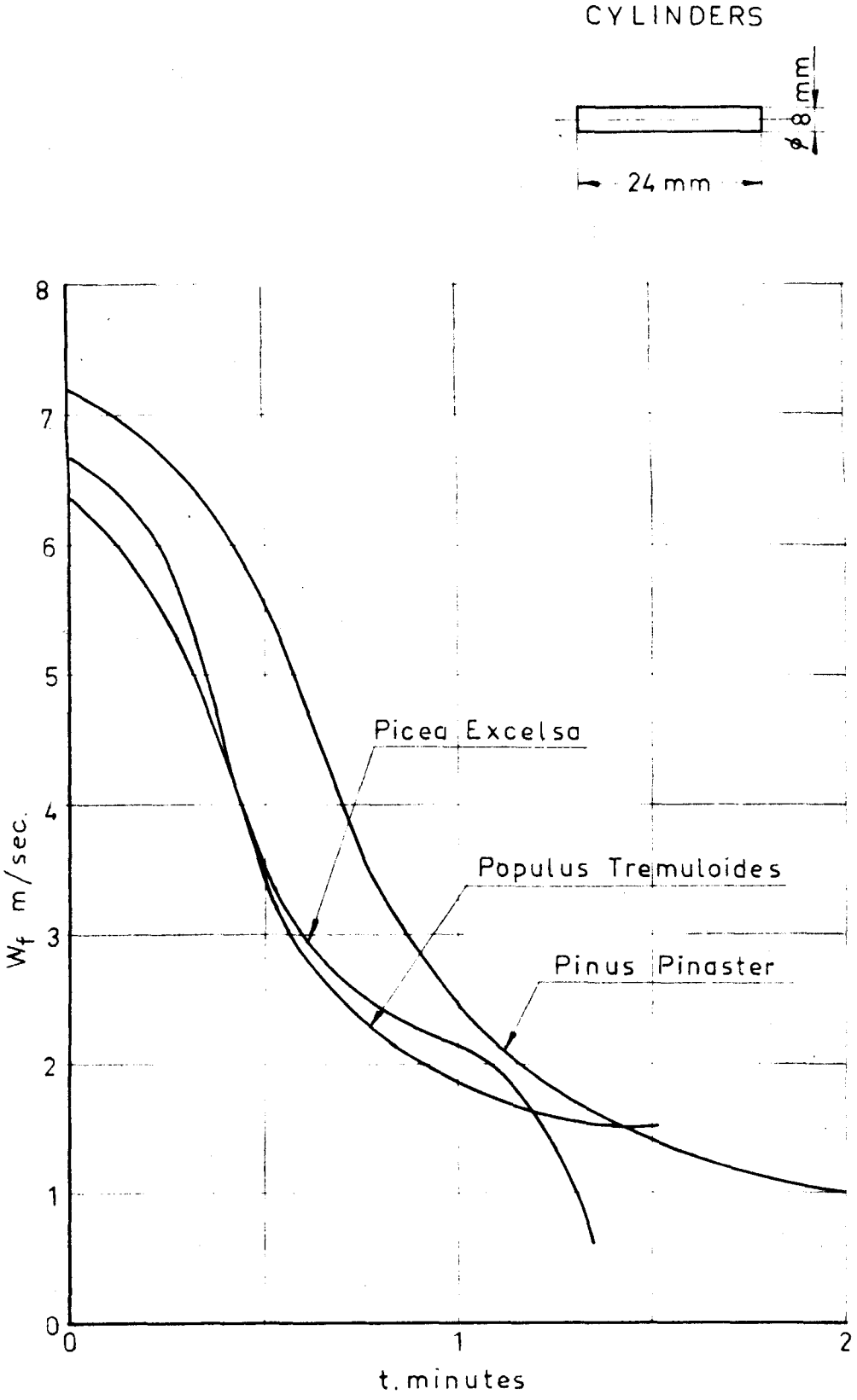


EXPERIMENTAL FINAL VELOCITIES

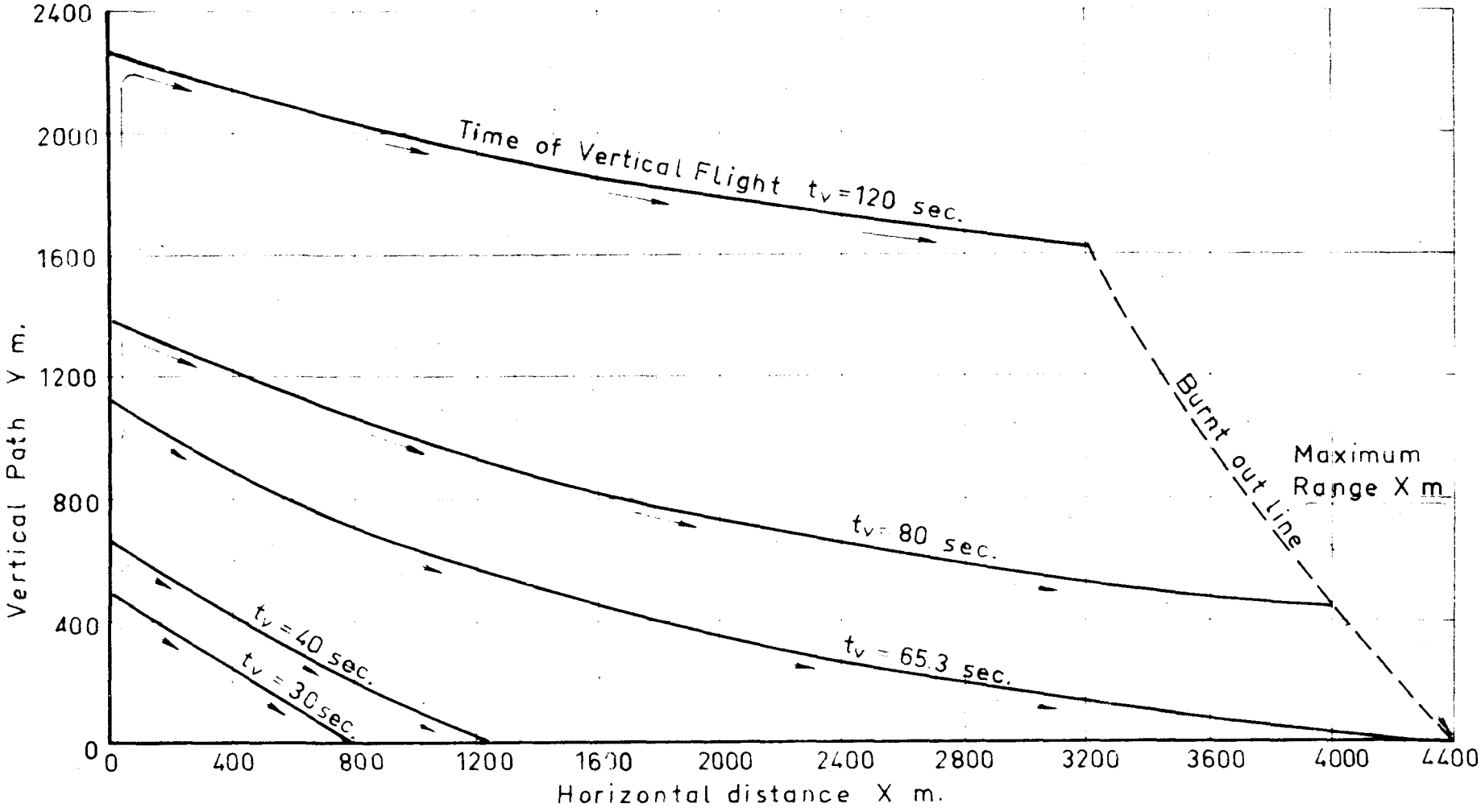


# FLIGHT PATHS OF BURNING SPHERES

PINUS PINASTER $D_o$=22 mm.

$u_y$ = 30 (m/sec.) for X=0

$u_x$ = 20 (m/sec.)

FIG. 47

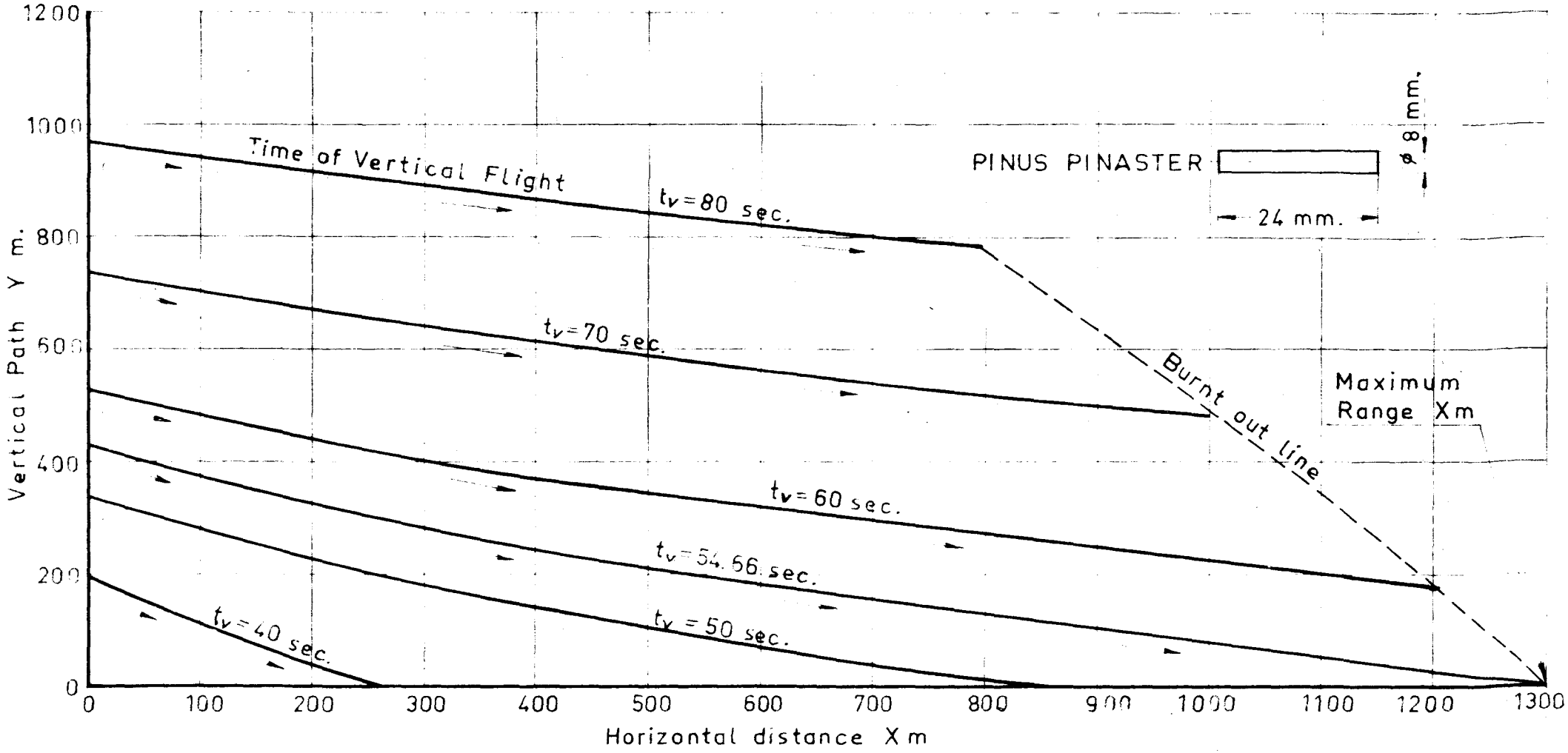


FLIGHT PATHS OF BURNING CYLINDERS

$u_y$ = 30 (m/sec.) for X=0
$u_x$ = 20 (m/sec.)

FIG. 48

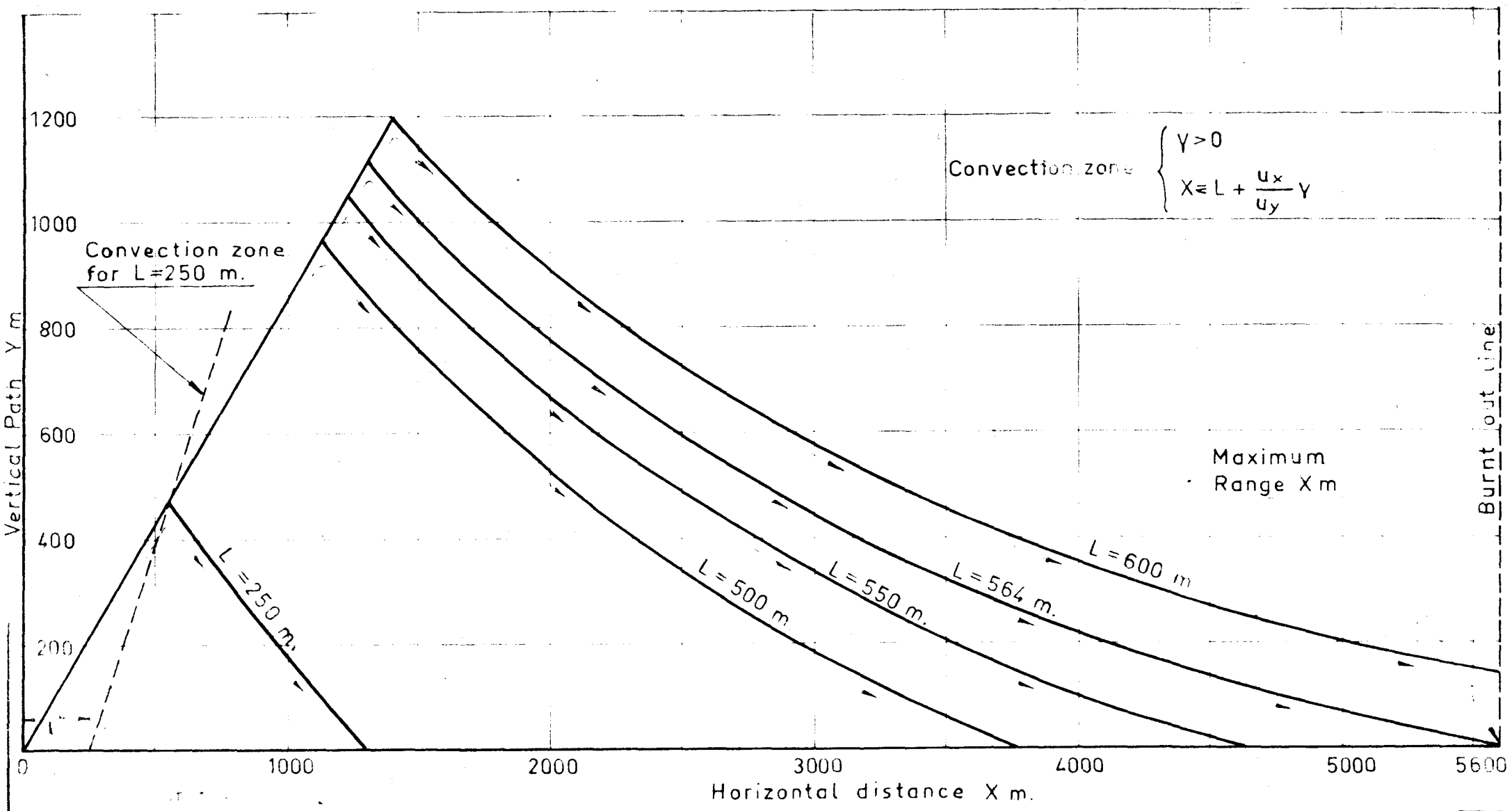


# FLIGHT PATHS OF BURNING SPHERES

P[illegible] P[illegible] $D_0$=[illegible] m

$u_y$ = 30 ( m/sec.) for $\leq L + \frac{u_x}{u_y} Y$

$u_x$ = 20 ( m/sec.)

67 - 11

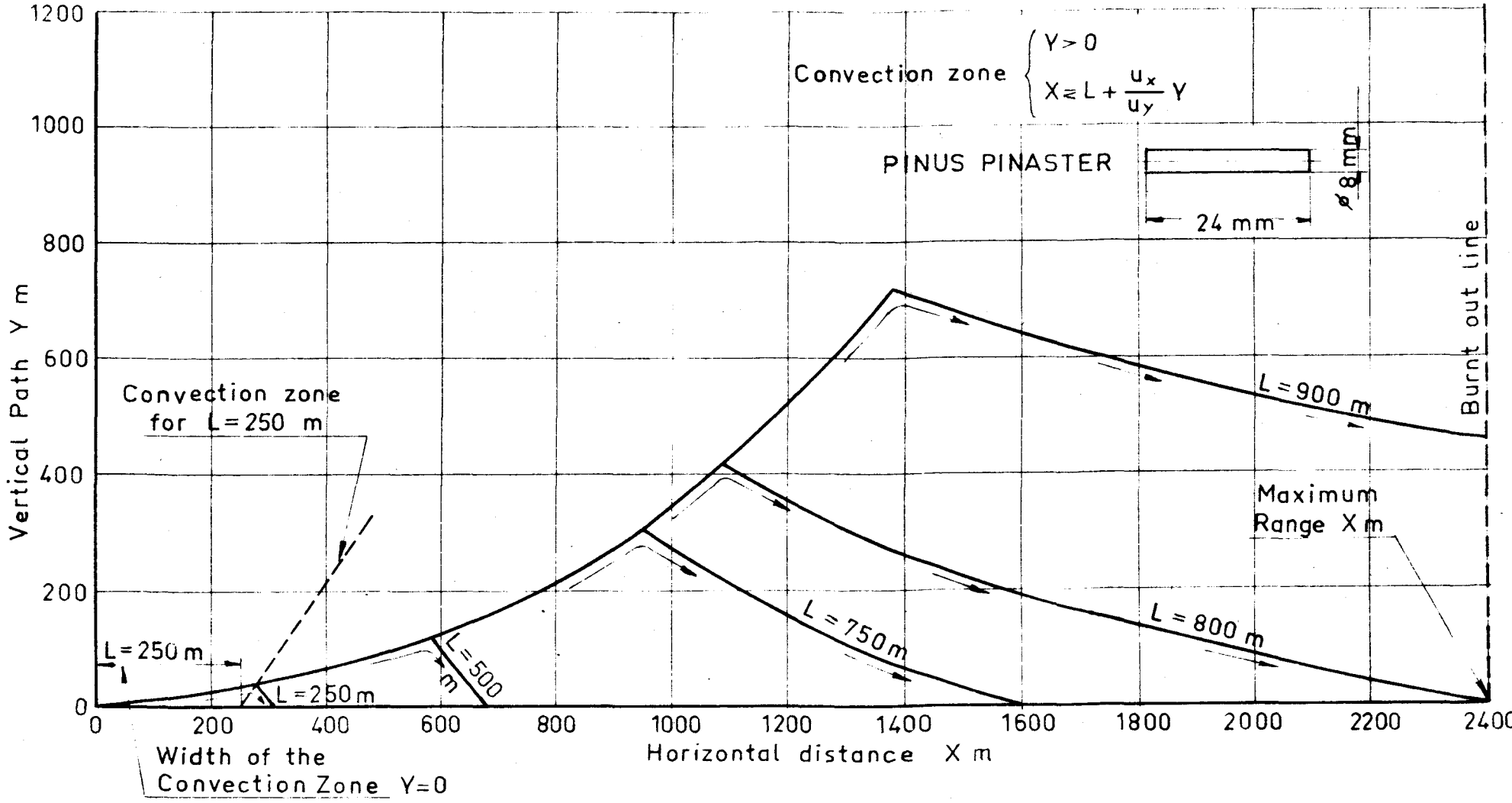


FLIGHT PATHS OF BURNING CYLINDERS

$u_y = 30$ (m/sec.) for $X \geq L + \frac{u_x}{u_y} Y$

$u_x = 20$ (m/sec.)

FIG. 50